



# Mitochondrial respiratory states and rates

**COST Action CA15203 MitoEAGLE preprint** Version: 2018-12-12 (50)

Corresponding author: Gnaiger E

Authors:

Gnaiger E, Aasander Frostner E, Abumrad NA, Acuna-Castroviejo D, Adiele RC, Ahn B, Ali SS, Alton L, Alves MG, Amati F, Amoedo ND, Andreadou I, Aragó M, Aral C, Arandarčikaitė O, Armand AS, Arnould T, Avram VF, Bailey DM, Bajpeyi S, Bajzikova M, Bakker BM, Barlow J, Bastos Sant'Anna Silva AC, Batterson P, Battino M, Bazil J, Beard DA, Bednarczyk P, Bello F, Ben-Shachar D, Bergdahl A, Berge RK, Bergmeister L, Bernardi P, Berridge MV, Bettinazzi S, Bishop D, Blier PU, Blindheim DF, Boardman NT, Boetker HE, Borchard S, Boros M, Børsheim E, Borutaite V, Botella Ruiz J, Bouillaud F, Bouitbir J, Boushel RC, Bovard J, Breton S, Brown DA, Brown GC, Brown RA, Brozinick JT, Buettner GR, Burtscher J, Calabria E, Calbet JA, Calzia E, Cannon DT, Cano Sanchez M, Canto AC, Cardoso LHD, Carvalho E, Casado Pinna M, Cassar S, Cassina AM, Castelo MP, Castro L, Cavalcanti-de-Albuquerque JP, Cervinkova Z, Chabi B, Chakrabarti L, Chakrabarti S, Chaurasia B, Chen Q, Chicco AJ, Chinopoulos C, Chowdhury SK, Cizmarova B, Clementi E, Coen PM, Cohen BH, Coker RH, Collin A, Crisóstomo L, Dahdah N, Dalgaard LT, Dambrova M, Danhelovska T, Darveau CA, Das AM, Dash RK, Davidova E, Davis MS, De Goede P, De Palma C, Dembinska-Kiec A, Detraux D, Devaux Y, Di Marcello M, Dias TR, Distefano G, Doermann N, Doerrier C, Dong L, Donnelly C, Drahota Z, Duarte FV, Dubouchaud H, Duchen MR, Dumas JF, Durham WJ, Dymkowska D, Dyrstad SE, Dyson A, Dzialowski EM, Eaton S, Ehinger J, Elmer E, Endlicher R, Engin AB, Escames G, Ezrova Z, Falk MJ, Fell DA, Ferdinandy P, Ferko M, Ferreira JCB, Ferreira R, Ferri A, Fessel JP, Filipovska A, Fisar Z, Fischer C, Fischer M, Fisher G, Fisher JJ, Ford E, Fornaro M, Galina A, Galkin A, Gallee L, Galli GL, Gan Z, Ganetzky R, Garcia-Rivas G, Garcia-Roves PM, Garcia-Souza LF, Garipi E, Garlid KD, Garrabou G, Garten A, Gastaldelli A, Gayen J, Genders AJ, Genova ML, Giovarelli M, Gonzalez-Armenta JL, Goncalo Teixeira da SR, Goncalves DF, Gonzalo H, Goodpaster BH, Gorr TA, Gourlay CW, Granata C, Grefte S, Guarch ME, Gueguen N, Gumeni S, Haas CB, Haavik J, Haendeler J, Haider M, Hamann A, Han J, Han WH, Hancock CR, Hand SC, Handl J, Hargreaves IP, Harper ME, Harrison DK, Hausenloy DJ, Heales SJR, Heiestad C, Hellgren KT, Hepple RT, Hernansanz-Agustin P, Hewakapuge S, Hickey AJ, Ho DH, Hoehn KL, Hoel F, Holland OJ, Holloway GP, Hoppel CL, Hoppel F, Houstek J, Huete-Ortega M, Hyrossova P, Iglesias-Gonzalez J, Irving BA, Isola R, Iyer S, Jackson CB, Jadiya P, Jana PF, Jang DH, Jang YC, Janowska J, Jansen K, Jansen-Dürr P, Jansone B, Jarmuszkiewicz W, Jaskiewicz A, Jedlicka J, Jespersen NR, Jha RK, Jurczak MJ, Jurk D, Kaambre T, Kaczor JJ, Kainulainen H, Kampa RP, Kandel SM, Kane DA, Kapferer W, Kappler L, Karabatsiakis A, Karkucinska-Wieckowska A, Kaur S, Keijer J, Keller MA, Keppner G, Khamoui AV, Kidere D, Kilbaugh T, Kim HK, Kim JKS, Klepinin A, Klepinina L, Klingenspor M, Komlodi T, Koopman WJH, Kopitar-Jerala N, Kowaltowski AJ, Kozlov AV, Krajcova A, Krako Jakovljevic N, Kristal BS, Krycer JR, Kuang J, Kucera O, Kuka J, Kwak HB, Kwast K, Laasmaa M, Labieniec-Watala M, Lai N, Land JM, Lane N, Laner V, Lanza IR, Larsen TS, Lavery GG, Lazou A, Lee HK, Leeuwenburgh C, Lehti M, Lemieux H, Lenaz G, Lerfall J, Li PA, Li Puma L, Liepins E, Lionett S, Liu J, López LC, Lucchinetti E, Ma T, Macedo MP, Maciej S, MacMillan-Crow LA, Majtnerova P, Makarova E, Makrecka-Kuka M, Malik AN, Markova M, Martin DS, Martins AD, Martins JD, Maseko TE, Maull F, Mazat JP, McKenna HT, Menze MA, Merz T, Meszaros AT, Methner A, Michalak S, Moellering DR, Moiso N, Molina AJA, Moutaigne D, Moore AL, Moreau K, Moreno-Sánchez R, Moreira BP, Mracek T, Muccini AM,

49 Muntane J, Muntean DM, Murray AJ, Musiol E, Myhre Pedersen T, Nair KS, Nehlin JO, Nemeč M,  
 50 Neuffer PD, Neuzil J, Neviere R, Newsom S, Nozickova K, O'Brien KA, O'Gorman D, Olgar Y, Oliveira  
 51 B, Oliveira MF, Oliveira MT, Oliveira PF, Oliveira PJ, Orynbayeva Z, Osiewacz HD, Pak YK, Pallotta  
 52 ML, Palmeira CM, Parajuli N, Passos JF, Passrigger M, Patel HH, Pavlova N, Pecina P, Pereira da  
 53 Silva Grilo da Silva F, Perez Valencia JA, Perks KL, Pesta D, Petit PX, Pettersen IKN, Pichaud N,  
 54 Pichler I, Piel S, Pietka TA, Pino MF, Pirkmajer S, Plangger M, Porter C, Porter RK, Procaccio V,  
 55 Prochownik EV, Prola A, Pulinilkunnit T, Puskarich MA, Puurand M, Radenkovic F, Ramzan R, Rattan  
 56 SIS, Reboredo P, Renner-Sattler K, Rial E, Robinson MM, Roden M, Rodriguez-Enriquez S, Rohlena  
 57 J, Rolo AP, Ropelle ER, Røslund GV, Rossignol R, Rossiter HB, Rubelj I, Rybacka-Mossakowska J,  
 58 Saada A, Safaei Z, Saharnaz S, Salin K, Salvadego D, Sandi C, Saner N, Sanz A, Sazanov LA, Scatena  
 59 R, Schartner M, Scheiby-Knudsen M, Schilling JM, Schlattner U, Schönfeld P, Schots PC, Schulz R,  
 60 Schwarzer C, Scott GR, Selman C, Shabalina IG, Sharma P, Sharma V, Shevchuk I, Siewiera K, Silber  
 61 AM, Silva AM, Sims CA, Singer D, Singh BK, Skolik R, Smenes BT, Smith J, Soares FAA, Sobotka  
 62 O, Sokolova I, Sonkar VK, Sowton AP, Sparagna GC, Sparks LM, Spinazzi M, Stankova P, Starr J,  
 63 Stary C, Stelfa G, Stepto NK, Stiban J, Stier A, Stocker R, Storder J, Sumbalova Z, Suomalainen A,  
 64 Suravajhala P, Svalbe B, Swerdlow RH, Swiniuch D, Szabo I, Szewczyk A, Szibor M, Tanaka M,  
 65 Tandler B, Tarnopolsky MA, Tausan D, Tavernarakis N, Tepp K, Thakkar H, Thapa M, Thyfault JP,  
 66 Tomar D, Ton R, Torp MK, Towheed A, Tretter L, Trifunovic A, Trivigno C, Tronstad KJ, Trougakos  
 67 IP, Truu L, Tuncay E, Turan B, Tyrrell DJ, Urban T, Valentine JM, Van Bergen NJ, Van Hove J,  
 68 Varricchio F, Vella J, Vendelin M, Vercesi AE, Victor VM, Vieira Ligo Teixeira C, Vidimce J, Viel C,  
 69 Vieyra A, Vilks K, Villena JA, Vincent V, Vinogradov AD, Viscomi C, Vitorino RMP, Vogt S, Volani  
 70 C, Volska K, Votion DM, Vujacic-Mirski K, Wagner BA, Ward ML, Warnsmann V, Wasserman DH,  
 71 Watala C, Wei YH, Whitfield J, Wickert A, Wieckowski MR, Wiesner RJ, Williams CM, Winwood-  
 72 Smith H, Wohlgemuth SE, Wohlwend M, Wolff JN, Wrutniak-Cabello C, Wüst RCI, Yokota T,  
 73 Zablocki K, Zanon A, Zaugg K, Zaugg M, Zdrzilova L, Zhang Y, Zhang YZ, Zíková A, Zischka H,  
 74 Zorzano A, Zvejniece L

75  
 76 **Updates and discussion:**

77 [http://www.mitoeagle.org/index.php/MitoEAGLE\\_preprint\\_2018-02-08](http://www.mitoeagle.org/index.php/MitoEAGLE_preprint_2018-02-08)

78  
 79 517 coauthors

80  
 81 Correspondence: Gnaiger E

82 *Chair COST Action CA15203 MitoEAGLE – <http://www.mitoeagle.org>*

83 *Department of Visceral, Transplant and Thoracic Surgery, D. Swarovski Research Laboratory,*

84 *Medical University of Innsbruck, Innrain 66/4, A-6020 Innsbruck, Austria*

85 *Email: mitoeagle@i-med.ac.at; Tel: +43 512 566796, Fax: +43 512 566796 20*

86



87	<b>Table of contents</b>
88	
89	<b>Abstract</b>
90	<b>Executive summary</b>
91	<b>1. Introduction – Box 1: In brief: Mitochondria and Bioblasts</b>
92	<b>2. Coupling states and rates in mitochondrial preparations</b>
93	2.1. <i>Cellular and mitochondrial respiration</i>
94	2.1.1. Aerobic and anaerobic catabolism and ATP turnover
95	2.1.2. Specification of biochemical dose
96	2.2. <i>Mitochondrial preparations</i>
97	2.3. <i>Electron transfer pathways</i>
98	2.4. <i>Respiratory coupling control</i>
99	2.4.1. Coupling
100	2.4.2. Phosphorylation, P <sub>s</sub> , and P <sub>s</sub> /O <sub>2</sub> ratio
101	2.4.3. Uncoupling
102	2.5. <i>Coupling states and respiratory rates</i>
103	2.5.1. <b>LEAK-state</b>
104	2.5.2. <b>OXPHOS-state</b>
105	2.5.3. <b>Electron transfer-state</b>
106	2.5.4. ROX state and <i>Rox</i>
107	2.5.5. Quantitative relations
108	2.5.6. The steady-state
109	2.6. <i>Classical terminology for isolated mitochondria</i>
110	2.6.1. State 1
111	2.6.2. State 2
112	2.6.3. State 3
113	2.6.4. State 4
114	2.6.5. State 5
115	2.7. <i>Control and regulation</i>
116	<b>3. What is a rate? – Box 2: Metabolic flows and fluxes: vectorial, vectorial, and scalar</b>
117	<b>4. Normalization of rate per sample</b>
118	4.1. <i>Flow: per object</i>
119	4.1.1. Number concentration
120	4.1.2. Flow per object
121	4.2. <i>Size-specific flux: per sample size</i>
122	4.2.1. Sample concentration
123	4.2.2. Size-specific flux
124	4.3. <i>Marker-specific flux: per mitochondrial content</i>
125	4.3.1. Mitochondrial concentration and mitochondrial markers
126	4.3.2. mt-Marker-specific flux
127	<b>5. Normalization of rate per system</b>
128	5.1. <i>Flow: per chamber</i>
129	5.2. <i>Flux: per chamber volume</i>
130	5.2.1. System-specific flux
131	5.2.2. Advancement per volume
132	<b>6. Conversion of units</b>
133	<b>7. Conclusions – Box 3: Recommendations for studies with mitochondrial preparations</b>
134	<b>Acknowledgements</b>
135	<b>Author contributions</b>
136	<b>Competing financial interests</b>
137	<b>References</b>
138	<b>Supplement</b>
139	S1. Manuscript phases and versions - an open-access approach
140	S2. Joining COST Actions
141	

142 **Abstract** As the knowledge base and importance of mitochondrial physiology to human health expands,  
 143 the necessity for harmonizing the terminology concerning mitochondrial respiratory states and rates has  
 144 become increasingly apparent. The chemiosmotic theory establishes the mechanism of energy  
 145 transformation and coupling in oxidative phosphorylation. The unifying concept of the protonmotive  
 146 force provides the framework for developing a consistent theoretical foundation of mitochondrial  
 147 physiology and bioenergetics. We follow guidelines of the International Union of Pure and Applied  
 148 Chemistry (IUPAC) on terminology in physical chemistry, extended by considerations of open systems  
 149 and thermodynamics of irreversible processes. The concept-driven constructive terminology  
 150 incorporates the meaning of each quantity and aligns concepts and symbols with the nomenclature of  
 151 classical bioenergetics. We endeavour to provide a balanced view of mitochondrial respiratory control  
 152 and a critical discussion on reporting data of mitochondrial respiration in terms of metabolic flows and  
 153 fluxes. Uniform standards for evaluation of respiratory states and rates will ultimately contribute to  
 154 reproducibility between laboratories and thus support the development of databases of mitochondrial  
 155 respiratory function in species, tissues, and cells. Clarity of concept and consistency of nomenclature  
 156 facilitate effective transdisciplinary communication, education, and ultimately further discovery.

157  
 158 *Keywords:* Mitochondrial respiratory control, coupling control, mitochondrial preparations,  
 159 protonmotive force, uncoupling, oxidative phosphorylation: OXPHOS, efficiency, electron transfer: ET,  
 160 electron transfer system: ETS, proton leak, ion leak and slip compensatory state: LEAK, residual oxygen  
 161 consumption: ROX, State 2, State 3, State 4, normalization, flow, flux, oxygen: O<sub>2</sub>  
 162

---

## 163 **Executive summary**

164  
 165 In view of the broad implications for health care, mitochondrial researchers face an increasing  
 166 responsibility to disseminate their fundamental knowledge and novel discoveries to a wide range of  
 167 stakeholders and scientists beyond the group of specialists. This requires implementation of a commonly  
 168 accepted terminology within the discipline and standardization in the translational context. Authors,  
 169 reviewers, journal editors, and lecturers are challenged to collaborate with the aim to harmonize the  
 170 nomenclature in the growing field of mitochondrial physiology and bioenergetics, from evolutionary  
 171 biology and comparative physiology to mitochondrial medicine. In the present communication we focus  
 172 on the following concepts in mitochondrial physiology:

- 173 1. Aerobic respiration depends on the coupling of phosphorylation (ADP → ATP) to O<sub>2</sub> flux in  
 174 catabolic reactions. Coupling in oxidative phosphorylation is mediated by the translocation of  
 175 protons across the mitochondrial inner membrane (mtIM) through proton pumps generating  
 176 or utilizing the protonmotive force that is maintained between the mitochondrial matrix and  
 177 intermembrane compartment or outer mitochondrial space. Compartmental coupling depends  
 178 on ion translocation across a semipermeable membrane, which is defined as vectorial  
 179 metabolism and distinguishes oxidative phosphorylation from cytosolic fermentation as  
 180 counterparts of cellular core energy metabolism (**Figure 1**). Cell respiration is thus  
 181 distinguished from fermentation: (1) Electron acceptors are supplied by external respiration  
 182 for the maintenance of redox balance, whereas fermentation is characterized by an internal  
 183 electron acceptor produced in intermediary metabolism. In aerobic cell respiration, redox  
 184 balance is maintained by O<sub>2</sub> as the electron acceptor. (2) Compartmental coupling in vectorial  
 185 oxidative phosphorylation contrasts to exclusively scalar substrate-level phosphorylation in  
 186 fermentation.
- 187 2. When measuring mitochondrial metabolism, the contribution of fermentation and other cytosolic  
 188 interactions must be excluded from analysis by disrupting the barrier function of the plasma  
 189 membrane. Selective removal or permeabilization of the plasma membrane yields  
 190 mitochondrial preparations—including isolated mitochondria, tissue and cellular  
 191 preparations—with structural and functional integrity. Subsequently, extra-mitochondrial  
 192 concentrations of fuel substrates, ADP, ATP, inorganic phosphate, and cations including H<sup>+</sup>  
 193 can be controlled to determine mitochondrial function under a set of conditions defined as  
 194 coupling control states. We strive to incorporate an easily recognized and understood concept-  
 195 driven terminology of bioenergetics with explicit terms and symbols that define the nature of  
 196 respiratory states.

- 197 3. Mitochondrial coupling states are defined according to the control of respiratory oxygen flux by  
 198 the protonmotive force. Capacities of oxidative phosphorylation and electron transfer are  
 199 measured at kinetically saturating concentrations of fuel substrates, ADP and inorganic  
 200 phosphate, and O<sub>2</sub>, or at optimal uncoupler concentrations, respectively, in the absence of  
 201 Complex IV inhibitors such as NO, CO, or H<sub>2</sub>S. Respiratory capacity is a measure of the upper  
 202 boundary of the rate of respiration; it depends on the substrate type undergoing oxidation, and  
 203 provides reference values for the diagnosis of health and disease, and for evaluation of the  
 204 effects of Evolutionary background, Age, Gender and sex, Lifestyle and Environment.  
 205

### 206 Figure 1. Internal and external respiration

207 Mitochondrial respiration is the oxidation of fuel  
 208 substrates (electron donors) and reduction of O<sub>2</sub>  
 209 catalysed by the electron transfer system, ETS:  
 210 (mt) mitochondrial catabolic respiration; (ce)  
 211 total cellular O<sub>2</sub> consumption; and (ext) external  
 212 respiration. All chemical reactions,  $r$ , that  
 213 consume O<sub>2</sub> in the cells of an organism,  
 214 contribute to cell respiration,  $J_{\text{O}_2}$ . In addition to  
 215 mitochondrial catabolic respiration, O<sub>2</sub> is  
 216 consumed by:

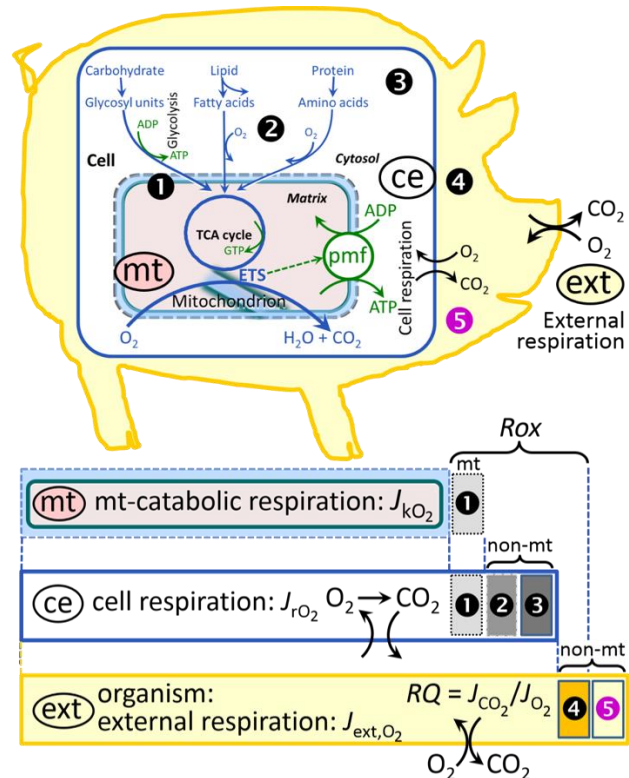
217 ❶ Mitochondrial residual oxygen consumption,  
 218  $R_{\text{ox}}$ . ❷ Non-mitochondrial O<sub>2</sub> consumption by  
 219 catabolic reactions, particularly peroxisomal  
 220 oxidases and microsomal cytochrome P450  
 221 systems. ❸ Non-mitochondrial  $R_{\text{ox}}$  by reactions  
 222 unrelated to catabolism. ❹ Extracellular  $R_{\text{ox}}$ . ❺  
 223 Aerobic microbial respiration. Bars are not at a  
 224 quantitative scale.

225 (mt) **Mitochondrial catabolic respiration**,  $J_{\text{K}_{\text{O}_2}}$ ,  
 226 is the O<sub>2</sub> consumption by the mitochondrial  
 227 ETS excluding  $R_{\text{ox}}$ .

228 (ce) **Cell respiration**,  $J_{\text{rO}_2}$ , takes into account  
 229 internal O<sub>2</sub>-consuming reactions,  $r$ , including catabolic respiration and  $R_{\text{ox}}$ . Catabolic cell respiration  
 230 is the O<sub>2</sub> consumption associated with catabolic pathways in the cell, including mitochondrial  
 231 catabolism in addition to peroxisomal and microsomal oxidation reactions (❷).

232 (ext) **External respiration** balances internal respiration at steady-state, including extracellular  $R_{\text{ox}}$  (❹)  
 233 and aerobic respiration by the microbiome (❺). O<sub>2</sub> is transported from the environment across the  
 234 respiratory cascade, *i.e.*, circulation between tissues and diffusion across cell membranes, to the  
 235 intracellular compartment. The respiratory quotient,  $RQ$ , is the molar CO<sub>2</sub>/O<sub>2</sub> exchange ratio; when  
 236 combined with the respiratory nitrogen quotient, N/O<sub>2</sub> (mol N given off per mol O<sub>2</sub> consumed), the  
 237  $RQ$  reflects the proportion of carbohydrate, lipid and protein utilized in cell respiration during  
 238 aerobically balanced steady-states. Bicarbonate and CO<sub>2</sub> are transported in reverse to the  
 239 extracellular milieu and the organismic environment. Hemoglobin provides the molecular paradigm  
 240 for the combination of O<sub>2</sub> and CO<sub>2</sub> exchange, as do lungs and gills on the morphological level.  
 241 Consult **Table 8** for a list of terms and symbols.  
 242

- 243 4. Incomplete tightness of coupling, *i.e.*, some degree of uncoupling relative to the substrate-  
 244 dependent coupling stoichiometry, is a characteristic of energy-transformations across  
 245 membranes. Uncoupling is caused by a variety of physiological, pathological, toxicological,  
 246 pharmacological and environmental conditions that exert an influence not only on the proton  
 247 leak and cation cycling, but also on proton slip within the proton pumps and the structural  
 248 integrity of the mitochondria. A more loosely coupled state is induced by stimulation of  
 249 mitochondrial superoxide formation and the bypass of proton pumps. In addition, the use of  
 250 protonophores represents an experimental uncoupling intervention to assess the transition  
 251 from a well-coupled to a noncoupled state of mitochondrial respiration.



- 252 5. Respiratory oxygen consumption rates have to be carefully normalized to enable meta-analytic  
 253 studies beyond the question of a particular experiment. Therefore, all raw data on rates and  
 254 variables for normalization should be published in an open access data repository.  
 255 Normalization of rates for: (1) the number of objects (cells, organisms); (2) the volume or  
 256 mass of the experimental sample; and (3) the concentration of mitochondrial markers in the  
 257 experimental chamber are sample-specific normalizations, which are distinguished from  
 258 system-specific normalization for the volume of the chamber (the measuring system).
- 259 6. The consistent use of terms and symbols will facilitate transdisciplinary communication and  
 260 support the further development of a collaborative database on bioenergetics and  
 261 mitochondrial physiology. The present considerations are focused on studies with  
 262 mitochondrial preparations. These will be extended in a series of reports on pathway control  
 263 of mitochondrial respiration, respiratory states in intact cells, and harmonization of  
 264 experimental procedures.  
 265

---

### 266 **Box 1: In brief – Mitochondria and Bioblasts**

267 *‘For the physiologist, mitochondria afforded the first opportunity for an experimental*  
 268 *approach to structure-function relationships, in particular those involved in active*  
 269 *transport, vectorial metabolism, and metabolic control mechanisms on a subcellular level’*  
 270 *(Ernster and Schatz 1981).*

271 Mitochondria are oxygen-consuming electrochemical generators that evolved from the endosymbiotic  
 272 alphaproteobacteria which became integrated into a host cell related to Asgard Archaea (Margulis 1970;  
 273 Lane 2005; Roger *et al.* 2017). They were described by Richard Altmann (1894) as ‘bioblasts’, which  
 274 include not only the mitochondria as presently defined, but also symbiotic and free-living bacteria. The  
 275 word ‘mitochondria’ (Greek mitos: thread; chondros: granule) was introduced by Carl Benda (1898).  
 276 Mitochondrion is singular and mitochondria is plural. Abbreviation: mt, as generally used in mtDNA.

277 Contrary to current textbook dogma, mitochondria form dynamic networks within eukaryotic  
 278 cells. Mitochondrial movement is supported by microtubules and morphology can change in response  
 279 to energy requirements of the cell via processes known as fusion and fission; these interactions allow  
 280 mitochondria to communicate within a network (Chan 2006). Mitochondria can even traverse cell  
 281 boundaries in a process known as horizontal mitochondrial transfer (Torralba *et al.* 2016). Another  
 282 defining characteristic of mitochondria is the double membrane. The mitochondrial inner membrane  
 283 (mtIM) forms dynamic tubular to disk-shaped cristae that separate the mitochondrial matrix, *i.e.*, the  
 284 negatively charged internal mitochondrial compartment, from the intermembrane space; the latter being  
 285 enclosed by the mitochondrial outer membrane (mtOM) and positively charged with respect to the  
 286 matrix.

287 The mtIM contains the non-bilayer phospholipid cardiolipin, which is not present in any other  
 288 eukaryotic cellular membrane. Cardiolipin has many regulatory functions (Oemer *et al.* 2018); in  
 289 particular, it stabilizes and promotes the formation of respiratory supercomplexes (SC I<sub>n</sub>III<sub>n</sub>IV<sub>n</sub>), which  
 290 are supramolecular assemblies based upon specific and dynamic interactions between individual  
 291 respiratory complexes (Greggio *et al.* 2017; Lenaz *et al.* 2017). The mitochondrial membrane is plastic  
 292 and exerts an influence on the functional properties of proteins incorporated in membranes  
 293 (Waczulikova *et al.* 2007). Intracellular stress factors may cause shrinking or swelling of the  
 294 mitochondrial matrix that can ultimately result in permeability transition (mtPT; Lemasters *et al.* 1998).

295 Mitochondria constitute the structural and functional elementary components of cell respiration.  
 296 Mitochondrial respiration is the reduction of molecular oxygen by electron transfer coupled to  
 297 electrochemical proton translocation across the mtIM. In the process of oxidative phosphorylation  
 298 (OXPHOS), the catabolic reaction of oxygen consumption is electrochemically coupled to the  
 299 transformation of energy in the form of adenosine triphosphate (ATP; Mitchell 1961, 2011).  
 300 Mitochondria are the powerhouses of the cell that contain the machinery of the OXPHOS-pathways,  
 301 including transmembrane respiratory complexes (proton pumps with FMN, Fe-S and cytochrome *b*, *c*,  
 302 *aa*<sub>3</sub> redox systems); alternative dehydrogenases and oxidases; the coenzyme ubiquinone (Q); F-ATPase  
 303 or ATP synthase; the enzymes of the tricarboxylic acid cycle (TCA), fatty acid and amino acid oxidation;  
 304 transporters of ions, metabolites and co-factors; iron/sulphur cluster synthesis; and mitochondrial  
 305 kinases related to catabolic pathways. The mitochondrial proteome comprises over 1,200 proteins  
 306 (Calvo *et al.* 2015; 2017), mostly encoded by nuclear DNA (nDNA), with a variety of functions, many  
 307 of which are relatively well known, *e.g.*, proteins regulating mitochondrial biogenesis or apoptosis,

308 while others are still under investigation, or need to be identified, *e.g.*, mtPT pore, alanine transporter.  
 309 The mammalian mitochondrial proteome can be used to discover and characterize the genetic basis of  
 310 mitochondrial diseases (Williams *et al.* 2016; Palmfeldt and Bross 2017).

311 Numerous cellular processes are orchestrated by a constant crosstalk between mitochondria and  
 312 other cellular components. For example, the crosstalk between mitochondria and the endoplasmic  
 313 reticulum is involved in the regulation of calcium homeostasis, cell division, autophagy, differentiation,  
 314 and anti-viral signaling (Murley and Nunnari 2016). Mitochondria contribute to the formation of  
 315 peroxisomes, which are hybrids of mitochondrial and ER-derived precursors (Sugiura *et al.* 2017).  
 316 Cellular mitochondrial homeostasis (mitostasis) is maintained through regulation at transcriptional,  
 317 post-translational and epigenetic levels, resulting in dynamic regulation of mitochondrial turnover by  
 318 biogenesis of new mitochondria and removal of damaged mitochondria by fusion, fission and mitophagy  
 319 (Singh *et al.* 2018). Cell signalling modules contribute to homeostatic regulation throughout the cell  
 320 cycle or even cell death by activating proteostatic modules, *e.g.*, the ubiquitin-proteasome and  
 321 autophagy-lysosome/vacuole pathways; specific proteases like LON, and genome stability modules in  
 322 response to varying energy demands and stress cues (Quiros *et al.* 2016). Several post-translational  
 323 modifications, including acetylation and nitrosylation, are also capable of influencing the bioenergetic  
 324 response, with clinically significant implications for health and disease (Carrico *et al.* 2018).

325 Mitochondria of higher eukaryotes typically maintain several copies of their own circular genome  
 326 known as mitochondrial DNA (mtDNA; hundred to thousands per cell; Cummins 1998), which is  
 327 maternally inherited in many species. However, biparental mitochondrial inheritance is documented in  
 328 some exceptional cases in humans (Luo *et al.* 2018), is widespread in birds, fish, reptiles and invertebrate  
 329 groups, and is even the norm in some bivalve taxonomic groups (Breton *et al.* 2007; White *et al.* 2008).  
 330 The mitochondrial genome of the angiosperm *Amborella* contains a record of six mitochondrial genome  
 331 equivalents acquired by horizontal transfer of entire genomes, two from angiosperms, three from algae  
 332 and one from mosses (Rice *et al.* 2016). In unicellular organisms, *i.e.*, protists, the structural organization  
 333 of mitochondrial genomes is highly variable and includes circular and linear DNA (Zikova *et al.* 2016).  
 334 While some of the free-living flagellates exhibit the largest known gene coding capacity, *e.g.*, jakobid  
 335 *Andalucia godoyi* mitochondrial DNA codes for 106 genes (Burger *et al.* 2013), some protist groups,  
 336 *e.g.*, alveolates, possess mitochondrial genomes with only three protein-coding genes and two rRNAs  
 337 (Feagin *et al.* 2012). The complete loss of mitochondrial genome is observed in the highly reduced  
 338 mitochondria of *Cryptosporidium* species (Liu *et al.* 2016). Reaching the final extreme, the microbial  
 339 eukaryote, oxymonad *Monocercomonoides*, has no mitochondrion whatsoever and lacks all typical  
 340 nuclear-encoded mitochondrial proteins, showing that while in 99% of organisms mitochondria play a  
 341 vital role, this organelle is not indispensable (Karnkowska *et al.* 2016).

342 In vertebrates, but not all invertebrates, mtDNA is compact (16.5 kB in humans) and encodes 13  
 343 protein subunits of the transmembrane respiratory Complexes CI, CIII, CIV and ATP synthase (F-  
 344 ATPase), 22 tRNAs, and two ribosomal RNAs. Additional gene content has been suggested to include  
 345 microRNAs, piRNA, smithRNAs, repeat associated RNA, and even additional proteins or peptides  
 346 (Duarte *et al.* 2014; Lee *et al.* 2015; Cobb *et al.* 2016). The mitochondrial genome requires nuclear-  
 347 encoded mitochondrially targeted proteins, *e.g.*, TFAM, for its maintenance and expression (Rackham  
 348 *et al.* 2012). The nuclear and the mitochondrial genomes encode peptides of the membrane spanning  
 349 redox pumps (CI, CIII and CIV) and F-ATPase, leading to strong constraints in the coevolution of both  
 350 genomes (Blier *et al.* 2001).

351 Given the multiple roles of mitochondria, it is perhaps not surprising that mitochondrial  
 352 dysfunction is associated with a wide variety of genetic and degenerative diseases. Robust mitochondrial  
 353 function is supported by physical exercise and caloric balance, and is central for sustained metabolic  
 354 health throughout life. Therefore, a more consistent set of definitions for mitochondrial physiology will  
 355 increase our understanding of the etiology of disease and improve the diagnostic repertoire of  
 356 mitochondrial medicine with a focus on protective medicine, lifestyle and healthy aging.  
 357

358  
 359

---

## 360 1. Introduction

361  
 362  
 363

Mitochondria are the powerhouses of the cell with numerous physiological, molecular, and genetic functions (**Box 1**). Every study of mitochondrial health and disease faces **Evolution, Age,**

364 **Gender and sex, Lifestyle, and Environment (MitoEAGLE)** as essential background conditions intrinsic  
 365 to the individual person or cohort, species, tissue and to some extent even cell line. As a large and  
 366 coordinated group of laboratories and researchers, the mission of the global MitoEAGLE Network is to  
 367 generate the necessary scale, type, and quality of consistent data sets and conditions to address this  
 368 intrinsic complexity. Harmonization of experimental protocols and implementation of a quality control  
 369 and data management system are required to interrelate results gathered across a spectrum of studies  
 370 and to generate a rigorously monitored database focused on mitochondrial respiratory function. In this  
 371 way, researchers from a variety of disciplines can compare their findings using clearly defined and  
 372 accepted international standards.

373 With an emphasis on quality of research, published data can be useful far beyond the specific  
 374 question of a particular experiment. For example, collaborative data sets support the development of  
 375 open-access databases such as those for National Institutes of Health sponsored research in genetics,  
 376 proteomics, and metabolomics. Indeed, enabling meta-analysis is the most economic way of providing  
 377 robust answers to biological questions (Cooper *et al.* 2009). However, the reproducibility of quantitative  
 378 results and databases depend on accurate measurements under strictly-defined conditions. Likewise,  
 379 meaningful interpretation and comparability of experimental outcomes requires standardisation of  
 380 protocols between research groups at different institutes. In addition to quality control, a conceptual  
 381 framework is also required to standardise and harmonise terminology and methodology. Vague or  
 382 ambiguous jargon can lead to confusion and may convert valuable signals to wasteful noise. For this  
 383 reason, measured values must be expressed in standard units for each parameter used to define  
 384 mitochondrial respiratory function. A consensus on fundamental nomenclature and conceptual  
 385 coherence, however, are missing in the expanding field of mitochondrial physiology. To fill this gap,  
 386 the present communication provides an in-depth review on harmonization of nomenclature and  
 387 definition of technical terms, which are essential to improve the awareness of the intricate meaning of  
 388 current and past scientific vocabulary. This is important for documentation and integration into  
 389 databases in general, and quantitative modelling in particular (Beard 2005).

390 In this review, we focus on coupling states and fluxes through metabolic pathways of aerobic  
 391 energy transformation in mitochondrial preparations as a first step in the attempt to generate a  
 392 conceptually-oriented nomenclature in bioenergetics and mitochondrial physiology. Respiratory control  
 393 by fuel substrates and specific inhibitors of respiratory enzymes, coupling states of intact cells, and  
 394 respiratory flux control ratios will be reviewed in subsequent communications, prepared in the frame of  
 395 the EU COST Action MitoEAGLE open to global bottom-up input.

396  
397

## 398 **2. Coupling states and rates in mitochondrial preparations**

399 *‘Every professional group develops its own technical jargon for talking about matters of critical*  
 400 *concern ... People who know a word can share that idea with other members of their group, and*  
 401 *a shared vocabulary is part of the glue that holds people together and allows them to create a*  
 402 *shared culture’* (Miller 1991).

403  
404  
405

### 404 *2.1. Cellular and mitochondrial respiration*

406 **2.1.1. Aerobic and anaerobic catabolism and ATP turnover:** In respiration, electron transfer  
 407 is coupled to the phosphorylation of ADP to ATP, with energy transformation mediated by the  
 408 protonmotive force, pmf (**Figure 2**). Anabolic reactions are coupled to catabolism, both by ATP as the  
 409 intermediary energy currency and by small organic precursor molecules as building blocks for  
 410 biosynthesis. Glycolysis involves substrate-level phosphorylation of ADP to ATP in fermentation  
 411 without utilization of O<sub>2</sub>, studied mainly in intact cells and organisms. Many cellular fuel substrates are  
 412 catabolized to acetyl-CoA or to glutamate, and further electron transfer reduces nicotinamide adenine  
 413 dinucleotide to NADH or flavin adenine dinucleotide to FADH<sub>2</sub>. Subsequent mitochondrial electron  
 414 transfer to O<sub>2</sub> is coupled to proton translocation for the control of the protonmotive force and  
 415 phosphorylation of ADP (**Figure 2B and 2C**). In contrast, extra-mitochondrial oxidation of fatty acids  
 416 and amino acids proceeds partially in peroxisomes without coupling to ATP production: acyl-CoA  
 417 oxidase catalyzes the oxidation of FADH<sub>2</sub> with electron transfer to O<sub>2</sub>; amino acid oxidases oxidize  
 418 flavin mononucleotide FMNH<sub>2</sub> or FADH<sub>2</sub> (**Figure 2A**).

419



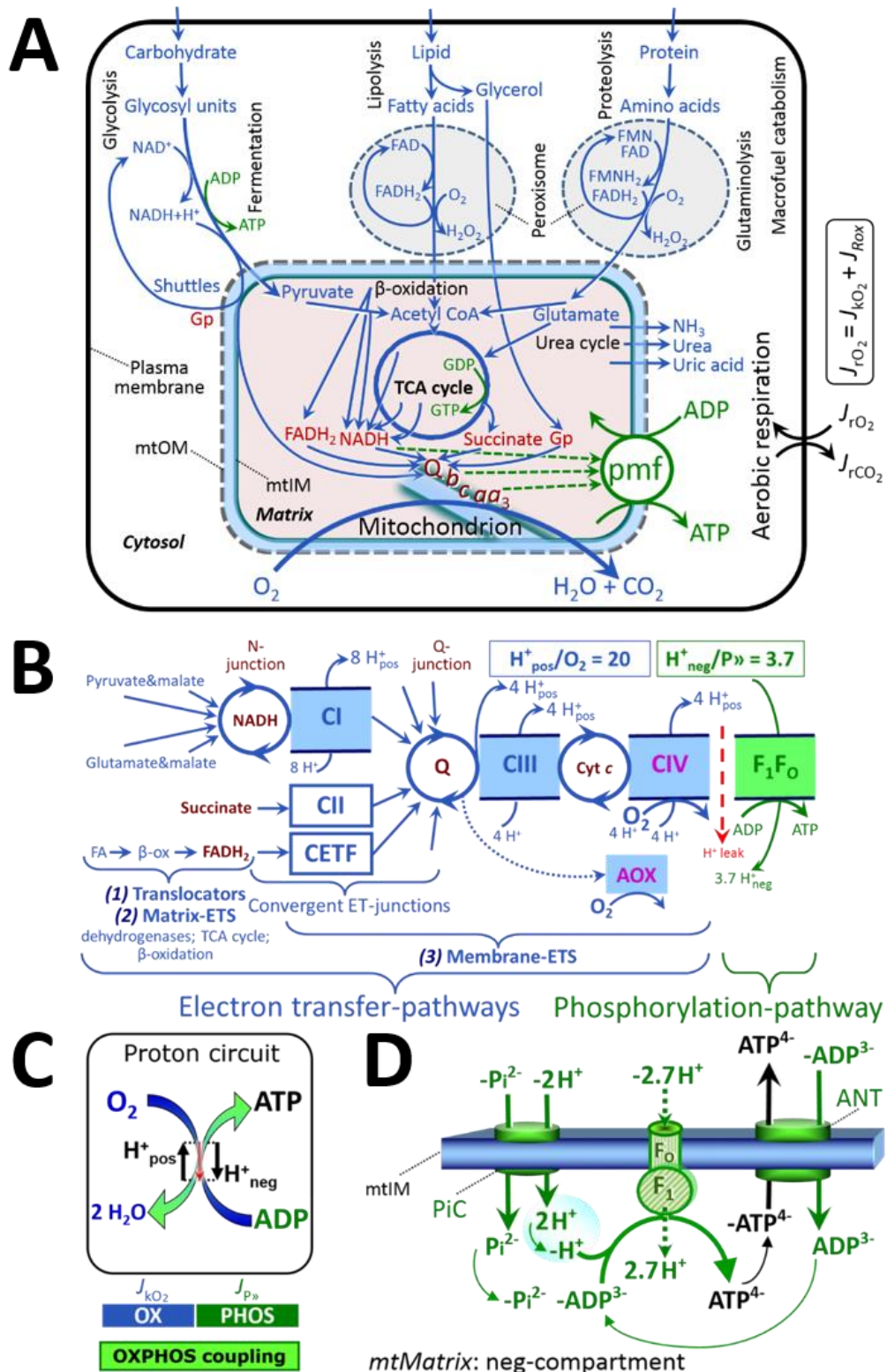


### Figure 2. Cell respiration and oxidative phosphorylation (OXPHOS)

Mitochondrial respiration is the oxidation of fuel substrates (electron donors) with electron transfer to  $O_2$  as the electron acceptor. For explanation of symbols see also **Figure 1**.

(A) Respiration of intact cells: Extra-mitochondrial catabolism of macromolecules and uptake of small molecules by the cell provide the mitochondrial fuel substrates. Dashed arrows indicate the connection between the redox proton pumps (respiratory Complexes CI, CIII and CIV) and the transmembrane protonmotive force, pmf. Coenzyme Q (Q) and the cytochromes *b*, *c*, and *aa<sub>3</sub>* are redox systems of the mitochondrial inner membrane, mtIM. Glycerol-3-phosphate, Gp.

420  
421  
422  
423  
424  
425  
426  
427  
428  
429

430 (B) Respiration in mitochondrial preparations: The mitochondrial electron transfer system  
 431 (ETS) is (1) fuelled by diffusion and transport of substrates across the mtOM and mtIM,  
 432 and in addition consists of the (2) matrix-ETS, and (3) membrane-ETS. Electron transfer  
 433 converges at the N-junction, and from CI, CII and electron transferring flavoprotein  
 434 complex (CETF) at the Q-junction. Unlabeled arrows converging at the Q-junction indicate  
 435 additional ETS-sections with electron entry into Q through glycerophosphate  
 436 dehydrogenase, dihydroorotate dehydrogenase, proline dehydrogenase, choline  
 437 dehydrogenase, and sulfide-ubiquinone oxidoreductase. The dotted arrow indicates the  
 438 branched pathway of oxygen consumption by alternative quinol oxidase (AOX). ET-  
 439 pathways are coupled to the phosphorylation-pathway. The  $H^+_{\text{pos}}/O_2$  ratio is the outward  
 440 proton flux from the matrix space to the positively (pos) charged vesicular compartment,  
 441 divided by catabolic  $O_2$  flux in the NADH-pathway. The  $H^+_{\text{neg}}/P_{\gg}$  ratio is the inward proton  
 442 flux from the inter-membrane space to the negatively (neg) charged matrix space, divided  
 443 by the flux of phosphorylation of ADP to ATP. These stoichiometries are not fixed because  
 444 of ion leaks and proton slip. Modified from Lemieux *et al.* (2017) and Rich (2013).  
 445 (C) OXPHOS coupling:  $O_2$  flux through the catabolic ET-pathway,  $J_{kO_2}$ , is coupled  
 446 by the  $H^+$  circuit to flux through the phosphorylation-pathway of ADP to ATP,  $J_{P_{\gg}}$ .  
 447 (D) Phosphorylation-pathway catalyzed by the proton pump  $F_1F_0$ -ATPase (F-ATPase,  
 448 ATP synthase), adenine nucleotide translocase (ANT), and inorganic phosphate carrier  
 449 (PiC). The  $H^+_{\text{neg}}/P_{\gg}$  stoichiometry is the sum of the coupling stoichiometry in the F-ATPase  
 450 reaction ( $-2.7 H^+_{\text{pos}}$  from the positive intermembrane space,  $2.7 H^+_{\text{neg}}$  to the matrix, *i.e.*, the  
 451 negative compartment) and the proton balance in the translocation of  $ADP^{3-}$ ,  $ATP^{4-}$  and  $P_i^{2-}$   
 452 (negative for substrates). Modified from Gnaiger (2014).  
 453

454 The plasma membrane separates the intracellular compartment including the cytosol, nucleus, and  
 455 organelles from the extracellular environment. The plasma membrane consists of a lipid bilayer with  
 456 embedded proteins and attached organic molecules that collectively control the selective permeability  
 457 of ions, organic molecules, and particles across the cell boundary. The intact plasma membrane prevents  
 458 the passage of many water-soluble mitochondrial substrates and inorganic ions—such as succinate,  
 459 adenosine diphosphate (ADP) and inorganic phosphate ( $P_i$ ) that must be precisely controlled at  
 460 kinetically-saturating concentrations for the analysis of mitochondrial respiratory capacities.  
 461 Respiratory capacities delineate, comparable to channel capacity in information theory (Schneider  
 462 2006), the upper boundary of the rate of  $O_2$  consumption measured in defined respiratory states. Despite  
 463 the activity of solute carriers, *e.g.*, the sodium-dependent dicarboxylate transporter SLC13A3 and the  
 464 sodium-dependent phosphate transporter SLC20A2, which transport specific metabolites across the  
 465 plasma membrane of various cell types, the intact plasma membrane limits the scope of investigations  
 466 into mitochondrial respiratory function in intact cells.

467 **2.1.2. Specification of biochemical dose:** Substrates, uncouplers, inhibitors, and other chemical  
 468 reagents are titrated to analyse cellular and mitochondrial function. Nominal concentrations of these  
 469 substances are usually reported as initial amount of substance concentration [ $\text{mol}\cdot\text{L}^{-1}$ ] in the incubation  
 470 medium. When aiming at the measurement of kinetically saturated processes—such as OXPHOS-  
 471 capacities—the concentrations for substrates can be chosen according to the apparent equilibrium  
 472 constant,  $K_m'$ . In the case of hyperbolic kinetics, only 80% of maximum respiratory capacity is obtained  
 473 at a substrate concentration of four times the  $K_m'$ , whereas substrate concentrations of 5, 9, 19 and 49  
 474 times the  $K_m'$  are theoretically required for reaching 83%, 90%, 95% or 98% of the maximal rate  
 475 (Gnaiger 2001). Other reagents are chosen to inhibit or alter a particular process. The amount of these  
 476 chemicals in an experimental incubation is selected to maximize effect, avoiding unacceptable off-target  
 477 consequences that would adversely affect the data being sought. Specifying the amount of substance in  
 478 an incubation as nominal concentration in the aqueous incubation medium can be ambiguous (Doskey  
 479 *et al.* 2015), particularly for cations (TPP<sup>+</sup>; fluorescent dyes such as safranin, TMRM; Chowdhury *et al.*  
 480 2015) and lipophilic substances (oligomycin, uncouplers, permeabilization agents; Doerrier *et al.* 2018),  
 481 which accumulate in the mitochondrial matrix or in biological membranes, respectively. Generally,  
 482 dose/exposure can be specified per unit of biological sample, *i.e.*, (nominal moles of  
 483 xenobiotic)/(number of cells) [ $\text{mol}\cdot\text{cell}^{-1}$ ] or, as appropriate, per mass of biological sample [ $\text{mol}\cdot\text{kg}^{-1}$ ].  
 484 This approach to specification of dose/exposure provides a scalable parameter that can be used to design

485 experiments, help interpret a wide variety of experimental results, and provide absolute information that  
486 allows researchers worldwide to make the most use of published data (Doskey *et al.* 2015).

487

## 488 2.2. Mitochondrial preparations

489

490 Mitochondrial preparations are defined as either isolated mitochondria or tissue and cellular  
491 preparations in which the barrier function of the plasma membrane is disrupted. Since this entails the  
492 loss of cell viability, mitochondrial preparations are not studied *in vivo*. In contrast to isolated  
493 mitochondria and tissue homogenate preparations, mitochondria in permeabilized tissues and cells are  
494 *in situ* relative to the plasma membrane. When studying mitochondrial preparations, substrate-  
495 uncoupler-inhibitor-titration (SUIT) protocols are used to establish respiratory coupling control states  
496 (CCS) and pathway control states (PCS) that provide reference values for various output variables  
497 (**Table 1**). Physiological conditions *in vivo* deviate from these experimentally obtained states; this is  
498 because kinetically-saturating concentrations, *e.g.*, of ADP, oxygen (O<sub>2</sub>; dioxygen) or fuel substrates,  
499 may not apply to physiological intracellular conditions. Further information is obtained in studies of  
500 kinetic responses to variations in fuel substrate concentrations, [ADP], or [O<sub>2</sub>] in the range between  
501 kinetically-saturating concentrations and anoxia (Gnaiger 2001).

502 The cholesterol content of the plasma membrane is high compared to mitochondrial membranes  
503 (Korn 1969). Therefore, mild detergents—such as digitonin and saponin—can be applied to selectively  
504 permeabilize the plasma membrane via interaction with cholesterol; this allows free exchange of organic  
505 molecules and inorganic ions between the cytosol and the immediate cell environment, while  
506 maintaining the integrity and localization of organelles, cytoskeleton, and the nucleus. Application of  
507 permeabilization agents (mild detergents or toxins) leads to washout of cytosolic marker enzymes—  
508 such as lactate dehydrogenase—and results in the complete loss of cell viability (tested by nuclear  
509 staining using plasma membrane-impermeable dyes), while mitochondrial function remains intact  
510 (tested by cytochrome *c* stimulation of respiration). Digitonin concentrations have to be optimized  
511 according to cell type, particularly since mitochondria from cancer cells contain significantly higher  
512 contents of cholesterol in both membranes (Baggetto and Testa-Perussini, 1990). For example, a dose  
513 of digitonin of 8 fmol·cell<sup>-1</sup> (10 pg·cell<sup>-1</sup>; 10 μg·10<sup>-6</sup> cells) is optimal for permeabilization of endothelial  
514 cells, and the concentration in the incubation medium has to be adjusted according to the cell density  
515 (Doerrier *et al.* 2018). Respiration of isolated mitochondria remains unaltered after the addition of low  
516 concentrations of digitonin or saponin. In addition to mechanical cell disruption during homogenization  
517 of tissue, permeabilization agents may be applied to ensure permeabilization of all cells in tissue  
518 homogenates.

519 Suspensions of cells permeabilized in the respiration chamber and crude tissue homogenates  
520 contain all components of the cell at highly dilute concentrations. All mitochondria are retained in  
521 chemically-permeabilized mitochondrial preparations and crude tissue homogenates. In the preparation  
522 of isolated mitochondria, however, the mitochondria are separated from other cell fractions and purified  
523 by differential centrifugation, entailing the loss of mitochondria at typical recoveries ranging from 30%  
524 to 80% of total mitochondrial content (Lai *et al.* 2018). Using Percoll or sucrose density gradients to  
525 maximize the purity of isolated mitochondria may compromise the mitochondrial yield or structural and  
526 functional integrity. Therefore, mitochondrial isolation protocols need to be optimized according to each  
527 study. The term, *mitochondrial preparation*, neither includes intact cells, nor submitochondrial particles  
528 and further fractionation of mitochondrial components.

529

## 530 2.3. Electron transfer pathways

531

532 Mitochondrial electron transfer (ET) pathways are fuelled by diffusion and transport of substrates  
533 across the mtOM and mtIM. In addition, the mitochondrial electron transfer system (ETS) consists of  
534 the matrix-ETS and membrane-ETS (**Figure 2B**). Upstream sections of ET-pathways converge at the  
535 NADH-junction (N-junction). NADH is mainly generated in the tricarboxylic acid (TCA) cycle and is  
536 oxidized by Complex I (CI), with further electron entry into the coenzyme Q-junction (Q-junction).  
537 Similarly, succinate is formed in the TCA cycle and oxidized by CII to fumarate. CII is part of both the  
538 TCA cycle and the ETS, and reduces FAD to FADH<sub>2</sub> with further reduction of ubiquinone to ubiquinol  
539 downstream of the TCA cycle in the Q-junction. Thus FADH<sub>2</sub> is not a substrate but is the product of  
540 CII, in contrast to erroneous metabolic maps shown in many publications. β-oxidation of fatty acids

541 (FA) supplies reducing equivalents via (1) FADH<sub>2</sub> as the substrate of electron transferring flavoprotein  
 542 complex (CETF); (2) acetyl-CoA generated by chain shortening; and (3) NADH generated via 3-  
 543 hydroxyacyl-CoA dehydrogenases. The ATP yield depends on whether acetyl-CoA enters the TCA  
 544 cycle, or is for example used in ketogenesis.

545 Selected mitochondrial catabolic pathways, *k*, of electron transfer from the oxidation of fuel  
 546 substrates to the reduction of O<sub>2</sub> are activated by addition of fuel substrates to the mitochondrial  
 547 respiration medium after depletion of endogenous substrates (**Figure 2B**). Substrate combinations and  
 548 specific inhibitors of ET-pathway enzymes are used to obtain defined pathway control states in  
 549 mitochondrial preparations (Gnaiger 2014).

550

## 551 2.4. Respiratory coupling control

552

553 **2.4.1. Coupling:** In mitochondrial electron transfer, vectorial transmembrane proton flux is  
 554 coupled through the redox proton pumps CI, CIII and CIV to the catabolic flux of scalar reactions,  
 555 collectively measured as O<sub>2</sub> flux,  $J_{kO_2}$  (**Figure 2**). Thus mitochondria are elementary components of  
 556 energy transformation. Energy is a conserved quantity and cannot be lost or produced in any internal  
 557 process (First Law of Thermodynamics). Open and closed systems can gain or lose energy only by  
 558 external fluxes—by exchange with the environment. Therefore, energy can neither be produced by  
 559 mitochondria, nor is there any internal process without energy conservation. Exergy or Gibbs energy  
 560 (‘free energy’) is the part of energy that can potentially be transformed into work under conditions of  
 561 constant temperature and pressure. *Coupling* is the interaction of an exergonic process (spontaneous,  
 562 negative exergy change) with an endergonic process (positive exergy change) in energy transformations  
 563 which conserve part of the exergy that would be irreversibly lost or dissipated in an uncoupled process.

564 Pathway control states (PCS) and coupling control states (CCS) are complementary, since  
 565 mitochondrial preparations depend on (1) an exogenous supply of pathway-specific fuel substrates and  
 566 oxygen, and (2) exogenous control of phosphorylation (**Figure 2**).

567 **2.4.2. Phosphorylation, P<sub>»</sub>, and P<sub>»</sub>/O<sub>2</sub> ratio:** Phosphorylation in the context of OXPHOS is  
 568 defined as phosphorylation of ADP by P<sub>i</sub> to form ATP. On the other hand, the term phosphorylation is  
 569 used generally in many contexts, *e.g.*, protein phosphorylation. This justifies consideration of a symbol  
 570 more discriminating and specific than P as used in the P/O ratio (phosphate to atomic oxygen ratio),  
 571 where P indicates phosphorylation of ADP to ATP or GDP to GTP (**Figure 2**). We propose the symbol  
 572 P<sub>»</sub> for the endergonic (uphill) direction of phosphorylation ADP→ATP, and likewise the symbol P<sub>«</sub> for  
 573 the corresponding exergonic (downhill) hydrolysis ATP→ADP. P<sub>»</sub> refers mainly to electrontransfer  
 574 phosphorylation but may also involve substrate-level phosphorylation as part of the TCA cycle  
 575 (succinyl-CoA ligase, phosphoglycerate kinase) and phosphorylation of ADP catalyzed by pyruvate  
 576 kinase, and of GDP phosphorylated by phosphoenolpyruvate carboxykinase. Transphosphorylation is  
 577 performed by adenylate kinase, creatine kinase (mtCK), hexokinase and nucleoside diphosphate kinase.  
 578 In isolated mammalian mitochondria, ATP production catalyzed by adenylate kinase (2 ADP ↔ ATP +  
 579 AMP) proceeds without fuel substrates in the presence of ADP (Kömldi and Tretter 2017). Kinase  
 580 cycles are involved in intracellular energy transfer and signal transduction for regulation of energy flux.

581 The P<sub>»</sub>/O<sub>2</sub> ratio (P<sub>»</sub>/4 e<sup>-</sup>) is two times the ‘P/O’ ratio (P<sub>»</sub>/2 e<sup>-</sup>). P<sub>»</sub>/O<sub>2</sub> is a generalized symbol, not  
 582 specific for reporting P<sub>i</sub> consumption (P<sub>i</sub>/O<sub>2</sub> flux ratio), ADP depletion (ADP/O<sub>2</sub> flux ratio), or ATP  
 583 production (ATP/O<sub>2</sub> flux ratio). The mechanistic P<sub>»</sub>/O<sub>2</sub> ratio—or P<sub>»</sub>/O<sub>2</sub> stoichiometry—is calculated  
 584 from the proton-to-O<sub>2</sub> and proton-to-phosphorylation coupling stoichiometries (**Figure 2B**):

$$586 \quad P_{\gg}/O_2 = \frac{H_{p_{\text{pos}}/O_2}^+}{H_{n_{\text{neg}}/P_{\gg}}^+} \quad (1)$$

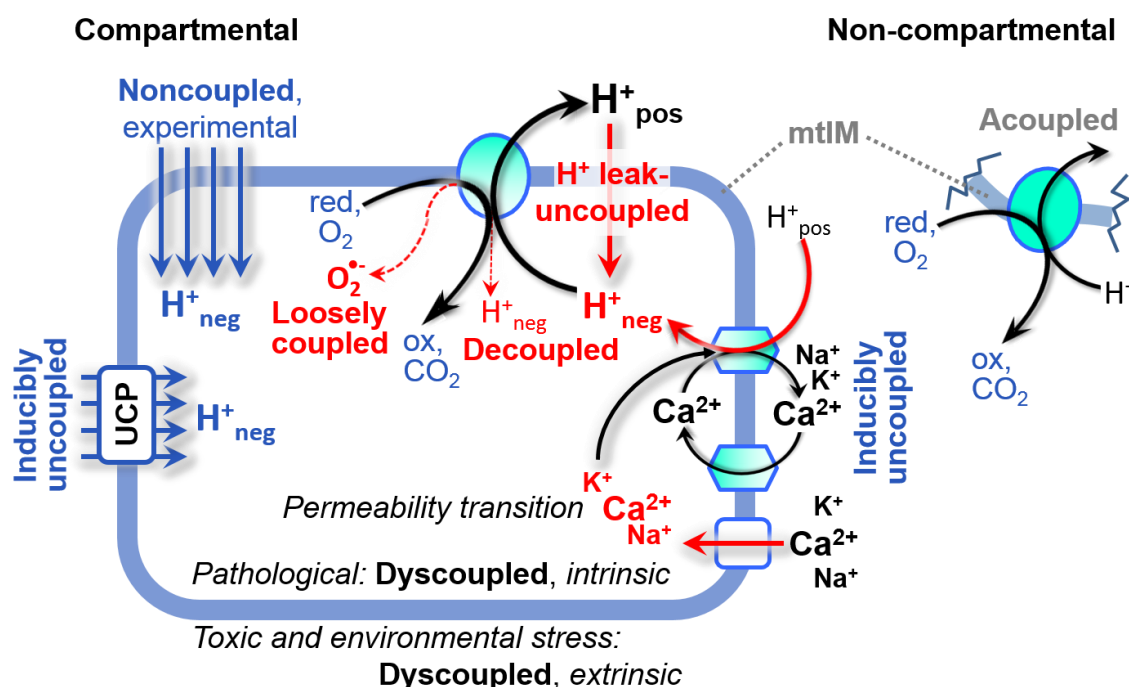
588 The H<sub>p<sub>pos</sub>/O<sub>2</sub></sub><sup>+</sup> coupling stoichiometry (referring to the full four electron reduction of O<sub>2</sub>) depends on the  
 589 relative involvement of the three coupling sites (respiratory Complexes CI, CIII and CIV) in the  
 590 catabolic ET-pathway from reduced fuel substrates (electron donors) to the reduction of O<sub>2</sub> (electron  
 591 acceptor). This varies with: (1) a bypass of CI by single or multiple electron input into the Q-junction;  
 592 and (2) a bypass of CIV by involvement of alternative oxidases, AOX. AOX are expressed in all plants,  
 593 some fungi, many protists, and several animal phyla, but are not expressed in vertebrate mitochondria  
 594 (McDonald *et al.* 2009).

595 The H<sub>p<sub>pos</sub>/O<sub>2</sub></sub><sup>+</sup> coupling stoichiometry equals 12 in the ET-pathways involving CIII and CIV as  
 596 proton pumps, increasing to 20 for the NADH-pathway through CI (**Figure 2B**), but a general consensus  
 597 on H<sub>p<sub>pos</sub>/O<sub>2</sub></sub><sup>+</sup> stoichiometries remains to be reached (Hinkle 2005; Wikström and Hummer 2012; Sazanov

598 2015). The  $H^+_{neg}/P_{\gg}$  coupling stoichiometry (3.7; **Figure 2B**) is the sum of 2.7  $H^+_{neg}$  required by the F-  
 599 ATPase of vertebrate and most invertebrate species (Watt *et al.* 2010) and the proton balance in the  
 600 translocation of ADP, ATP and  $P_i$  (**Figure 2C**). Taken together, the mechanistic  $P_{\gg}/O_2$  ratio is calculated  
 601 at 5.4 and 3.3 for NADH- and succinate-linked respiration, respectively (Eq. 1). The corresponding  
 602 classical  $P_{\gg}/O$  ratios (referring to the 2 electron reduction of  $0.5 O_2$ ) are 2.7 and 1.6 (Watt *et al.* 2010),  
 603 in agreement with the measured  $P_{\gg}/O$  ratio for succinate of  $1.58 \pm 0.02$  (Gnaiger *et al.* 2000).

604 **2.4.3. Uncoupling:** The effective  $P_{\gg}/O_2$  flux ratio ( $Y_{P_{\gg}/O_2} = J_{P_{\gg}}/J_{K_{O_2}}$ ) is diminished relative to the  
 605 mechanistic  $P_{\gg}/O_2$  ratio by intrinsic and extrinsic uncoupling or dyscoupling (**Figure 3**). Such  
 606 generalized uncoupling is different from switching to mitochondrial pathways that involve fewer than  
 607 three proton pumps ('coupling sites': Complexes CI, CIII and CIV), bypassing CI through multiple  
 608 electron entries into the Q-junction, or CIII and CIV through AOX (**Figure 2B**). Reprogramming of  
 609 mitochondrial pathways leading to different types of substrates being oxidized may be considered as a  
 610 switch of gears (changing the stoichiometry by altering the substrate that is oxidized) rather than  
 611 uncoupling (loosening the tightness of coupling relative to a fixed stoichiometry). In addition,  $Y_{P_{\gg}/O_2}$   
 612 depends on several experimental conditions of flux control, increasing as a hyperbolic function of [ADP]  
 613 to a maximum value (Gnaiger 2001).

614



615

616

### 617 **Figure 3. Mechanisms of respiratory uncoupling**

618 An intact mitochondrial inner membrane, mtIM, is required for vectorial, compartmental coupling.  
 619 'Acoupled' respiration is the consequence of structural disruption with catalytic activity of non-  
 620 compartmental mitochondrial fragments. Inducible uncoupling, *e.g.*, by activation of UCP1, increases  
 621 LEAK-respiration; experimentally noncoupled respiration provides an estimate of ET-capacity obtained  
 622 by titration of protonophores stimulating respiration to maximum  $O_2$  flux.  $H^+$  leak-uncoupled,  
 623 decoupled, and loosely coupled respiration are components of intrinsic uncoupling (**Table 2**).  
 624 Pathological dysfunction may affect all types of uncoupling, including permeability transition (mtPT),  
 625 causing intrinsically dyscoupled respiration. Similarly, toxicological and environmental stress factors  
 626 can cause extrinsically dyscoupled respiration. Reduced fuel substrates, red; oxidized products, ox.

627 Uncoupling of mitochondrial respiration is a general term comprising diverse mechanisms:

- 628 1. Proton leak across the mtIM from the positive to the negative compartment ( $H^+$  leak-uncoupled;  
 629 **Figure 3**).
- 630 2. Cycling of other cations, strongly stimulated by mtPT; comparable to the use of protonophores,  
 631 cation cycling is experimentally induced by valinomycin in the presence of  $K^+$ ;
- 632 3. Decoupling by proton slip in the redox proton pumps when protons are effectively not pumped  
 633 (CI, CIII and CIV) or are not driving phosphorylation (F-ATPase);

- 634 4. Loss of vesicular (compartmental) integrity when electron transfer is acoupled;  
 635 5. Electron leak in the loosely coupled univalent reduction of O<sub>2</sub> to superoxide (O<sub>2</sub><sup>•-</sup>; superoxide  
 636 anion radical).

637 Differences of terms—uncoupled *vs.* noncoupled—are easily overlooked, although they relate to  
 638 different meanings of uncoupling (**Figure 3** and **Table 2**).

639

## 640 2.5. Coupling states and respiratory rates

641

642 To extend the classical nomenclature on mitochondrial coupling states (Section 2.6) by a concept-  
 643 driven terminology that explicitly incorporates information on the meaning of respiratory states, the  
 644 terminology must be general and not restricted to any particular experimental protocol or mitochondrial  
 645 preparation (Gnaiger 2009). Concept-driven nomenclature aims at mapping the meaning and concept  
 646 behind the words and acronyms onto the forms of words and acronyms (Miller 1991). The focus of  
 647 concept-driven nomenclature is primarily the conceptual *why*, along with clarification of the  
 648 experimental *how*.

649

650 **Table 1. Coupling states and residual oxygen consumption in mitochondrial**  
 651 **preparations in relation to respiration- and phosphorylation-flux,  $J_{\text{KO}_2}$  and  $J_{\text{P}}$ , and**  
 652 **protonmotive force, pmf. Coupling states are established at kinetically-saturating**  
 653 **concentrations of fuel substrates and O<sub>2</sub>.**

State	$J_{\text{KO}_2}$	$J_{\text{P}}$	pmf	Inducing factors	Limiting factors
LEAK	<i>L</i> ; low, cation leak-dependent respiration	0	max.	back-flux of cations including proton leak, proton slip	$J_{\text{P}} = 0$ : (1) without ADP, $L_{\text{N}}$ ; (2) max. ATP/ADP ratio, $L_{\text{T}}$ ; or (3) inhibition of the phosphorylation-pathway, $L_{\text{Omy}}$
OXPHOS	<i>P</i> ; high, ADP-stimulated respiration, OXPHOS-capacity	max.	high	kinetically-saturating [ADP] and [P <sub>i</sub> ]	$J_{\text{P}}$ by phosphorylation-pathway capacity; or $J_{\text{KO}_2}$ by ET-capacity
ET	<i>E</i> ; max., noncoupled respiration, ET-capacity	0	low	optimal external uncoupler concentration for max. $J_{\text{O}_2, \text{E}}$	$J_{\text{KO}_2}$ by ET-capacity
ROX	<i>Rox</i> ; min., residual O <sub>2</sub> consumption	0	0	$J_{\text{O}_2, \text{Rox}}$ in non-ET-pathway oxidation reactions	inhibition of all ET-pathways; or absence of fuel substrates

654

655 To provide a diagnostic reference for respiratory capacities of core energy metabolism, the  
 656 capacity of oxidative phosphorylation, OXPHOS, is measured at kinetically-saturating concentrations  
 657 of ADP and P<sub>i</sub>. The oxidative ET-capacity reveals the limitation of OXPHOS-capacity mediated by the  
 658 phosphorylation-pathway. The ET- and phosphorylation-pathways comprise coupled segments of the  
 659 OXPHOS-system. By application of external uncouplers, ET-capacity is measured as noncoupled  
 660 respiration. The contribution of intrinsically uncoupled O<sub>2</sub> consumption is studied by preventing the  
 661 stimulation of phosphorylation either in the absence of ADP or by inhibition of the phosphorylation-  
 662 pathway. The corresponding states are collectively classified as LEAK-states when O<sub>2</sub> consumption  
 663 compensates mainly for ion leaks, including the proton leak. Defined coupling states are induced by: (1)  
 664 adding cation chelators such as EGTA, binding free Ca<sup>2+</sup> and thus limiting cation cycling; (2) adding  
 665 ADP and P<sub>i</sub>; (3) inhibiting the phosphorylation-pathway; and (4) uncoupler titrations, while maintaining  
 666 a defined ET-pathway state with constant fuel substrates and inhibitors of specific branches of the ET-  
 667 pathway.

668 The three coupling states, ET, LEAK and OXPHOS, are shown schematically with the  
 669 corresponding respiratory rates, abbreviated as *E*, *L* and *P*, respectively (**Figure 4**). We distinguish

670 metabolic *pathways* from metabolic *states* and the corresponding metabolic *rates*; for example: ET-  
 671 pathways, ET-states, and ET-capacities,  $E$ , respectively (**Table 1**). The protonmotive force is *high* in  
 672 the OXPHOS-state when it drives phosphorylation, *maximum* in the LEAK-state of coupled  
 673 mitochondria, driven by LEAK-respiration at a minimum back-flux of cations to the matrix side, and  
 674 *very low* in the ET-state when uncouplers short-circuit the proton cycle (**Table 1**).

675

676 **Figure 4. Four-compartment**  
 677 **model of oxidative**  
 678 **phosphorylation**

679 Respiratory states (ET, OXPHOS,  
 680 LEAK; **Table 1**) and corresponding  
 681 rates ( $E$ ,  $P$ ,  $L$ ) are connected by the  
 682 protonmotive force, pmf. (1) ET-  
 683 capacity,  $E$ , is partitioned into (2)  
 684 dissipative LEAK-respiration,  $L$ ,  
 685 when the Gibbs energy change of  
 686 catabolic  $O_2$  flux is irreversibly lost,  
 687 (3) net OXPHOS-capacity,  $P-L$ , with  
 688 partial conservation of the capacity to perform work, and (4) the excess capacity,  $E-P$ . Modified from  
 689 Gnaiger (2014).

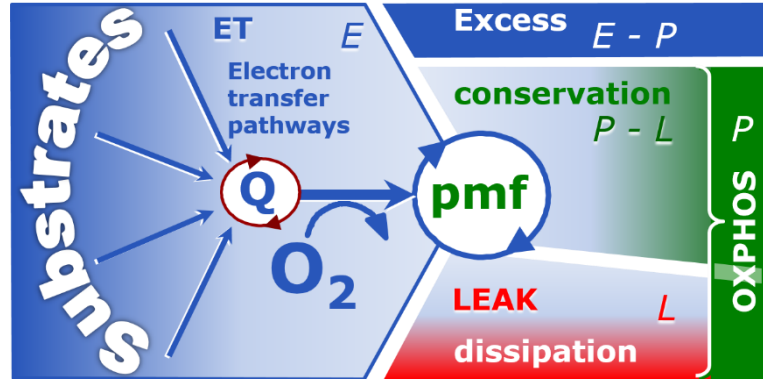
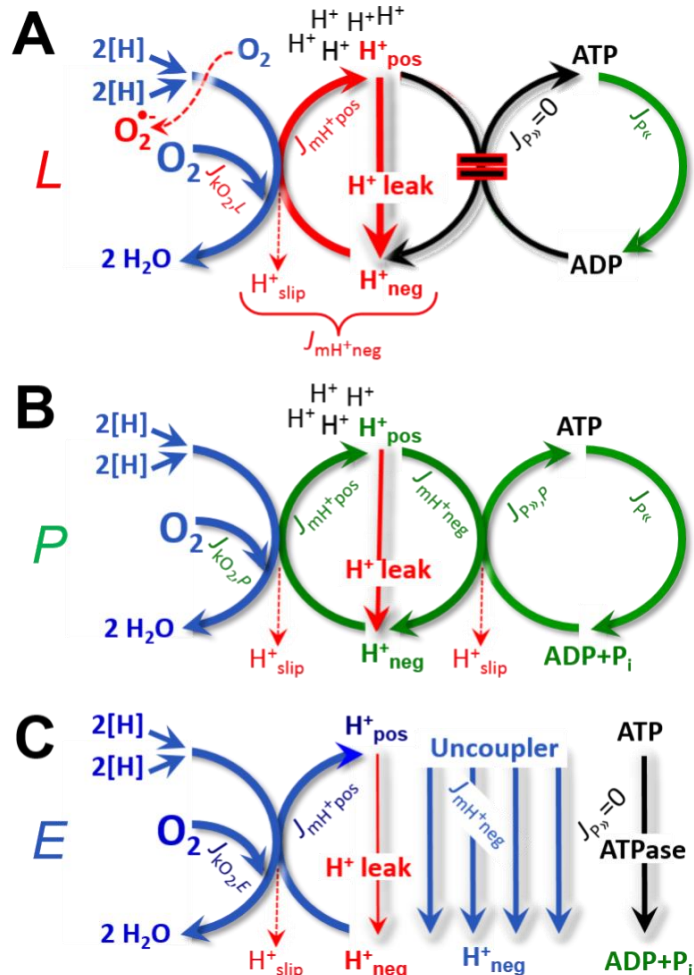


**Figure 5. Respiratory coupling states**

(A) **LEAK-state and rate,  $L$** : Oxidation only, since phosphorylation is arrested,  $J_{P\gg} = 0$ , and catabolic  $O_2$  flux,  $J_{kO_2,L}$ , is controlled mainly by the proton leak and slip,  $J_{mH^+neg}$ , at maximum protonmotive force (**Figure 4**). Extramitochondrial ATP may be hydrolyzed by extramitochondrial ATPases,  $J_{P\ll}$ ; then phosphorylation must be blocked.

(B) **OXPHOS-state and rate,  $P$** : Oxidation coupled to phosphorylation,  $J_{P\gg}$ , which is stimulated by kinetically-saturating [ADP] and  $[P_i]$ , supported by a high protonmotive force.  $O_2$  flux,  $J_{kO_2,P}$ , is well-coupled at a  $P\gg/O_2$  flux ratio of  $J_{P\gg,P} \cdot J_{O_2,P}^{-1}$ . Extramitochondrial ATPases may recycle ATP,  $J_{P\ll}$ .

(C) **ET-state and rate,  $E$** : Oxidation only, since phosphorylation is zero,  $J_{P\gg} = 0$ , at optimum exogenous uncoupler concentration when noncoupled respiration,  $J_{kO_2,E}$ , is maximum. The F-ATPase may hydrolyze extramitochondrial ATP.



690

691

692 **2.5.1. LEAK-state (Figure 5A)**: The LEAK-state is defined as a state of mitochondrial  
 693 respiration when  $O_2$  flux mainly compensates for ion leaks in the absence of ATP synthesis, at  
 kinetically-saturating concentrations of  $O_2$ , respiratory fuel substrates and  $P_i$ . LEAK-respiration is

694 measured to obtain an estimate of intrinsic uncoupling without addition of an experimental uncoupler:  
 695 (1) in the absence of adenylates, *i.e.*, AMP, ADP and ATP; (2) after depletion of ADP at a maximum  
 696 ATP/ADP ratio; or (3) after inhibition of the phosphorylation-pathway by inhibitors of F-ATPase—such  
 697 as oligomycin, or of adenine nucleotide translocase—such as carboxyatractyloside. Adjustment of the  
 698 nominal concentration of these inhibitors to the density of biological sample applied can minimize or  
 699 avoid inhibitory side-effects exerted on ET-capacity or even some dyscoupling.

700

701 **Table 2. Terms on respiratory coupling and uncoupling.**

Term	$J_{\text{kO}_2}$	$P \gg O_2$	Notes	
acoupled		0	electron transfer in mitochondrial fragments without vectorial proton translocation ( <b>Figure 3</b> )	
intrinsic, no protonophore added	uncoupled	$L$	0	non-phosphorylating <b>LEAK-respiration</b> ( <b>Figure 5A</b> )
	proton leak-uncoupled		0	component of $L$ , $H^+$ diffusion across the mtIM ( <b>Figure 3</b> )
	decoupled		0	component of $L$ , proton slip ( <b>Figure 3</b> )
	loosely coupled		0	component of $L$ , lower coupling due to superoxide formation and bypass of proton pumps by electron leak ( <b>Figure 3</b> )
	dyscoupled		0	pathologically, toxicologically, environmentally increased uncoupling, mitochondrial dysfunction
	inducibly uncoupled		0	by UCP1 or cation ( <i>e.g.</i> , $Ca^{2+}$ ) cycling ( <b>Figure 3</b> )
noncoupled	$E$	0	ET-capacity, non-phosphorylating respiration stimulated to maximum flux at optimum exogenous protonophore concentration ( <b>Figure 5C</b> )	
well-coupled	$P$	high	<b>OXPPOS-capacity</b> , phosphorylating respiration with an intrinsic LEAK component ( <b>Figure 5B</b> )	
fully coupled	$P - L$	max.	<b>OXPPOS-capacity</b> corrected for LEAK-respiration ( <b>Figure 4</b> )	

702

703

704

705

706

707

708

709

710

711

712

713

714

715

716

717

718

719

720

721

722

723

- **Proton leak and uncoupled respiration:** The intrinsic proton leak is the *uncoupled* leak current of protons in which protons diffuse across the mtIM in the dissipative direction of the downhill protonmotive force without coupling to phosphorylation (**Figure 5A**). The proton leak flux depends non-linearly on the protonmotive force (Garlid *et al.* 1989; Divakaruni and Brand 2011), which is a temperature-dependent property of the mtIM and may be enhanced due to possible contamination by free fatty acids. Inducible uncoupling mediated by uncoupling protein 1 (UCP1) is physiologically controlled, *e.g.*, in brown adipose tissue. UCP1 is a member of the mitochondrial carrier family that is involved in the translocation of protons across the mtIM (Klingenberg 2017). Consequently, this short-circuit lowers the protonmotive force and stimulates electron transfer, respiration, and heat dissipation in the absence of phosphorylation of ADP.
- **Cation cycling:** There can be other cation contributors to leak current including calcium and probably magnesium. Calcium influx is balanced by mitochondrial  $Na^+/Ca^{2+}$  or  $H^+/Ca^{2+}$  exchange, which is balanced by  $Na^+/H^+$  or  $K^+/H^+$  exchanges. This is another effective uncoupling mechanism different from proton leak (**Table 2**).
- **Proton slip and decoupled respiration:** Proton slip is the *decoupled* process in which protons are only partially translocated by a redox proton pump of the ET-pathways and slip back to the original vesicular compartment. The proton leak is the dominant contributor to the overall leak current in mammalian mitochondria incubated under physiological conditions at 37 °C, whereas proton slip increases at lower experimental temperature (Canton *et al.* 1995). Proton slip can also happen in association with the F-ATPase, in which the proton slips downhill across the pump to



724 the matrix without contributing to ATP synthesis. In each case, proton slip is a property of the  
725 proton pump and increases with the pump turnover rate.

- 726 • **Electron leak and loosely coupled respiration:** Superoxide production by the ETS leads to a  
727 bypass of redox proton pumps and correspondingly lower  $P_{\gg}/O_2$  ratio. This depends on the actual  
728 site of electron leak and the scavenging of hydrogen peroxide by cytochrome *c*, whereby electrons  
729 may re-enter the ETS with proton translocation by CIV.
- 730 • **Loss of compartmental integrity and acoupled respiration:** Electron transfer and catabolic  $O_2$   
731 flux proceed without compartmental proton translocation in disrupted mitochondrial fragments.  
732 Such fragments are an artefact of mitochondrial isolation, and may not fully fuse to re-establish  
733 structurally intact mitochondria. Loss of mtIM integrity, therefore, is the cause of acoupled  
734 respiration, which is a nonvectorial dissipative process without control by the protonmotive force.
- 735 • **Dyscoupled respiration:** Mitochondrial injuries may lead to *dyscoupling* as a pathological or  
736 toxicological cause of *uncoupled* respiration. Dyscoupling may involve any type of uncoupling  
737 mechanism, *e.g.*, opening the mtPT pore. Dyscoupled respiration is distinguished from the  
738 experimentally induced *noncoupled* respiration in the ET-state (**Table 2**).

740 **2.5.2. OXPHOS-state (Figure 5B):** The OXPHOS-state is defined as the respiratory state with  
741 kinetically-saturating concentrations of  $O_2$ , respiratory and phosphorylation substrates, and absence of  
742 exogenous uncoupler, which provides an estimate of the maximal respiratory capacity in the OXPHOS-  
743 state for any given ET-pathway state. Respiratory capacities at kinetically-saturating substrate  
744 concentrations provide reference values or upper limits of performance, aiming at the generation of data  
745 sets for comparative purposes. Physiological activities and effects of substrate kinetics can be evaluated  
746 relative to the OXPHOS-capacity.

747 As discussed previously, 0.2 mM ADP does not fully saturate flux in isolated mitochondria  
748 (Gnaiger 2001; Puchowicz *et al.* 2004); greater [ADP] is required, particularly in permeabilized muscle  
749 fibres and cardiomyocytes, to overcome limitations by intracellular diffusion and by the reduced  
750 conductance of the mtOM (Jepihhina *et al.* 2011; Illaste *et al.* 2012; Simson *et al.* 2016), either through  
751 interaction with tubulin (Rostovtseva *et al.* 2008) or other intracellular structures (Birkedal *et al.* 2014).  
752 In addition, saturating ADP concentrations need to be evaluated under different experimental conditions  
753 such as temperature (Lemieux *et al.* 2017) and with different animal models (Blier and Guderley, 1993).  
754 In permeabilized muscle fibre bundles of high respiratory capacity, the apparent  $K_m$  for ADP increases  
755 up to 0.5 mM (Saks *et al.* 1998), consistent with experimental evidence that >90% saturation is reached  
756 only at >5 mM ADP (Pesta and Gnaiger 2012). Similar ADP concentrations are also required for  
757 accurate determination of OXPHOS-capacity in human clinical cancer samples and permeabilized cells  
758 (Klepinin *et al.* 2016; Koit *et al.* 2017). 2.5 to 5 mM ADP is sufficient to obtain the actual OXPHOS-  
759 capacity in many types of permeabilized tissue and cell preparations, but experimental validation is  
760 required in each specific case.

761 **2.5.3. Electron transfer-state (Figure 5C):**  $O_2$  flux determined in the ET-state yields an estimate  
762 of ET-capacity. The ET-state is defined as the *noncoupled* state with kinetically-saturating  
763 concentrations of  $O_2$ , respiratory substrate and optimum exogenous uncoupler concentration for  
764 maximum  $O_2$  flux. Uncouplers are weak lipid-soluble acids which function as protonophores. These  
765 disrupt the barrier function of the mtIM and thus short circuit the protonmotive system, functioning like  
766 a clutch in a mechanical system. As a consequence of the nearly collapsed protonmotive force, the  
767 driving force is insufficient for phosphorylation, and  $J_{P_{\gg}} = 0$ . The most frequently used uncouplers are  
768 carbonyl cyanide *m*-chloro phenyl hydrazone (CCCP), carbonyl cyanide *p*-  
769 trifluoromethoxyphenylhydrazone (FCCP), or dinitrophenol (DNP). Stepwise titration of uncouplers  
770 stimulates respiration up to or above the level of  $O_2$  consumption rates in the OXPHOS-state; respiration  
771 is inhibited, however, above optimum uncoupler concentrations (Mitchell 2011). Data obtained with a  
772 single dose of uncoupler must be evaluated with caution, particularly when a fixed uncoupler  
773 concentration is used in studies exploring a treatment or disease that may alter the mitochondrial content  
774 or mitochondrial sensitivity to inhibition by uncouplers. There is a need for new protonophoric  
775 uncouplers that drive maximal respiration across a broad dosing range and do not inhibit respiration at  
776 high concentrations (Kenwood *et al.* 2013). The effect on ET-capacity of the reversed function of F-  
777 ATPase ( $J_{P_{\ll}}$ ; **Figure 5C**) can be evaluated in the presence and absence of extramitochondrial ATP.

778 **2.5.4. ROX state and Rox:** Besides the three fundamental coupling states of mitochondrial  
779 preparations, the state of residual  $O_2$  consumption, ROX, which although not a coupling state, is relevant

780 to assess respiratory function (**Figure 1**). The rate of residual oxygen consumption, *Rox*, is defined as  
 781 O<sub>2</sub> consumption due to oxidative reactions measured after inhibition of ET with rotenone, malonic acid  
 782 and antimycin A. Cyanide and azide inhibit not only CIV but catalase and several peroxidases involved  
 783 in *Rox*. High concentrations of antimycin A, but not rotenone or cyanide, inhibit peroxisomal acyl-CoA  
 784 oxidase and D-amino acid oxidase (Vamecq *et al.* 1987). *Rox* represents a baseline used to correct  
 785 respiration measured in defined coupling control states. *Rox*-corrected *L*, *P* and *E* not only lower the  
 786 values of total fluxes, but also change the flux control ratios *L/P* and *L/E*. *Rox* is not necessarily  
 787 equivalent to non-mitochondrial reduction of O<sub>2</sub>, considering O<sub>2</sub>-consuming reactions in mitochondria  
 788 that are not related to ET—such as O<sub>2</sub> consumption in reactions catalyzed by monoamine oxidases (type  
 789 A and B), monooxygenases (cytochrome P450 monooxygenases), dioxygenase (sulfur dioxygenase and  
 790 trimethyllysine dioxygenase), and several hydroxylases. Even isolated mitochondrial fractions,  
 791 especially those obtained from liver, may be contaminated by peroxisomes, as shown by transmission  
 792 electron microscopy. This fact makes the exact determination of mitochondrial O<sub>2</sub> consumption and  
 793 mitochondria-associated generation of reactive oxygen species complicated (Schönfeld *et al.* 2009;  
 794 Speijer 2016; **Figure 2**). The dependence of ROX-linked O<sub>2</sub> consumption needs to be studied in detail  
 795 together with non-ET enzyme activities, availability of specific substrates, O<sub>2</sub> concentration, and  
 796 electron leakage leading to the formation of reactive oxygen species.

797 **2.5.5. Quantitative relations:** *E* may exceed or be equal to *P*.  $E > P$  is observed in many types  
 798 of mitochondria, varying between species, tissues and cell types (Gnaiger 2009). *E-P* is the excess ET-  
 799 capacity pushing the phosphorylation-flux (**Figure 2C**) to the limit of its capacity for utilizing the  
 800 protonmotive force. In addition, the magnitude of *E-P* depends on the tightness of respiratory coupling  
 801 or degree of uncoupling, since an increase of *L* causes *P* to increase towards the limit of *E*. The *excess*  
 802 *E-P* capacity, *E-P*, therefore, provides a sensitive diagnostic indicator of specific injuries of the  
 803 phosphorylation-pathway, under conditions when *E* remains constant but *P* declines relative to controls  
 804 (**Figure 4**). Substrate cocktails supporting simultaneous convergent electron transfer to the Q-junction  
 805 for reconstitution of TCA cycle function establish pathway control states with high ET-capacity, and  
 806 consequently increase the sensitivity of the *E-P* assay.

807 *E* cannot theoretically be lower than *P*.  $E < P$  must be discounted as an artefact, which may be  
 808 caused experimentally by: (1) loss of oxidative capacity during the time course of the respirometric  
 809 assay, since *E* is measured subsequently to *P*; (2) using insufficient uncoupler concentrations; (3) using  
 810 high uncoupler concentrations which inhibit ET (Gnaiger 2008); (4) high oligomycin concentrations  
 811 applied for measurement of *L* before titrations of uncoupler, when oligomycin exerts an inhibitory effect  
 812 on *E*. On the other hand, the excess ET-capacity is overestimated if non-saturating [ADP] or [P<sub>i</sub>] are  
 813 used. See State 3 in the next section.

814 The net OXPHOS-capacity is calculated by subtracting *L* from *P* (**Figure 4**). The net P<sub>»</sub>/O<sub>2</sub> equals  
 815  $P_{»}/(P-L)$ , wherein the dissipative LEAK component in the OXPHOS-state may be overestimated. This  
 816 can be avoided by measuring LEAK-respiration in a state when the protonmotive force is adjusted to its  
 817 slightly lower value in the OXPHOS-state by titration of an ET inhibitor (Divakaruni and Brand 2011).  
 818 Any turnover-dependent components of proton leak and slip, however, are underestimated under these  
 819 conditions (Garlid *et al.* 1993). In general, it is inappropriate to use the term *ATP production* or *ATP*  
 820 *turnover* for the difference of O<sub>2</sub> flux measured in the OXPHOS and LEAK states. *P-L* is the upper limit  
 821 of OXPHOS-capacity that is freely available for ATP production (corrected for LEAK-respiration) and  
 822 is fully coupled to phosphorylation with a maximum mechanistic stoichiometry (**Figure 4**).

823 LEAK-respiration and OXPHOS-capacity depend on (1) the tightness of coupling under the  
 824 influence of the respiratory uncoupling mechanisms (**Figure 3**), and (2) the coupling stoichiometry,  
 825 which varies as a function of the substrate type undergoing oxidation in ET-pathways with either two  
 826 or three coupling sites (**Figure 2B**). When cocktails with NADH-linked substrates and succinate are  
 827 used, the relative contribution of ET-pathways with three or two coupling sites cannot be controlled  
 828 experimentally, is difficult to determine, and may shift in transitions between LEAK-, OXPHOS- and  
 829 ET-states (Gnaiger 2014). Under these experimental conditions, we cannot separate the tightness of  
 830 coupling *versus* coupling stoichiometry as the mechanisms of respiratory control in the shift of *L/P*  
 831 ratios. The tightness of coupling and fully coupled O<sub>2</sub> flux, *P-L* (**Table 2**), therefore, are obtained from  
 832 measurements of coupling control of LEAK-respiration, OXPHOS- and ET-capacities in well-defined  
 833 pathway states, using either pyruvate and malate as substrates or the classical succinate and rotenone  
 834 substrate-inhibitor combination (**Figure 2B**).

835 **2.5.6. The steady-state:** Mitochondria represent a thermodynamically open system in non-  
 836 equilibrium states of biochemical energy transformation. State variables (protonmotive force; redox  
 837 states) and metabolic *rates* (fluxes) are measured in defined mitochondrial respiratory *states*. Steady-  
 838 states can be obtained only in open systems, in which changes by internal transformations, *e.g.*, O<sub>2</sub>  
 839 consumption, are instantaneously compensated for by external fluxes, *e.g.*, O<sub>2</sub> supply, preventing a  
 840 change of O<sub>2</sub> concentration in the system (Gnaiger 1993b). Mitochondrial respiratory states monitored  
 841 in closed systems satisfy the criteria of pseudo-steady states for limited periods of time, when changes  
 842 in the system (concentrations of O<sub>2</sub>, fuel substrates, ADP, P<sub>i</sub>, H<sup>+</sup>) do not exert significant effects on  
 843 metabolic fluxes (respiration, phosphorylation). Such pseudo-steady states require respiratory media  
 844 with sufficient buffering capacity and substrates maintained at kinetically-saturating concentrations, and  
 845 thus depend on the kinetics of the processes under investigation.  
 846

#### 847 2.6. Classical terminology for isolated mitochondria

848 *'When a code is familiar enough, it ceases appearing like a code; one forgets that there is a*  
 849 *decoding mechanism. The message is identical with its meaning'* (Hofstadter 1979).  
 850

851 Chance and Williams (1955; 1956) introduced five classical states of mitochondrial respiration  
 852 and cytochrome redox states. **Table 3** shows a protocol with isolated mitochondria in a closed  
 853 respirometric chamber, defining a sequence of respiratory states. States and rates are not specifically  
 854 distinguished in this nomenclature.  
 855

856 **Table 3. Metabolic states of mitochondria (Chance and**  
 857 **Williams, 1956; Table V).**  
 858

State	[O <sub>2</sub> ]	ADP level	Substrate level	Respiration rate	Rate-limiting substance
1	>0	low	low	slow	ADP
2	>0	high	~0	slow	substrate
3	>0	high	high	fast	respiratory chain
4	>0	low	high	slow	ADP
5	0	high	high	0	oxygen

859 **2.6.1. State 1** is obtained after addition of isolated mitochondria to air-saturated  
 860 isoosmotic/isotonic respiration medium containing P<sub>i</sub>, but no fuel substrates and no adenylates.  
 861

862 **2.6.2. State 2** is induced by addition of a 'high' concentration of ADP (typically 100 to 300 μM),  
 863 which stimulates respiration transiently on the basis of endogenous fuel substrates and phosphorylates  
 864 only a small portion of the added ADP. State 2 is then obtained at a low respiratory activity limited by  
 865 exhausted endogenous fuel substrate availability (**Table 3**). If addition of specific inhibitors of  
 866 respiratory complexes such as rotenone does not cause a further decline of O<sub>2</sub> flux, State 2 is equivalent  
 867 to the ROX state (See below.). If inhibition is observed, undefined endogenous fuel substrates are a  
 868 confounding factor of pathway control, contributing to the effect of subsequently externally added  
 869 substrates and inhibitors. In contrast to the original protocol, an alternative sequence of titration steps is  
 870 frequently applied, in which the alternative 'State 2' has an entirely different meaning when this second  
 871 state is induced by addition of fuel substrate without ADP or ATP (LEAK-state; in contrast to State 2  
 872 defined in **Table 1** as a ROX state). Some researchers have called this condition as 'pseudostate 4'  
 873 because it has no significant concentrations of adenine nucleotides and hence it is not a near-  
 874 physiological condition, although it should be used for calculating the net OXPHOS-capacity, *P-L*.  
 875

876 **2.6.3. State 3** is the state stimulated by addition of fuel substrates while the ADP concentration  
 877 is still high (**Table 3**) and supports coupled energy transformation through oxidative phosphorylation.  
 878 'High ADP' is a concentration of ADP specifically selected to allow the measurement of State 3 to State  
 879 4 transitions of isolated mitochondria in a closed respirometric chamber. Repeated ADP titration re-  
 880 establishes State 3 at 'high ADP'. Starting at O<sub>2</sub> concentrations near air-saturation (193 or 238 μM O<sub>2</sub>  
 881 at 37 °C or 25 °C and sea level at 1 atm or 101.32 kPa, and an oxygen solubility of respiration medium  
 at 0.92 times that of pure water; Forstner and Gnaiger 1983), the total ADP concentration added must

882 be low enough (typically 100 to 300  $\mu\text{M}$ ) to allow phosphorylation to ATP at a coupled  $\text{O}_2$  flux that  
 883 does not lead to  $\text{O}_2$  depletion during the transition to State 4. In contrast, kinetically-saturating ADP  
 884 concentrations usually are 10-fold higher than 'high ADP', e.g., 2.5 mM in isolated mitochondria. The  
 885 abbreviation State 3u is occasionally used in bioenergetics, to indicate the state of respiration after  
 886 titration of an uncoupler, without sufficient emphasis on the fundamental difference between OXPHOS-  
 887 capacity (*well-coupled* with an endogenous uncoupled component) and ET-capacity (*noncoupled*).

888 **2.6.4. State 4** is a LEAK-state that is obtained only if the mitochondrial preparation is intact and  
 889 well-coupled. Depletion of ADP by phosphorylation to ATP causes a decline of  $\text{O}_2$  flux in the transition  
 890 from State 3 to State 4. Under the conditions of State 4, a maximum protonmotive force and high  
 891 ATP/ADP ratio are maintained. The gradual decline of  $Y_{\text{P}}/\text{O}_2$  towards diminishing [ADP] at State 4 must  
 892 be taken into account for calculation of  $\text{P}_{\text{P}}/\text{O}_2$  ratios (Gnaiger 2001). State 4 respiration,  $L_{\text{T}}$  (**Table 1**),  
 893 reflects intrinsic proton leak and ATP hydrolysis activity.  $\text{O}_2$  flux in State 4 is an overestimation of  
 894 LEAK-respiration if the contaminating ATP hydrolysis activity recycles some ATP to ADP,  $J_{\text{P}_{\text{L}}}$ , which  
 895 stimulates respiration coupled to phosphorylation,  $J_{\text{P}_{\text{S}}} > 0$ . Some degree of mechanical disruption and  
 896 loss of mitochondrial integrity allows the exposed mitochondrial F-ATPases to hydrolyze the ATP  
 897 synthesized by the fraction of coupled mitochondria. This can be tested by inhibition of the  
 898 phosphorylation-pathway using oligomycin, ensuring that  $J_{\text{P}_{\text{S}}} = 0$  (State 4o). On the other hand, the State  
 899 4 respiration reached after exhaustion of added ADP is a more physiological condition, i.e., presence of  
 900 ATP, ADP and even AMP. Sequential ADP titrations re-establish State 3, followed by State 3 to State  
 901 4 transitions while sufficient  $\text{O}_2$  is available. Anoxia may be reached, however, before exhaustion of  
 902 ADP (State 5).

903 **2.6.5. State 5** 'may be obtained by antimycin A treatment or by anaerobiosis' (Chance and  
 904 Williams, 1955) '. These definitions give State 5 two different meanings of ROX or anoxia, respectively.  
 905 Anoxia is obtained after exhaustion of  $\text{O}_2$  in a closed respirometric chamber. Diffusion of  $\text{O}_2$  from the  
 906 surroundings into the aqueous solution may be a confounding factor preventing complete anoxia  
 907 (Gnaiger 2001).

908 In **Table 3**, only States 3 and 4 are coupling control states, with the restriction that rates in State  
 909 3 may be limited kinetically by non-saturating ADP concentrations.

## 911 2.7. Control and regulation

912  
 913 The terms metabolic *control* and *regulation* are frequently used synonymously, but are  
 914 distinguished in metabolic control analysis: "We could understand the regulation as the mechanism that  
 915 occurs when a system maintains some variable constant over time, in spite of fluctuations in external  
 916 conditions (homeostasis of the internal state). On the other hand, metabolic control is the power to  
 917 change the state of the metabolism in response to an external signal" (Fell 1997). Respiratory control  
 918 may be induced by experimental control signals that exert an influence on: (1) ATP demand and ADP  
 919 phosphorylation-rate; (2) fuel substrate composition, pathway competition; (3) available amounts of  
 920 substrates and  $\text{O}_2$ , e.g., starvation and hypoxia; (4) the protonmotive force, redox states, flux-force  
 921 relationships, coupling and efficiency; (5)  $\text{Ca}^{2+}$  and other ions including  $\text{H}^+$ ; (6) inhibitors, e.g., nitric  
 922 oxide or intermediary metabolites such as oxaloacetate; (7) signalling pathways and regulatory proteins,  
 923 e.g., insulin resistance, transcription factor hypoxia inducible factor 1.

924 Mechanisms of respiratory control and regulation include adjustments of: (1) enzyme activities  
 925 by allosteric mechanisms and phosphorylation; (2) enzyme content, concentrations of cofactors and  
 926 conserved moieties such as adenylates, nicotinamide adenine dinucleotide [ $\text{NAD}^+/\text{NADH}$ ], coenzyme  
 927 Q, cytochrome *c*; (3) metabolic channeling by supercomplexes; and (4) mitochondrial density (enzyme  
 928 concentrations and membrane area) and morphology (cristae folding, fission and fusion). Mitochondria  
 929 are targeted directly by hormones, e.g., progesterone and glucacorticoids, which affect their energy  
 930 metabolism (Lee *et al.* 2013; Gerö and Szabo 2016; Price and Dai 2016; Moreno *et al.* 2017; Singh *et al.*  
 931 2018). Evolutionary or acquired differences in the genetic and epigenetic basis of mitochondrial  
 932 function (or dysfunction) between individuals; age; biological sex, and hormone concentrations; life  
 933 style including exercise and nutrition; and environmental issues including thermal, atmospheric, toxic  
 934 and pharmacological factors, exert an influence on all control mechanisms listed above. For reviews,  
 935 see Brown 1992; Gnaiger 1993a, 2009; 2014; Paradies *et al.* 2014; Morrow *et al.* 2017.

936 Lack of control by a metabolic pathway, e.g., phosphorylation-pathway, means that there will  
 937 be no response to a variable activating it, e.g., [ADP]. The reverse, however, is not true as the absence

938 of a response to [ADP] does not exclude the phosphorylation-pathway from having some degree of  
 939 control. The degree of control of a component of the OXPHOS-pathway on an output variable, such as  
 940 O<sub>2</sub> flux, will in general be different from the degree of control on other outputs, such as phosphorylation-  
 941 flux or proton leak flux. Therefore, it is necessary to be specific as to which input and output are under  
 942 consideration (Fell 1997).

943 Respiratory control refers to the ability of mitochondria to adjust O<sub>2</sub> flux in response to external  
 944 control signals by engaging various mechanisms of control and regulation. Respiratory control is  
 945 monitored in a mitochondrial preparation under conditions defined as respiratory states, preferentially  
 946 under near-physiological conditions of temperature, pH, and medium ionic composition, to generate  
 947 data of higher biological relevance. When phosphorylation of ADP to ATP is stimulated or depressed,  
 948 an increase or decrease is observed in electron transfer measured as O<sub>2</sub> flux in respiratory coupling states  
 949 of intact mitochondria ('controlled states' in the classical terminology of bioenergetics). Alternatively,  
 950 coupling of electron transfer with phosphorylation is diminished by uncouplers. The corresponding  
 951 coupling control state is characterized by a high respiratory rate without control by P» (noncoupled or  
 952 'uncontrolled state').

953  
 954

### 955 3. What is a rate?

956

957 The term *rate* is not adequately defined to be useful for reporting data. Normalization of 'rates'  
 958 leads to a diversity of formats. Application of common and defined units is required for direct transfer  
 959 of reported results into a database. The second [s] is the SI unit for the base quantity *time*. It is also the  
 960 standard time-unit used in solution chemical kinetics.

961 The inconsistency of the meanings of rate becomes apparent when considering Galileo Galilei's  
 962 famous principle, that 'bodies of different weight all fall at the same rate (have a constant acceleration)'  
 963 (Coopersmith 2010). A rate may be an extensive quantity, which is a *flow*, *I*, when expressed per object  
 964 (per number of cells or organisms) or per chamber (per system). 'System' is defined as the open or  
 965 closed chamber of the measuring device. A rate is a *flux*, *J*, when expressed as a size-specific quantity  
 966 (Figure 6A; Box 2).

967 • **Extensive quantities:** An extensive quantity increases proportionally with system size. For  
 968 example, mass and volume are extensive quantities. Flow is an extensive quantity. The  
 969 magnitude of an extensive quantity is completely additive for non-interacting subsystems.  
 970 The magnitude of these quantities depends on the extent or size of the system (Cohen *et al.*  
 971 2008).

972 • **Size-specific quantities:** 'The adjective *specific* before the name of an extensive quantity is  
 973 often used to mean *divided by mass*' (Cohen *et al.* 2008). In this system-paradigm, mass-  
 974 specific flux is flow divided by mass of the system (the total mass of everything within the  
 975 measuring chamber or reactor). Rates are frequently expressed as volume-specific flux. A  
 976 mass-specific or volume-specific quantity is independent of the extent of non-interacting  
 977 homogenous subsystems. Tissue-specific quantities (related to the *sample* in contrast to the  
 978 *system*) are of fundamental interest in the field of comparative mitochondrial physiology,  
 979 where *specific* refers to the *type of the sample* rather than *mass of the system*. The term  
 980 *specific*, therefore, must be clarified; *sample-specific*, *e.g.*, muscle mass-specific  
 981 normalization, is distinguished from *system-specific* quantities (mass or volume; Figure 6).

982 • **Intensive quantities:** In contrast to size-specific properties, forces are intensive quantities  
 983 defined as the change of an extensive quantity per advancement of an energy transformation  
 984 (Gnaiger 1993b).

985 • **Formats:** The quantity of a sample *X* can be expressed in different formats.  $n_X$ ,  $N_X$ , and  $m_X$   
 986 are the molar amount, number, and mass of *X*, respectively. When different formats are  
 987 indicated in symbols of derived quantities, the format ( $\underline{n}$ ,  $\underline{N}$ ,  $\underline{m}$ ) is shown as a subscript  
 988 (*underlined italic*), as in  $I_{O_2/\underline{N}X}$  and  $J_{O_2/\underline{m}X}$ . Oxygen flow and flux are expressed in the molar  
 989 format,  $n_{O_2}$  [mol], but in the volume format,  $V_{O_2}$  [m<sup>3</sup>] in ergometry. For mass-specific flux  
 990 these formats can be distinguished as  $J_{\underline{n}O_2/\underline{m}X}$  and  $J_{\underline{V}O_2/\underline{m}X}$ , respectively. Further examples are  
 991 given in Figure 6 and Table 4.

992

993 **Figure 6. Flow and flux, and**  
 994 **normalization in structure-**  
 995 **function analysis**

996 (A) When expressing metabolic  
 997 ‘rate’ measured in a chamber, a  
 998 fundamental distinction is made  
 999 between relating the rate to the  
 1000 experimental sample (left) or  
 1001 chamber (right). The different  
 1002 meanings of rate need to be  
 1003 specified by the chosen  
 1004 normalization. Left: Results are  
 1005 expressed as mass-specific flux,  $J_{mX}$ ,  
 1006 per mg protein, dry or wet mass.  
 1007 Cell volume,  $V_{ce}$ , may be used for  
 1008 normalization (volume-specific  
 1009 flux,  $J_{Vce}$ ). Right: Flow per chamber,  
 1010  $I$ , or flux per chamber volume,  $J_V$ ,  
 1011 are merely reported for  
 1012 methodological reasons.

1013 (B)  $O_2$  flow per cell,  $I_{O_2/Nce}$ , is the  
 1014 product of mitochondria-specific  
 1015 flux, mt-density and mass per cell.  
 1016 Unstructured analysis: performance  
 1017 is the product of mass-specific flux,  
 1018  $J_{O_2/MX}$  [ $\text{mol}\cdot\text{s}^{-1}\cdot\text{kg}^{-1}$ ], and size  
 1019 (mass per cell). Structured analysis:  
 1020 performance is the product of  
 1021 mitochondrial function (mt-specific  
 1022 flux) and structure (mt-content).  
 1023 Modified from Gnaiger (2014). For  
 1024 further details see **Table 4**.

1025  
1026  
1027  
1028  
1029

1030 **Box 2: Metabolic flows and fluxes: vectoral, vectorial, and scalar**

1031

1032

1033

1034

1035

1036

1037

1038

1039

1040

1041

1042

1043

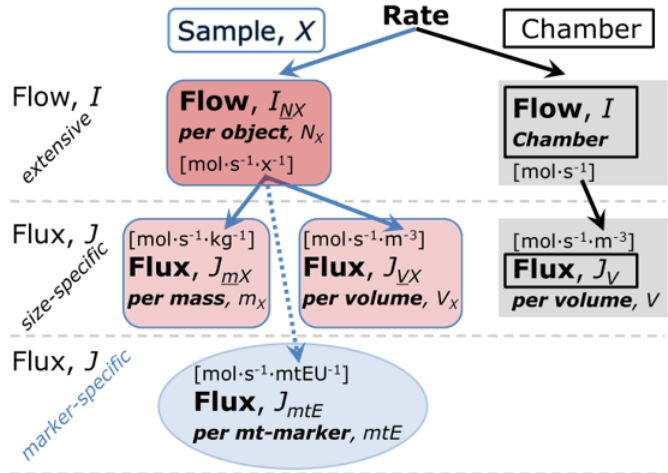
1044

1045

1046

1047

**A**



**B**

$$\text{Flow per cell} = \text{mt-specific Flux} \times \text{mt-Density} \times \text{Mass per cell}$$

$$\frac{I_{O_2/Nce}}{\text{mol}\cdot\text{s}^{-1}} = \frac{J_{O_2/CS}}{\text{mol}\cdot\text{s}^{-1}} \cdot \frac{D_{CS}}{\text{IU}/\text{kg}} \cdot \frac{M_{ce}}{\text{kg}/\text{x}}$$

Size

$$\text{Flow per cell} = \text{Mass-specific Flux} \times \text{Mass per cell}$$

$$\frac{I_{O_2/Nce}}{\text{mol}\cdot\text{s}^{-1}} = \frac{J_{O_2/Mce}}{\text{mol}\cdot\text{s}^{-1}\cdot\text{kg}^{-1}} \cdot \frac{M_{ce}}{\text{kg}/\text{x}}$$

Structure

$$\text{Flow per cell} = \text{mt-specific Flux} \times \text{mt-Content per cell}$$

$$\frac{I_{O_2/Nce}}{\text{mol}\cdot\text{s}^{-1}} = \frac{J_{O_2/CS}}{\text{mol}\cdot\text{s}^{-1}} \cdot \frac{CS_{Nce}}{\text{IU}/\text{kg} \cdot \text{kg}/\text{x}}$$

$$\text{Aerobic cell performance} = \begin{cases} \text{mt-Quality} \times \text{mt-Quantity} \\ \text{mt-Function} \times \text{mt-Structure} \end{cases}$$

In a generalization of electrical terms, flow as an extensive quantity ( $I$ ; per system) is distinguished from flux as a size-specific quantity ( $J$ ; per system size). *Flows*,  $I_{tr}$ , are defined for all transformations as extensive quantities. Electric charge per unit time is electric flow or current,  $I_{el} = dQ_{el} \cdot dt^{-1}$  [ $A \equiv C \cdot s^{-1}$ ]. When dividing  $I_{el}$  by size of the system (cross-sectional area of a ‘wire’), we obtain flux as a size-specific quantity, which is the current density (surface-density of flow) perpendicular to the direction of flux,  $J_{el} = I_{el} \cdot A^{-1}$  [ $A \cdot m^{-2}$ ] (Cohen et al. 2008). Fluxes with *spatial* geometric direction and magnitude are *vectors*. Vector and scalar *fluxes* are related to flows as  $J_{tr} = I_{tr} \cdot A^{-1}$  [ $\text{mol}\cdot\text{s}^{-1}\cdot\text{m}^{-2}$ ] and  $J_{tr} = I_{tr} \cdot V^{-1}$  [ $\text{mol}\cdot\text{s}^{-1}\cdot\text{m}^{-3}$ ], expressing flux as an area-specific vector or volume-specific vectorial or scalar quantity, respectively (Gnaiger 1993b). We use the metre–kilogram–second–ampere (MKSA) international system of units (SI) for general cases ([m], [kg], [s] and [A]), with decimal SI prefixes for specific applications (**Table 4**).

We suggest defining: (1) *vectoral* fluxes, which are translocations as functions of *gradients* with direction in geometric space in continuous systems; (2) *vectorial* fluxes, which describe translocations in discontinuous systems and are restricted to information on *compartmental differences* (transmembrane proton flux); and (3) *scalar* fluxes, which are transformations in a *homogenous* system (catabolic  $O_2$  flux,  $J_{kO_2}$ ).

1048 **4. Normalization of rate per sample**

1049

1050 The challenges of measuring mitochondrial respiratory flux are matched by those of  
 1051 normalization. Normalization (**Table 4**) is guided by physicochemical principles, methodological  
 1052 considerations, and conceptual strategies (**Figure 6**).

1053

1054 **Table 4. Sample concentrations and normalization of flux.**

1055

Expression	Symbol	Definition	Unit	Notes
<b>Sample</b>				
identity of sample	$X$	object: cell, tissue, animal, patient		
number of sample entities $X$	$N_X$	number of objects	x	1
mass of sample $X$	$m_X$		kg	2
mass of object $X$	$M_X$	$M_X = m_X \cdot N_X^{-1}$	$\text{kg} \cdot \text{x}^{-1}$	2
<b>Mitochondria</b>				
mitochondria	mt	$X = \text{mt}$		
amount of mt-elementary components	$mtE$	quantity of mt-marker	mtEU	
<b>Concentrations</b>				
object number concentration	$C_{NX}$	$C_{NX} = N_X \cdot V^{-1}$	$\text{x} \cdot \text{m}^{-3}$	3
sample mass concentration	$C_{mX}$	$C_{mX} = m_X \cdot V^{-1}$	$\text{kg} \cdot \text{m}^{-3}$	
mitochondrial concentration	$C_{mtE}$	$C_{mtE} = mtE \cdot V^{-1}$	$\text{mtEU} \cdot \text{m}^{-3}$	4
specific mitochondrial density	$D_{mtE}$	$D_{mtE} = mtE \cdot m_X^{-1}$	$\text{mtEU} \cdot \text{kg}^{-1}$	5
mitochondrial content, $mtE$ per object $X$	$mtE_{NX}$	$mtE_{NX} = mtE \cdot N_X^{-1}$	$\text{mtEU} \cdot \text{x}^{-1}$	6
<b>O<sub>2</sub> flow and flux</b>				
flow, system	$I_{O_2}$	internal flow	$\text{mol} \cdot \text{s}^{-1}$	7
volume-specific flux	$J_{V,O_2}$	$J_{V,O_2} = I_{O_2} \cdot V^{-1}$	$\text{mol} \cdot \text{s}^{-1} \cdot \text{m}^{-3}$	8
flow per object $X$	$I_{O_2/NX}$	$I_{O_2/NX} = J_{V,O_2} \cdot C_{NX}^{-1}$	$\text{mol} \cdot \text{s}^{-1} \cdot \text{x}^{-1}$	9
mass-specific flux	$J_{O_2/mX}$	$J_{O_2/mX} = J_{V,O_2} \cdot C_{mX}^{-1}$	$\text{mol} \cdot \text{s}^{-1} \cdot \text{kg}^{-1}$	10
mt-marker-specific flux	$J_{O_2/mtE}$	$J_{O_2/mtE} = J_{V,O_2} \cdot C_{mtE}^{-1}$	$\text{mol} \cdot \text{s}^{-1} \cdot \text{mtEU}^{-1}$	11

1056

1057

1058

1059

1060

1061

1062

1063

1064

1065

1066

1067

1068

1069

1070

1071

1072

1073

- The unit x for a number is not used by IUPAC. To avoid confusion, the units [ $\text{kg} \cdot \text{x}^{-1}$ ] and [kg] distinguish the mass per object from the mass of a sample that may contain any number of objects. Similarly, the units for flow per system *versus* flow per object are [ $\text{mol} \cdot \text{s}^{-1}$ ] (Note 8) and [ $\text{mol} \cdot \text{s}^{-1} \cdot \text{x}^{-1}$ ] (Note 10).
- Units are given in the MKSA system (**Box 2**). The SI prefix k is used for the SI base unit of mass (kg = 1,000 g). In praxis, various SI prefixes are used for convenience, to make numbers easily readable, e.g., 1 mg tissue, cell or mitochondrial mass instead of 0.000001 kg.
- In case of cells (sample  $X = \text{cells}$ ), the object number concentration is  $C_{N_{ce}} = N_{ce} \cdot V^{-1}$ , and volume may be expressed in [ $\text{dm}^3 \equiv \text{L}$ ] or [ $\text{cm}^3 = \text{mL}$ ]. See **Table 5** for different object types.
- mt-concentration is an experimental variable, dependent on sample concentration: (1)  $C_{mtE} = mtE \cdot V^{-1}$ ; (2)  $C_{mtE} = mtE_X \cdot C_{NX}$ ; (3)  $C_{mtE} = C_{mX} \cdot D_{mtE}$ .
- If the amount of mitochondria,  $mtE$ , is expressed as mitochondrial mass, then  $D_{mtE}$  is the mass fraction of mitochondria in the sample. If  $mtE$  is expressed as mitochondrial volume,  $V_{mt}$ , and the mass of sample,  $m_X$ , is replaced by volume of sample,  $V_X$ , then  $D_{mtE}$  is the volume fraction of mitochondria in the sample.
- $mtE_{NX} = mtE \cdot N_X^{-1} = C_{mtE} \cdot C_{NX}^{-1}$ .
- $O_2$  can be replaced by other chemicals to study different reactions, e.g., ATP,  $H_2O_2$ , or vesicular compartmental translocations, e.g.,  $Ca^{2+}$ .

- 1074 8  $I_{O_2}$  and  $V$  are defined per instrument chamber as a system of constant volume (and constant  
 1075 temperature), which may be closed or open.  $I_{O_2}$  is abbreviated for  $I_{rO_2}$ , *i.e.*, the metabolic or internal  
 1076  $O_2$  flow of the chemical reaction  $r$  in which  $O_2$  is consumed, hence the negative stoichiometric  
 1077 number,  $\nu_{O_2} = -1$ .  $I_{rO_2} = d_r n_{O_2} / dt \cdot \nu_{O_2}^{-1}$ . If  $r$  includes all chemical reactions in which  $O_2$  participates, then  
 1078  $d_r n_{O_2} = dn_{O_2} - d_e n_{O_2}$ , where  $dn_{O_2}$  is the change in the amount of  $O_2$  in the instrument chamber and  $d_e n_{O_2}$   
 1079 is the amount of  $O_2$  added externally to the system. At steady state, by definition  $dn_{O_2} = 0$ , hence  $d_r n_{O_2}$   
 1080  $= -d_e n_{O_2}$ . Note that in this context ‘external’,  $e$ , refers to the system, whereas in Figure 1 ‘external’,  
 1081  $ext$ , refers to the organism.  
 1082 9  $J_{V,O_2}$  is an experimental variable, expressed per volume of the instrument chamber.  
 1083 10  $I_{O_2/NX}$  is a physiological variable, depending on the size of entity  $X$ .  
 1084 11 There are many ways to normalize for a mitochondrial marker, that are used in different experimental  
 1085 approaches: (1)  $J_{O_2/mtE} = J_{V,O_2} \cdot C_{mtE}^{-1}$ ; (2)  $J_{O_2/mtE} = J_{V,O_2} \cdot C_{mX}^{-1} \cdot D_{mtE}^{-1} = J_{O_2/mX} \cdot D_{mtE}^{-1}$ ; (3)  $J_{O_2/mtE} =$   
 1086  $J_{V,O_2} \cdot C_{NX}^{-1} \cdot mtE_{NX}^{-1} = I_{O_2/NX} \cdot mtE_{NX}^{-1}$ ; (4)  $J_{O_2/mtE} = I_{O_2} \cdot mtE^{-1}$ . The mt-elementary unit [mtEU] varies depending  
 1087 on the mt-marker.  
 1088  
 1089  
 1090

**Table 5. Sample types, X, abbreviations, and quantification.**

Identity of sample	$X$	$N_X$	Mass <sup>a</sup>	Volume	mt-Marker
mitochondrial preparation		[x]	[kg]	[m <sup>3</sup> ]	[mtEU]
isolated mitochondria	imt		$m_{mt}$	$V_{mt}$	$mtE$
tissue homogenate	thom		$m_{thom}$		$mtE_{thom}$
permeabilized tissue	pti		$m_{pti}$		$mtE_{pti}$
permeabilized fibre	pfi		$m_{pfi}$		$mtE_{pfi}$
permeabilized cell	pce	$N_{pce}$	$M_{pce}$	$V_{pce}$	$mtE_{pce}$
cells <sup>b</sup>	ce	$N_{ce}$	$M_{ce}$	$V_{ce}$	$mtE_{ce}$
intact cell, viable cell	vce	$N_{vce}$	$M_{vce}$	$V_{vce}$	
dead cell	dce	$N_{dce}$	$M_{dce}$	$V_{dce}$	
organism	org	$N_{org}$	$M_{org}$	$V_{org}$	

<sup>a</sup> Instead of mass, the wet weight or dry weight is frequently stated,  $W_w$  or  $W_d$ .  $m_X$  is mass of the sample [kg],  $M_X$  is mass of the object [kg·x<sup>-1</sup>] (Table 4).

<sup>b</sup> Total cell count,  $N_{ce} = N_{vce} + N_{dce}$

#### 4.1. Flow: per object

**4.1.1. Number concentration,  $C_{NX}$ :** Normalization per sample concentration is routinely required to report respiratory data.  $C_{NX}$  is the experimental number concentration of sample  $X$ . In the case of animals, *e.g.*, nematodes,  $C_{NX} = N_X \cdot V^{-1}$  [x·L<sup>-1</sup>], where  $N_X$  is the number of organisms in the chamber. Similarly, the number of cells per chamber volume is the number concentration of permeabilized or intact cells  $C_{Nce} = N_{ce} \cdot V^{-1}$  [x·L<sup>-1</sup>], where  $N_{ce}$  is the number of cells in the chamber (Table 4).

**4.1.2. Flow per object,  $I_{O_2/NX}$ :**  $O_2$  flow per cell is calculated from volume-specific  $O_2$  flux,  $J_{V,O_2}$  [nmol·s<sup>-1</sup>·L<sup>-1</sup>] (per  $V$  of the measurement chamber [L]), divided by the number concentration of cells. The total cell count is the sum of viable and dead cells,  $N_{ce} = N_{vce} + N_{dce}$  (Table 5). The cell viability index,  $VI = N_{vce} \cdot N_{ce}^{-1}$ , is the ratio of viable cells ( $N_{vce}$ ; before experimental permeabilization) per total cell count. After experimental permeabilization, all cells are permeabilized,  $N_{pce} = N_{ce}$ . The cell viability index can be used to normalize respiration for the number of cells that have been viable before experimental permeabilization,  $I_{O_2/Nvce} = I_{O_2/Nce} \cdot VI^{-1}$ , considering that mitochondrial respiratory dysfunction in dead cells should be eliminated as a confounding factor.

The complexity changes when the object is a whole organism studied as an experimental model. The scaling law in respiratory physiology reveals a strong interaction between  $O_2$  flow and individual body mass: *basal* metabolic rate (flow) does not increase linearly with body mass, whereas *maximum* mass-specific  $O_2$  flux,  $\dot{V}_{O_2max}$  or  $\dot{V}_{O_2peak}$ , is approximately constant across a large range of individual body mass (Weibel and Hoppeler 2005). Individuals, breeds and species, however, deviate substantially from this relationship.  $\dot{V}_{O_2peak}$  of human endurance athletes is 60 to 80 mL  $O_2 \cdot \text{min}^{-1} \cdot \text{kg}^{-1}$  body mass, converted to  $J_{O_2peak/Morg}$  of 45 to 60 nmol·s<sup>-1</sup>·g<sup>-1</sup> (Gnaiger 2014; Table 6).



#### 1117 4.2. Size-specific flux: per sample size

1118  
1119 **4.2.1. Sample concentration,  $C_{mX}$ :** Considering permeabilized tissue, homogenate or cells as the  
1120 sample,  $X$ , the sample mass is  $m_X$  [mg], which is frequently measured as wet or dry weight,  $W_w$  or  $W_d$   
1121 [mg], respectively, or as amount of protein,  $m_{\text{Protein}}$ . The sample concentration is the mass of the  
1122 subsample per volume of the measurement chamber,  $C_{mX} = m_X \cdot V^{-1}$  [ $\text{g} \cdot \text{L}^{-1} = \text{mg} \cdot \text{mL}^{-1}$ ].  $X$  is the type of  
1123 sample—isolated mitochondria, tissue homogenate, permeabilized fibres or cells (**Table 5**).

1124 **4.2.2. Size-specific flux:** Cellular  $\text{O}_2$  flow can be compared between cells of identical size. To  
1125 take into account changes and differences in cell size, normalization is required to obtain cell size-  
1126 specific or mitochondrial marker-specific  $\text{O}_2$  flux (Renner *et al.* 2003).

- 1127 • **Mass-specific flux,  $J_{\text{O}_2/mX}$  [ $\text{mol} \cdot \text{s}^{-1} \cdot \text{kg}^{-1}$ ]:** Mass-specific flux is obtained by expressing  
1128 respiration per mass of sample,  $m_X$  [mg]. Flow per cell is divided by mass per cell,  $J_{\text{O}_2/mce} =$   
1129  $I_{\text{O}_2/Nce} \cdot M_{Nce}^{-1}$ . Or chamber volume-specific flux,  $J_{V,\text{O}_2}$ , is divided by mass concentration of  $X$  in  
1130 the chamber,  $J_{\text{O}_2/mX} = J_{V,\text{O}_2} \cdot C_{mX}^{-1}$ .
- 1131 • **Cell volume-specific flux,  $J_{\text{O}_2/VX}$  [ $\text{mol} \cdot \text{s}^{-1} \cdot \text{m}^{-3}$ ]:** Sample volume-specific flux is obtained by  
1132 expressing respiration per volume of sample. For example, in the case of using cells as sample  
1133 will be the volume of cells added to the chamber (**Figure 6**).

1134 If size-specific  $\text{O}_2$  flux is constant and independent of sample size, then there is no interaction  
1135 between the subsystems. For example, a 1.5 mg and a 3.0 mg muscle sample respire at identical mass-  
1136 specific flux. Mass-specific  $\text{O}_2$  flux, however, may change with the mass of a tissue sample, cells or  
1137 isolated mitochondria in the measuring chamber, in which the nature of the interaction becomes an issue.  
1138 Therefore, cell density must be optimized, particularly in experiments carried out in wells, considering  
1139 the confluency of the cell monolayer or clumps of cells (Salabei *et al.* 2014).

#### 1141 4.3. Marker-specific flux: per mitochondrial content

1142  
1143 Tissues can contain multiple cell populations that may have distinct mitochondrial subtypes.  
1144 Mitochondria undergo dynamic fission and fusion cycles, and can exist in multiple stages and sizes that  
1145 may be altered by a range of factors. The isolation of mitochondria (often achieved through differential  
1146 centrifugation) can therefore yield a subsample of the mitochondrial types present in a tissue, depending  
1147 on the isolation protocols utilized, *e.g.*, centrifugation speed. This possible bias should be taken into  
1148 account when planning experiments using isolated mitochondria. Different sizes of mitochondria are  
1149 enriched at specific centrifugation speeds, which can be used strategically for isolation of mitochondrial  
1150 subpopulations.

1151 Part of the mitochondrial content of a tissue is lost during preparation of isolated mitochondria.  
1152 The fraction of isolated mitochondria obtained from a tissue sample is expressed as mitochondrial  
1153 recovery. At a high mitochondrial recovery, the fraction of isolated mitochondria is more representative  
1154 of the total mitochondrial population than in preparations characterized by low recovery. Determination  
1155 of the mitochondrial recovery and yield is based on measurement of the concentration of a mitochondrial  
1156 marker in the stock of isolated mitochondria,  $C_{mtE,\text{stock}}$ , and crude tissue homogenate,  $C_{mtE,\text{thom}}$ , which  
1157 simultaneously provides information on the specific mitochondrial density in the sample,  $D_{mtE}$  (**Table**  
1158 **4**).

1159 When discussing concepts of normalization, it is essential to consider the question posed by the  
1160 study. If the study aims at comparing tissue performance—such as the effects of a treatment on a specific  
1161 tissue, then normalization for tissue mass or protein content is appropriate. However, if the aim is to  
1162 find differences in mitochondrial function independent of mitochondrial density (**Table 4**), then  
1163 normalization to a mitochondrial marker is imperative (**Figure 6**). One cannot assume that quantitative  
1164 changes in various markers—such as mitochondrial proteins—necessarily occur in parallel with one  
1165 another. It should be established that the marker chosen is not selectively altered by the performed  
1166 treatment. In conclusion, the normalization must reflect the question under investigation to reach a  
1167 satisfying answer. On the other hand, the goal of comparing results across projects and institutions  
1168 requires standardization on normalization for entry into a databank.

1169 **4.3.1. Mitochondrial concentration,  $C_{mtE}$ , and mitochondrial markers:** Mitochondrial  
1170 organelles compose a dynamic cellular reticulum in various states of fusion and fission. Hence, the  
1171 definition of an ‘amount’ of mitochondria is often misconceived: mitochondria cannot be counted  
1172 reliably as a number of occurring elementary components. Therefore, quantification of the amount of

1173 mitochondria depends on the measurement of chosen mitochondrial markers. “Mitochondria are the  
 1174 structural and functional elementary units of cell respiration” (Gnaiger 2014). The quantity of a  
 1175 mitochondrial marker can reflect the amount of *mitochondrial elementary components*,  $mtE$ , expressed  
 1176 in various mitochondrial elementary units [mtEU] specific for each measured mt-marker (**Table 4**).  
 1177 However, since mitochondrial quality may change in response to stimuli—particularly in mitochondrial  
 1178 dysfunction (Campos *et al.* 2017) and after exercise training (Pesta *et al.* 2011) and during aging (Daum  
 1179 *et al.* 2013)—some markers can vary while others are unchanged: (1) Mitochondrial volume and  
 1180 membrane area are structural markers, whereas mitochondrial protein mass is commonly used as a  
 1181 marker for isolated mitochondria. (2) Molecular and enzymatic mitochondrial markers (amounts or  
 1182 activities) can be selected as matrix markers, *e.g.*, citrate synthase activity, mtDNA; mtIM-markers, *e.g.*,  
 1183 cytochrome *c* oxidase activity,  $aa_3$  content, cardiolipin, or mtOM-markers, *e.g.*, the voltage-dependent  
 1184 anion channel (VDAC), TOM20. (3) Extending the measurement of mitochondrial marker enzyme  
 1185 activity to mitochondrial pathway capacity, ET- or OXPHOS-capacity can be considered as an  
 1186 integrative functional mitochondrial marker.

1187 Depending on the type of mitochondrial marker, the mitochondrial elementary component,  $mtE$ ,  
 1188 is expressed in marker-specific units. Mitochondrial concentration in the measurement chamber and the  
 1189 tissue of origin are quantified as (1) a quantity for normalization in functional analyses,  $C_{mtE}$ , and (2) a  
 1190 physiological output that is the result of mitochondrial biogenesis and degradation,  $D_{mtE}$ , respectively  
 1191 (**Table 4**). It is recommended, therefore, to distinguish *experimental mitochondrial concentration*,  $C_{mtE}$   
 1192  $= mtE \cdot V^{-1}$  and *physiological mitochondrial density*,  $D_{mtE} = mtE \cdot m_X^{-1}$ . Then mitochondrial density is the  
 1193 amount of mitochondrial elementary components per mass of tissue, which is a biological variable  
 1194 (**Figure 6**). The experimental variable is mitochondrial density multiplied by sample mass concentration  
 1195 in the measuring chamber,  $C_{mtE} = D_{mtE} \cdot C_{mX}$ , or mitochondrial content multiplied by sample number  
 1196 concentration,  $C_{mtE} = mtE_X \cdot C_{NX}$  (**Table 4**).

1197 **4.3.2. mt-Marker-specific flux,  $J_{O_2/mtE}$ :** Volume-specific metabolic  $O_2$  flux depends on: (1) the  
 1198 sample concentration in the volume of the instrument chamber,  $C_{mX}$ , or  $C_{NX}$ ; (2) the mitochondrial  
 1199 density in the sample,  $D_{mtE} = mtE \cdot m_X^{-1}$  or  $mtE_X = mtE \cdot N_X^{-1}$ ; and (3) the specific mitochondrial activity or  
 1200 performance per elementary mitochondrial unit,  $J_{O_2/mtE} = J_{V,O_2} \cdot C_{mtE}^{-1}$  [ $\text{mol} \cdot \text{s}^{-1} \cdot \text{mtEU}^{-1}$ ] (**Table 4**).  
 1201 Obviously, the numerical results for  $J_{O_2/mtE}$  vary with the type of mitochondrial marker chosen for  
 1202 measurement of  $mtE$  and  $C_{mtE} = mtE \cdot V^{-1}$  [ $\text{mtEU} \cdot \text{m}^{-3}$ ].

1203 Different methods are involved in the quantification of mitochondrial markers and have different  
 1204 strengths. Some problems are common for all mitochondrial markers,  $mtE$ : (1) Accuracy of  
 1205 measurement is crucial, since even a highly accurate and reproducible measurement of  $O_2$  flux results  
 1206 in an inaccurate and noisy expression if normalized by a biased and noisy measurement of a  
 1207 mitochondrial marker. This problem is acute in mitochondrial respiration because the denominators used  
 1208 (the mitochondrial markers) are often small moieties of which accurate and precise determination is  
 1209 difficult. This problem can be avoided when  $O_2$  fluxes measured in substrate-uncoupler-inhibitor  
 1210 titration protocols are normalized for flux in a defined respiratory reference state, which is used as an  
 1211 *internal* marker and yields flux control ratios, *FCRs*. *FCRs* are independent of externally measured  
 1212 markers and, therefore, are statistically robust, considering the limitations of ratios in general (Jasienski  
 1213 and Bazzaz 1999). *FCRs* indicate qualitative changes of mitochondrial respiratory control, with highest  
 1214 quantitative resolution, separating the effect of mitochondrial density or concentration on  $J_{O_2/mX}$  and  
 1215  $I_{O_2/NX}$  from that of function per elementary mitochondrial marker,  $J_{O_2/mtE}$  (Pesta *et al.* 2011; Gnaiger  
 1216 2014). (2) If mitochondrial quality does not change and only the amount of mitochondria varies as a  
 1217 determinant of mass-specific flux, any marker is equally qualified in principle; then in practice selection  
 1218 of the optimum marker depends only on the accuracy and precision of measurement of the mitochondrial  
 1219 marker. (3) If mitochondrial flux control ratios change, then there may not be any best mitochondrial  
 1220 marker. In general, measurement of multiple mitochondrial markers enables a comparison and  
 1221 evaluation of normalization for these mitochondrial markers. Particularly during postnatal development,  
 1222 the activity of marker enzymes—such as cytochrome *c* oxidase and citrate synthase—follows different  
 1223 time courses (Drahota *et al.* 2004). Evaluation of mitochondrial markers in healthy controls is  
 1224 insufficient for providing guidelines for application in the diagnosis of pathological states and specific  
 1225 treatments.

1226 In line with the concept of the respiratory control ratio (Chance and Williams 1955a), the most  
 1227 readily used normalization is that of flux control ratios and flux control factors (Gnaiger 2014). Selection  
 1228 of the state of maximum flux in a protocol as the reference state has the advantages of: (1) internal

1229 normalization; (2) statistically validated linearization of the response in the range of 0 to 1; and (3)  
 1230 consideration of maximum flux for integrating a large number of elementary steps in the OXPHOS- or  
 1231 ET-pathways. This reduces the risk of selecting a functional marker that is specifically altered by the  
 1232 treatment or pathology, yet increases the chance that the highly integrative pathway is disproportionately  
 1233 affected, *e.g.*, the OXPHOS- rather than ET-pathway in case of an enzymatic defect in the  
 1234 phosphorylation-pathway. In this case, additional information can be obtained by reporting flux control  
 1235 ratios based on a reference state that indicates stable tissue-mass specific flux.

1236 Stereological determination of mitochondrial content via two-dimensional transmission electron  
 1237 microscopy can have limitations due to the dynamics of mitochondrial size (Meinild Lundby *et al.*  
 1238 2017). Accurate determination of three-dimensional volume by two-dimensional microscopy can be  
 1239 both time consuming and statistically challenging (Larsen *et al.* 2012).

1240 The validity of using mitochondrial marker enzymes (citrate synthase activity, CI to CIV amount  
 1241 or activity) for normalization of flux is limited in part by the same factors that apply to flux control  
 1242 ratios. Strong correlations between various mitochondrial markers and citrate synthase activity  
 1243 (Reichmann *et al.* 1985; Boushel *et al.* 2007; Mogensen *et al.* 2007) are expected in a specific tissue of  
 1244 healthy persons and in disease states not specifically targeting citrate synthase. Citrate synthase activity  
 1245 is acutely modifiable by exercise (Tonkonogi *et al.* 1997; Leek *et al.* 2001). Evaluation of mitochondrial  
 1246 markers related to a selected age and sex cohort cannot be extrapolated to provide recommendations for  
 1247 normalization in respirometric diagnosis of disease, in different states of development and ageing,  
 1248 different cell types, tissues, and species. mtDNA normalized to nDNA via qPCR is correlated to  
 1249 functional mitochondrial markers including OXPHOS- and ET-capacity in some cases (Puntschart *et al.*  
 1250 1995; Wang *et al.* 1999; Menshikova *et al.* 2006; Boushel *et al.* 2007; Ehinger *et al.* 2015), but lack of  
 1251 such correlations have been reported (Menshikova *et al.* 2005; Schultz and Wiesner 2000; Pesta *et al.*  
 1252 2011). Several studies indicate a strong correlation between cardiolipin content and increase in  
 1253 mitochondrial function with exercise (Menshikova *et al.* 2005; Menshikova *et al.* 2007; Larsen *et al.*  
 1254 2012; Faber *et al.* 2014), but it has not been evaluated as a general mitochondrial biomarker in disease.  
 1255 With no single best mitochondrial marker, a good strategy is to quantify several different biomarkers to  
 1256 minimize the decorrelating effects caused by diseases, treatments, or other factors. Determination of  
 1257 multiple markers, particularly a matrix marker and a marker from the mtIM, allows tracking changes in  
 1258 mitochondrial quality defined by their ratio.

1259  
 1260

## 1261 5. Normalization of rate per system

1262  
 1263  
 1264

### 1263 5.1. Flow: per chamber

1265 The experimental system (experimental chamber) is part of the measurement instrument,  
 1266 separated from the environment as an isolated, closed, open, isothermal or non-isothermal system  
 1267 (Table 4). Reporting O<sub>2</sub> flows per respiratory chamber,  $I_{O_2}$  [nmol·s<sup>-1</sup>], restricts the analysis to intra-  
 1268 experimental comparison of relative differences.

1269  
 1270

### 1270 5.2. Flux: per chamber volume

1271

1272 **5.2.1. System-specific flux,  $J_{V,O_2}$ :** We distinguish between (1) the *system* with volume  $V$  and mass  
 1273  $m$  defined by the system boundaries, and (2) the *sample* or *objects* with volume  $V_X$  and mass  $m_X$  that are  
 1274 enclosed in the experimental chamber (Figure 6). Metabolic O<sub>2</sub> flow per object,  $I_{O_2/N_X}$ , is the total O<sub>2</sub>  
 1275 flow in the system divided by the number of objects,  $N_X$ , in the system.  $I_{O_2/N_X}$  increases as the mass of  
 1276 the object is increased. Sample mass-specific O<sub>2</sub> flux,  $J_{O_2/m_X}$  should be independent of the mass of the  
 1277 sample studied in the instrument chamber, but system volume-specific O<sub>2</sub> flux,  $J_{V,O_2}$  (per volume of the  
 1278 instrument chamber), increases in proportion to the mass of the sample in the chamber. Although  $J_{V,O_2}$   
 1279 depends on mass-concentration of the sample in the chamber, it should be independent of the chamber  
 1280 (system) volume at constant sample mass-concentration. There are practical limitations to increasing the  
 1281 mass-concentration of the sample in the chamber, when one is concerned about crowding effects and  
 1282 instrumental time resolution.

1283 **5.2.2. Advancement per volume:** When the reactor volume does not change during the reaction,  
 1284 which is typical for liquid phase reactions, the volume-specific flux of a chemical reaction  $r$  is the time

1285 derivative of the advancement of the reaction per unit volume,  $J_{V,rB} = d_{r\zeta_B}/dt \cdot V^{-1}$  [(mol·s<sup>-1</sup>)·L<sup>-1</sup>]. The *rate*  
 1286 *of concentration change* is  $dc_B/dt$  [(mol·L<sup>-1</sup>)·s<sup>-1</sup>], where concentration is  $c_B = n_B \cdot V^{-1}$ . There is a difference  
 1287 between (1)  $J_{V,rO_2}$  [mol·s<sup>-1</sup>·L<sup>-1</sup>] and (2) rate of concentration change [mol·L<sup>-1</sup>·s<sup>-1</sup>]. These merge into a  
 1288 single expression only in closed systems. In open systems, internal transformations (catabolic flux, O<sub>2</sub>  
 1289 consumption) are distinguished from external flux (such as O<sub>2</sub> supply). External fluxes of all substances  
 1290 are zero in closed systems. In a closed chamber O<sub>2</sub> consumption (internal flux of catabolic reactions  $k$ ;  
 1291  $I_{kO_2}$  [pmol·s<sup>-1</sup>]) causes a decline in the amount of O<sub>2</sub> in the system,  $n_{O_2}$  [nmol]. Normalization of these  
 1292 quantities for the volume of the system,  $V$  [L  $\equiv$  dm<sup>3</sup>], yields volume-specific O<sub>2</sub> flux,  $J_{V,kO_2} = I_{kO_2}/V$   
 1293 [nmol·s<sup>-1</sup>·L<sup>-1</sup>], and O<sub>2</sub> concentration, [O<sub>2</sub>] or  $c_{O_2} = n_{O_2} \cdot V^{-1}$  [ $\mu$ mol·L<sup>-1</sup> =  $\mu$ M = nmol·mL<sup>-1</sup>]. Instrumental  
 1294 background O<sub>2</sub> flux is due to external flux into a non-ideal closed respirometer, so total volume-specific  
 1295 flux has to be corrected for instrumental background O<sub>2</sub> flux—O<sub>2</sub> diffusion into or out of the  
 1296 instrumental chamber.  $J_{V,kO_2}$  is relevant mainly for methodological reasons and should be compared with  
 1297 the accuracy of instrumental resolution of background-corrected flux, *e.g.*,  $\pm 1$  nmol·s<sup>-1</sup>·L<sup>-1</sup> (Gnaiger  
 1298 2001). ‘Catabolic’ indicates O<sub>2</sub> flux,  $J_{kO_2}$ , corrected for: (1) instrumental background O<sub>2</sub> flux; (2)  
 1299 chemical background O<sub>2</sub> flux due to autoxidation of chemical components added to the incubation  
 1300 medium; and (3) *Rox* for O<sub>2</sub>-consuming side reactions unrelated to the catabolic pathway  $k$ .

1301  
1302

## 1303 6. Conversion of units

1304

1305 Many different units have been used to report the O<sub>2</sub> consumption rate, OCR (Table 6). SI base  
 1306 units provide the common reference to introduce the theoretical principles (Figure 6), and are used with  
 1307 appropriately chosen SI prefixes to express numerical data in the most practical format, with an effort  
 1308 towards unification within specific areas of application (Table 7). Reporting data in SI units—including  
 1309 the mole [mol], coulomb [C], joule [J], and second [s]—should be encouraged, particularly by journals  
 1310 that propose the use of SI units.

1311

1312 **Table 6. Conversion of various formats and units used in respirometry and**  
 1313 **ergometry.**  $e^-$  is the number of electrons or reducing equivalents.  $z_B$  is the charge number  
 1314 of entity B.  
1315

Format	1 Unit		Multiplication factor	SI-unit	Notes
$\underline{n}$	ng.atom O·s <sup>-1</sup>	(2 $e^-$ )	0.5	nmol O <sub>2</sub> ·s <sup>-1</sup>	
$\underline{n}$	ng.atom O·min <sup>-1</sup>	(2 $e^-$ )	8.33	pmol O <sub>2</sub> ·s <sup>-1</sup>	
$\underline{n}$	natom O·min <sup>-1</sup>	(2 $e^-$ )	8.33	pmol O <sub>2</sub> ·s <sup>-1</sup>	
$\underline{n}$	nmol O <sub>2</sub> ·min <sup>-1</sup>	(4 $e^-$ )	16.67	pmol O <sub>2</sub> ·s <sup>-1</sup>	
$\underline{n}$	nmol O <sub>2</sub> ·h <sup>-1</sup>	(4 $e^-$ )	0.2778	pmol O <sub>2</sub> ·s <sup>-1</sup>	
$\underline{V}$ to $\underline{n}$	mL O <sub>2</sub> ·min <sup>-1</sup> at STPD <sup>a</sup>		0.744	$\mu$ mol O <sub>2</sub> ·s <sup>-1</sup>	1
$\underline{e}$ to $\underline{n}$	W = J/s at -470 kJ/mol O <sub>2</sub>		-2.128	$\mu$ mol O <sub>2</sub> ·s <sup>-1</sup>	
$\underline{e}$ to $\underline{n}$	mA = mC·s <sup>-1</sup>	( $z_{H^+} = 1$ )	10.36	nmol H <sup>+</sup> ·s <sup>-1</sup>	2
$\underline{e}$ to $\underline{n}$	mA = mC·s <sup>-1</sup>	( $z_{O_2} = 4$ )	2.59	nmol O <sub>2</sub> ·s <sup>-1</sup>	2
$\underline{n}$ to $\underline{e}$	nmol H <sup>+</sup> ·s <sup>-1</sup>	( $z_{H^+} = 1$ )	0.09649	mA	3
$\underline{n}$ to $\underline{e}$	nmol O <sub>2</sub> ·s <sup>-1</sup>	( $z_{O_2} = 4$ )	0.38594	mA	3

1316 1 At standard temperature and pressure dry (STPD: 0 °C = 273.15 K and 1 atm = 101.325 kPa =  
 1317 760 mmHg), the molar volume of an ideal gas,  $V_m$ , and  $V_{m,O_2}$  is 22.414 and 22.392 L·mol<sup>-1</sup>,  
 1318 respectively. Rounded to three decimal places, both values yield the conversion factor of 0.744.  
 1319 For comparison at normal temperature and pressure dry (NTPD: 20 °C),  $V_{m,O_2}$  is 24.038 L·mol<sup>-1</sup>.  
 1320 Note that the SI standard pressure is 100 kPa.

1321 2 The multiplication factor is  $10^6/(z_B \cdot F)$ .

1322 3 The multiplication factor is  $z_B \cdot F/10^6$ .

1323

1324

**Table 7. Conversion of units with preservation of numerical values.**

Name	Frequently used unit	Equivalent unit	Notes
volume-specific flux, $J_{V,O_2}$	$\text{pmol}\cdot\text{s}^{-1}\cdot\text{mL}^{-1}$	$\text{nmol}\cdot\text{s}^{-1}\cdot\text{L}^{-1}$	1
cell-specific flow, $I_{O_2/\text{cell}}$	$\text{mmol}\cdot\text{s}^{-1}\cdot\text{L}^{-1}$	$\text{mol}\cdot\text{s}^{-1}\cdot\text{m}^{-3}$	
	$\text{pmol}\cdot\text{s}^{-1}\cdot 10^{-6}$ cells	$\text{amol}\cdot\text{s}^{-1}\cdot\text{cell}^{-1}$	2
cell number concentration, $C_{Nce}$	$\text{pmol}\cdot\text{s}^{-1}\cdot 10^{-9}$ cells	$\text{zmol}\cdot\text{s}^{-1}\cdot\text{cell}^{-1}$	3
	$10^6$ cells $\cdot\text{mL}^{-1}$	$10^9$ cells $\cdot\text{L}^{-1}$	
mitochondrial protein concentration, $C_{mtE}$	$0.1$ mg $\cdot\text{mL}^{-1}$	$0.1$ g $\cdot\text{L}^{-1}$	
mass-specific flux, $J_{O_2/m}$	$\text{pmol}\cdot\text{s}^{-1}\cdot\text{mg}^{-1}$	$\text{nmol}\cdot\text{s}^{-1}\cdot\text{g}^{-1}$	4
catabolic power, $P_k$	$\mu\text{W}\cdot 10^{-6}$ cells	$\text{pW}\cdot\text{cell}^{-1}$	1
volume	1,000 L	$\text{m}^3$ (1,000 kg)	
	L	$\text{dm}^3$ (kg)	
	mL	$\text{cm}^3$ (g)	
	$\mu\text{L}$	$\text{mm}^3$ (mg)	
	fL	$\mu\text{m}^3$ (pg)	5
amount of substance concentration	$\text{M} = \text{mol}\cdot\text{L}^{-1}$	$\text{mol}\cdot\text{dm}^{-3}$	

1325 1 pmol: picomole =  $10^{-12}$  mol1326 2 amol: attomole =  $10^{-18}$  mol1327 3 zmol: zeptomole =  $10^{-21}$  mol

1328

1329 Although volume is expressed as  $\text{m}^3$  using the SI base unit, the litre [ $\text{dm}^3$ ] is a conventional unit  
 1330 of volume for concentration and is used for most solution chemical kinetics. If one multiplies  $I_{O_2/Nce}$  by  
 1331  $C_{Nce}$ , then the result will not only be the amount of  $\text{O}_2$  [mol] consumed per time [ $\text{s}^{-1}$ ] in one litre [ $\text{L}^{-1}$ ],  
 1332 but also the change in  $\text{O}_2$  concentration per second (for any volume of an ideally closed system). This  
 1333 is ideal for kinetic modeling as it blends with chemical rate equations where concentrations are typically  
 1334 expressed in  $\text{mol}\cdot\text{L}^{-1}$  (Wagner *et al.* 2011). In studies of multinuclear cells—such as differentiated  
 1335 skeletal muscle cells—it is easy to determine the number of nuclei but not the total number of cells. A  
 1336 generalized concept, therefore, is obtained by substituting cells by nuclei as the sample entity. This does  
 1337 not hold, however, for non-nucleated platelets.

1338 For studies of cells, we recommend that respiration be expressed, as far as possible, as: (1)  $\text{O}_2$   
 1339 flux normalized for a mitochondrial marker, for separation of the effects of mitochondrial quality and  
 1340 content on cell respiration (this includes  $FCRs$  as a normalization for a functional mitochondrial  
 1341 marker); (2)  $\text{O}_2$  flux in units of cell volume or mass, for comparison of respiration of cells with different  
 1342 cell size (Renner *et al.* 2003) and with studies on tissue preparations, and (3)  $\text{O}_2$  flow in units of attomole  
 1343 ( $10^{-18}$  mol) of  $\text{O}_2$  consumed per second by each cell [ $\text{amol}\cdot\text{s}^{-1}\cdot\text{cell}^{-1}$ ], numerically equivalent to  
 1344 [ $\text{pmol}\cdot\text{s}^{-1}\cdot 10^{-6}$  cells]. This convention allows information to be easily used when designing experiments  
 1345 in which  $\text{O}_2$  flow must be considered. For example, to estimate the volume-specific  $\text{O}_2$  flux in an  
 1346 instrument chamber that would be expected at a particular cell number concentration, one simply needs  
 1347 to multiply the flow per cell by the number of cells per volume of interest. This provides the amount of  
 1348  $\text{O}_2$  [mol] consumed per time [ $\text{s}^{-1}$ ] per unit volume [ $\text{L}^{-1}$ ]. At an  $\text{O}_2$  flow of  $100$   $\text{amol}\cdot\text{s}^{-1}\cdot\text{cell}^{-1}$  and a cell  
 1349 density of  $10^9$  cells $\cdot\text{L}^{-1}$  ( $10^6$  cells $\cdot\text{mL}^{-1}$ ), the volume-specific  $\text{O}_2$  flux is  $100$   $\text{nmol}\cdot\text{s}^{-1}\cdot\text{L}^{-1}$  ( $100$   
 1350  $\text{pmol}\cdot\text{s}^{-1}\cdot\text{mL}^{-1}$ ).

1351 ET-capacity in human cell types including HEK 293, primary HUVEC, and fibroblasts ranges  
 1352 from  $50$  to  $180$   $\text{amol}\cdot\text{s}^{-1}\cdot\text{cell}^{-1}$ , measured in intact cells in the noncoupled state (see Gnaiger 2014). At  
 1353  $100$   $\text{amol}\cdot\text{s}^{-1}\cdot\text{cell}^{-1}$  corrected for  $Rox$ , the current across the mt-membranes,  $I_{H+e}$ , approximates  $193$   
 1354  $\text{pA}\cdot\text{cell}^{-1}$  or  $0.2$  nA per cell. See Rich (2003) for an extension of quantitative bioenergetics from the  
 1355 molecular to the human scale, with a transmembrane proton flux equivalent to  $520$  A in an adult at a  
 1356 catabolic power of  $-110$  W. Modelling approaches illustrate the link between protonmotive force and  
 1357 currents (Willis *et al.* 2016).

1358 We consider isolated mitochondria as powerhouses and proton pumps as molecular machines to  
 1359 relate experimental results to energy metabolism of the intact cell. The cellular  $P_{\gg/O_2}$  based on oxidation

of glycogen is increased by the glycolytic (fermentative) substrate-level phosphorylation of 3 P<sub>»</sub>/Glyc or 0.5 mol P<sub>»</sub> for each mol O<sub>2</sub> consumed in the complete oxidation of a mol glycosyl unit (Glyc). Adding 0.5 to the mitochondrial P<sub>»</sub>/O<sub>2</sub> ratio of 5.4 yields a bioenergetic cell physiological P<sub>»</sub>/O<sub>2</sub> ratio close to 6. Two NADH equivalents are formed during glycolysis and transported from the cytosol into the mitochondrial matrix, either by the malate-aspartate shuttle or by the glycerophosphate shuttle (**Figure 2A**) resulting in different theoretical yields of ATP generated by mitochondria, the energetic cost of which potentially must be taken into account. Considering also substrate-level phosphorylation in the TCA cycle, this high P<sub>»</sub>/O<sub>2</sub> ratio not only reflects proton translocation and OXPHOS studied in isolation, but integrates mitochondrial physiology with energy transformation in the living cell (Gnaiger 1993a).

## 7. Conclusions

Catabolic cell respiration is the process of exergonic and exothermic energy transformation in which scalar redox reactions are coupled to vectorial ion translocation across a semipermeable membrane, which separates the small volume of a bacterial cell or mitochondrion from the larger volume of its surroundings. The electrochemical exergy can be partially conserved in the phosphorylation of ADP to ATP or in ion pumping, or dissipated in an electrochemical short-circuit. Respiration is thus clearly distinguished from fermentation as the counterparts of cellular core energy metabolism. An O<sub>2</sub> flux balance scheme illustrates the relationships and general definitions (**Figures 1 and 2**).

---

### Box 3: Recommendations for studies with mitochondrial preparations

- Normalization of respiratory rates should be provided as far as possible:
  1. *Biophysical normalization*: on a per cell basis as O<sub>2</sub> flow; this may not be possible when dealing with coenocytic organisms, *e.g.*, filamentous fungi, or tissues without cross-walls separating individual cells, *e.g.*, muscle fibers.
  2. *Cellular normalization*: per g protein; per cell- or tissue-mass as mass-specific O<sub>2</sub> flux; per cell volume as cell volume-specific flux.
  3. *Mitochondrial normalization*: per mitochondrial marker as mt-specific flux.
- With information on cell size and the use of multiple normalizations, maximum potential information is available (Renner *et al.* 2003; Wagner *et al.* 2011; Gnaiger 2014). Reporting flow in a respiratory chamber [nmol·s<sup>-1</sup>] is discouraged, since it restricts the analysis to intra-experimental comparison of relative (qualitative) differences.
- Catabolic mitochondrial respiration is distinguished from residual O<sub>2</sub> consumption. Fluxes in mitochondrial coupling states should be, as far as possible, corrected for residual O<sub>2</sub> consumption.
- Different mechanisms of uncoupling should be distinguished by defined terms. The tightness of coupling relates to these uncoupling mechanisms, whereas the coupling stoichiometry varies as a function the substrate type involved in ET-pathways with either three or two redox proton pumps operating in series. Separation of tightness of coupling from the pathway-dependent coupling stoichiometry is possible only when the substrate type undergoing oxidation remains the same for respiration in LEAK-, OXPHOS-, and ET-states. In studies of the tightness of coupling, therefore, simple substrate-inhibitor combinations should be applied to exclude a shift in substrate competition that may occur when providing physiological substrate cocktails.
- In studies of isolated mitochondria, the mitochondrial recovery and yield should be reported. Experimental criteria such as transmission electron microscopy for evaluation of purity versus integrity should be considered. Mitochondrial markers—such as citrate synthase activity as an enzymatic matrix marker—provide a link to the tissue of origin on the basis of calculating the mitochondrial recovery, *i.e.*, the fraction of mitochondrial marker obtained from a unit mass of tissue. Total mitochondrial protein is frequently applied as a mitochondrial marker, which is restricted to isolated mitochondria.
- In studies of permeabilized cells, the viability of the cell culture or cell suspension of origin should be reported. Normalization should be evaluated for total cell count or viable cell count.
- Terms and symbols are summarized in **Table 8**. Their use will facilitate transdisciplinary communication and support further development of a consistent theory of bioenergetics and mitochondrial physiology. Technical terms related to and defined with normal words can be used as

1416 index terms in databases, support the creation of ontologies towards semantic information processing  
 1417 (MitoPedia), and help in communicating analytical findings as impactful data-driven stories.  
 1418 ‘Making data available without making it understandable may be worse than not making it available  
 1419 at all’ (National Academies of Sciences, Engineering, and Medicine 2018). Success will depend on  
 1420 taking further steps: (1) exhaustive text-mining considering Omics data and functional data; (2)  
 1421 network analysis of Omics data with bioinformatics tools; (3) cross-validation with distinct  
 1422 bioinformatics approaches; (4) correlation with functional data; (5) guidelines for biological  
 1423 validation of network data. This is a call to carefully contribute to FAIR principles (Findable,  
 1424 Accessible, Interoperable, Reusable) for the sharing of scientific data.

1426  
1427  
1428 **Table 8. Terms, symbols, and units.**

1431 1432	Term	Symbol	Unit	Links and comments
1433	alternative quinol oxidase	AOX		Figure 2B
1434	adenosine monophosphate	AMP		2 ADP ↔ ATP+AMP
1435	adenosine diphosphate	ADP		Table 1; Figures 1, 2 and 5
1436	adenosine triphosphate	ATP		Figures 2 and 5
1437	adenylates	AMP, ADP, ATP		Section 2.5.1
1438	amount of substance B	$n_B$	[mol]	
1439	ATP yield per O <sub>2</sub>	$Y_{P\gg/O_2}$		P <sub>2</sub> /O <sub>2</sub> ratio measured in any respiratory state
1440	catabolic reaction	k		Figures 1 and 3
1441	catabolic respiration	$J_{kO_2}$	<i>varies</i>	Figures 1 and 3
1442	cell respiration	$J_{rO_2}$	<i>varies</i>	Figure 1
1443	cell viability index	VI		$VI = N_{vce} \cdot N_{ce}^{-1} = 1 - N_{dce} \cdot N_{ce}^{-1}$
1444	charge number of entity B	$z_B$		Table 6; $z_{O_2} = 4$
1445	Complexes I to IV	CI to CIV		respiratory ET Complexes; Figure 2B
1446	concentration of substance B	$c_B = n_B \cdot V^{-1}$ ; [B]	[mol·m <sup>-3</sup> ]	Box 2
1447	coupling control state	CCS		Section 2.4.1
1448	dead cell number	$N_{dce}$	[x]	non-viable cells, loss of plasma membrane barrier function; Table 5
1449	electric format	$\underline{e}$	[C]	Table 6
1450	electron transfer system	ETS		state; Figures 2B and 4
1451	ET state	ET		Table 1; Figures 2B and 4; State 3u
1452	ET-capacity	$E$	<i>varies</i>	Table 1; Figure 4
1453	flow, for substance B	$I_B$	[mol·s <sup>-1</sup> ]	system-related extensive quantity; Figure 6
1454	flux, for substance B	$J_B$	<i>varies</i>	size-specific quantity; Figure 6
1455	inorganic phosphate	P <sub>i</sub>		Figure 2C
1456	inorganic phosphate carrier	PiC		Figure 2C
1457	intact cell number, viable cell number	$N_{vce}$	[x]	viable cells, intact plasma membrane barrier function; Table 5
1458	LEAK state	LEAK		state; Table 1; Figure 4; compare State 4
1459	LEAK-respiration	$L$	<i>varies</i>	Table 1; Figure 4
1460	mass format	$\underline{m}$	[kg]	Table 4; Figure 6
1461	mass of sample X	$m_X$	[kg]	Table 4
1462	mass, dry mass	$m_d$	[kg]	mass of sample X; Figure 6 (frequently called dry weight)
1463	mass, wet mass	$m_w$	[kg]	mass of sample X; Figure 6 (frequently called wet weight)

1474	mass of object $X$	$M_X = m_X \cdot N_X^{-1}$	$[\text{kg} \cdot \text{x}^{-1}]$	mass of entity $X$ ; Table 4
1475	MITOCARTA			<a href="https://www.broadinstitute.org/scientific-community/science/programs/metabolic-disease-program/publications/mitocarta/mitocarta-in-0">https://www.broadinstitute.org/scientific-community/science/programs/metabolic-disease-program/publications/mitocarta/mitocarta-in-0</a>
1476				
1477				
1478				
1479				
1480	MitoPedia			<a href="http://www.bioblast.at/index.php/MitoPedia">http://www.bioblast.at/index.php/MitoPedia</a>
1481	mitochondria or mitochondrial	mt		Box 1
1482	mitochondrial DNA	mtDNA		Box 1
1483	mitochondrial concentration	$C_{mtE} = mtE \cdot V^{-1}$	$[\text{mtEU} \cdot \text{m}^{-3}]$	Table 4
1484	mitochondrial content	$mtE_X$	$[\text{mtEU} \cdot \text{x}^{-1}]$	$mtE_X = mtE \cdot N_X^{-1}$ ; Table 4
1485	mitochondrial			
1486	elementary component	$mtE$	$[\text{mtEU}]$	quantity of mt-marker; Table 4
1487	mitochondrial elementary unit	mtEU	<i>varies</i>	specific units for mt-marker; Table 4
1488	mitochondrial inner membrane	mtIM		MIM is widely used; the first M is replaced by mt; Figure 2; Box 1
1489				
1490	mitochondrial outer membrane	mtOM		MOM is widely used; the first M is replaced by mt; Figure 2; Box 1
1491				
1492	mitochondrial recovery	$Y_{mtE}$		fraction of $mtE$ recovered in sample from the tissue of origin
1493				
1494	mitochondrial yield	$Y_{mtE/m}$		mt-yield per tissues mass; $Y_{mtE/m} = Y_{mtE} \cdot D_{mtE}$
1495				
1496	molar format	$\underline{n}$	$[\text{mol}]$	Table 6
1497	negative	neg		Figure 4
1498	number concentration of $X$	$C_{NX}$	$[\text{x} \cdot \text{m}^{-3}]$	Table 4
1499	number format	$\underline{N}$	$[\text{x}]$	Table 4; Figure 6
1500	number of cells	$N_{ce}$	$[\text{x}]$	$N_{ce} = N_{vce} + N_{dce}$ ; Table 5
1501	number of entities $X$	$N_X$	$[\text{x}]$	Table 4; Figure 6
1502	number of entity $B$	$N_B$	$[\text{x}]$	Table 4
1503	oxidative phosphorylation	OXPHOS		state; Table 1; Figure 4
1504	OXPHOS state	OXPHOS		Table 1; State 3 if [ADP] and [P <sub>i</sub> ] are saturating
1505				
1506	OXPHOS-capacity	$P$	<i>varies</i>	Table 1; Figure 4
1507	oxygen concentration	$c_{O_2} = n_{O_2} \cdot V^{-1}$	$[\text{mol} \cdot \text{m}^{-3}]$	[O <sub>2</sub> ]; Section 3.2
1508	oxygen flux, in reaction $r$	$J_{rO_2}$	<i>varies</i>	Figure 1
1509	pathway control state	PCS		Section 2.2
1510	permeability transition	mtPT		Figure 3; Section 2.4.3; MPT is widely used; M is replaced by mt
1511				
1512	permeabilized cell number	$N_{pce}$	$[\text{x}]$	experimental permeabilization of plasma membrane; Table 5
1513				
1514	phosphorylation of ADP to ATP	$P \gg$		Section 2.2
1515	$P \gg / O_2$ ratio	$P \gg / O_2$		mechanistic $Y_{P \gg / O_2}$ , calculated from pump stoichiometries; Figure 2B
1516				
1517	positive	pos		Figure 4
1518	proton in the negative compartment	$H^{+}_{neg}$		Figure 4
1519	proton in the positive compartment	$H^{+}_{pos}$		Figure 4
1520	protonmotive force	pmf	$[\text{V}]$	Figures 1, 2A and 4; Table 1
1521	rate of electron transfer in ET state	$E$	<i>varies</i>	ET-capacity; Table 1
1522	rate of LEAK-respiration	$L$	<i>varies</i>	Table 1
1523	rate of oxidative phosphorylation	$P$	<i>varies</i>	OXPHOS-capacity; Table 1
1524	rate of residual oxygen consumption	$ROx$		Table 1; Figure 1
1525	residual oxygen consumption	ROX		state; Table 1
1526	respiratory supercomplex	SC I <sub>n</sub> III <sub>n</sub> IV <sub>n</sub>		supramolecular assemblies composed of variable copy numbers ( $n$ ) of CI, CIII and CIV; Box 1
1527				
1528				
1529	specific mitochondrial density	$D_{mtE} = mtE \cdot m_X^{-1}$	$[\text{mtEU} \cdot \text{kg}^{-1}]$	Table 4



1530	substrate-uncoupler-inhibitor-			
1531	titration protocol	SUIT		Section 2.2
1532	volume	$V$	$[m^{-3}]$	Table 7
1533	volume format	$\underline{V}$	$[m^{-3}]$	Table 6

---

1535  
1536 Experimentally, respiration is separated in mitochondrial preparations from the interactions with  
1537 the fermentative pathways of the intact cell. OXPHOS analysis is based on the study of mitochondrial  
1538 preparations complementary to bioenergetic investigations of (1) submitochondrial particles and  
1539 molecular structures, (2) intact cells, and (3) organisms—from model organisms to the human species  
1540 including healthy and diseased persons (patients). Different mechanisms of respiratory uncoupling have  
1541 to be distinguished (**Figure 3**). Metabolic fluxes measured in defined coupling and pathway control  
1542 states (**Figures 5 and 6**) provide insights into the meaning of cellular and organismic respiration.

1543 The optimal choice for expressing mitochondrial and cell respiration as  $O_2$  flow per biological  
1544 sample, and normalization for specific tissue-markers (volume, mass, protein) and mitochondrial  
1545 markers (volume, protein, content, mtDNA, activity of marker enzymes, respiratory reference state) is  
1546 guided by the scientific question under study. Interpretation of the data depends critically on appropriate  
1547 normalization (**Figure 6**).

1548 MitoEAGLE can serve as a gateway to better diagnose mitochondrial respiratory adaptations and  
1549 defects linked to genetic variation, age-related health risks, sex-specific mitochondrial performance,  
1550 lifestyle with its effects on degenerative diseases, and thermal and chemical environment. The present  
1551 recommendations on coupling control states and rates, linked to the concept of the protonmotive force,  
1552 are focused on studies using mitochondrial preparations (**Box 3**). These will be extended in a series of  
1553 reports on pathway control of mitochondrial respiration, respiratory states in intact cells, and  
1554 harmonization of experimental procedures.

#### 1556 **Acknowledgements**

1557 We thank Beno M for management assistance, and Rich PR for valuable discussions. This publication  
1558 is based upon work from COST Action CA15203 MitoEAGLE, supported by COST (European  
1559 Cooperation in Science and Technology), in cooperation with COST Actions CA16225 EU-  
1560 CARDIOPROTECTION and CA17129 CardioRNA, and K-Regio project MitoFit (E.G.).

#### 1562 **Author contributions**

1563 This manuscript developed as an open invitation to scientists and students to join as coauthors in the bottom-up  
1564 spirit of COST, based upon a first draft written by the corresponding author, who edited all versions. Many  
1565 coauthors have focused on a particular section, contributed to the scope and quality of the manuscript, and are  
1566 listed in alphabetical order. Coauthors confirm that they have read the final manuscript and agree to implement  
1567 the recommendations into future manuscripts, presentations and teaching materials.

1569 **Competing financial interests:** E.G. is founder and CEO of Oroboros Instruments, Innsbruck, Austria.

#### 1571 **References**

- 1572  
1573 Altmann R (1894) Die Elementarorganismen und ihre Beziehungen zu den Zellen. Zweite vermehrte Auflage.  
1574 Verlag Von Veit & Comp, Leipzig:160 pp.  
1575 Baggeto LG, Testa-Perussini R (1990) Role of acetoin on the regulation of intermediate metabolism of Ehrlich  
1576 ascites tumor mitochondria: its contribution to membrane cholesterol enrichment modifying passive proton  
1577 permeability. Arch Biochem Biophys 283:341-8.  
1578 Beard DA (2005) A biophysical model of the mitochondrial respiratory system and oxidative phosphorylation.  
1579 PLoS Comput Biol 1(4):e36.  
1580 Benda C (1898) Weitere Mitteilungen über die Mitochondria. Verh Dtsch Physiol Ges:376-83.  
1581 Birkedal R, Laasmaa M, Vendelin M (2014) The location of energetic compartments affects energetic  
1582 communication in cardiomyocytes. Front Physiol 5:376.  
1583 Blier PU, Dufresne F, Burton RS (2001) Natural selection and the evolution of mtDNA-encoded peptides:  
1584 evidence for intergenomic co-adaptation. Trends Genet 17:400-6.  
1585 Blier PU, Guderley HE (1993) Mitochondrial activity in rainbow trout red muscle: the effect of temperature on  
1586 the ADP-dependence of ATP synthesis. J Exp Biol 176:145-58.

- 1587 Breton S, Beaupré HD, Stewart DT, Hoeh WR, Blier PU (2007) The unusual system of doubly uniparental  
 1588 inheritance of mtDNA: isn't one enough? *Trends Genet* 23:465-74.
- 1589 Brown GC (1992) Control of respiration and ATP synthesis in mammalian mitochondria and cells. *Biochem J*  
 1590 284:1-13.
- 1591 Burger G, Gray MW, Forget L, Lang BF (2013) Strikingly bacteria-like and gene-rich mitochondrial genomes  
 1592 throughout jakobid protists. *Genome Biol Evol* 5:418-38.
- 1593 Calvo SE, Klauser CR, Mootha VK (2016) MitoCarta2.0: an updated inventory of mammalian mitochondrial  
 1594 proteins. *Nucleic Acids Research* 44:D1251-7.
- 1595 Calvo SE, Julien O, Clauser KR, Shen H, Kamer KJ, Wells JA, Mootha VK (2017) Comparative analysis of  
 1596 mitochondrial N-termini from mouse, human, and yeast. *Mol Cell Proteomics* 16:512-23.
- 1597 Campos JC, Queliconi BB, Bozi LHM, Bechara LRG, Dourado PMM, Andres AM, Jannig PR, Gomes KMS,  
 1598 Zambelli VO, Rocha-Resende C, Guatimosim S, Brum PC, Mochly-Rosen D, Gottlieb RA, Kowaltowski AJ,  
 1599 Ferreira JCB (2017) Exercise reestablishes autophagic flux and mitochondrial quality control in heart failure.  
 1600 *Autophagy* 13:1304-317.
- 1601 Canton M, Luvisetto S, Schmehl I, Azzone GF (1995) The nature of mitochondrial respiration and discrimination  
 1602 between membrane and pump properties. *Biochem J* 310:477-81.
- 1603 Carrico C, Meyer JG, He W, Gibson BW, Verdin E (2018) The mitochondrial acylome emerges: proteomics,  
 1604 regulation by Sirtuins, and metabolic and disease implications. *Cell Metab* 27:497-512.
- 1605 Chan DC (2006) Mitochondria: dynamic organelles in disease, aging, and development. *Cell* 125:1241-52.
- 1606 Chance B, Williams GR (1955a) Respiratory enzymes in oxidative phosphorylation. I. Kinetics of oxygen  
 1607 utilization. *J Biol Chem* 217:383-93.
- 1608 Chance B, Williams GR (1955b) Respiratory enzymes in oxidative phosphorylation: III. The steady state. *J Biol*  
 1609 *Chem* 217:409-27.
- 1610 Chance B, Williams GR (1955c) Respiratory enzymes in oxidative phosphorylation. IV. The respiratory chain. *J*  
 1611 *Biol Chem* 217:429-38.
- 1612 Chance B, Williams GR (1956) The respiratory chain and oxidative phosphorylation. *Adv Enzymol Relat Subj*  
 1613 *Biochem* 17:65-134.
- 1614 Chowdhury SK, Djordjevic J, Albensi B, Fernyhough P (2015) Simultaneous evaluation of substrate-dependent  
 1615 oxygen consumption rates and mitochondrial membrane potential by TMRM and safranin in cortical  
 1616 mitochondria. *Biosci Rep* 36:e00286.
- 1617 Cobb LJ, Lee C, Xiao J, Yen K, Wong RG, Nakamura HK, Mehta HH, Gao Q, Ashur C, Huffman DM, Wan J,  
 1618 Muzumdar R, Barzilai N, Cohen P (2016) Naturally occurring mitochondrial-derived peptides are age-  
 1619 dependent regulators of apoptosis, insulin sensitivity, and inflammatory markers. *Aging (Albany NY)* 8:796-  
 1620 809.
- 1621 Cohen ER, Cvitas T, Frey JG, Holmström B, Kuchitsu K, Marquardt R, Mills I, Pavese F, Quack M, Stohner J,  
 1622 Strauss HL, Takami M, Thor HL (2008) Quantities, units and symbols in physical chemistry, IUPAC Green  
 1623 Book, 3rd Edition, 2nd Printing, IUPAC & RSC Publishing, Cambridge.
- 1624 Cooper H, Hedges LV, Valentine JC, eds (2009) The handbook of research synthesis and meta-analysis. Russell  
 1625 Sage Foundation.
- 1626 Coopersmith J (2010) Energy, the subtle concept. The discovery of Feynman's blocks from Leibnitz to Einstein.  
 1627 Oxford University Press:400 pp.
- 1628 Cummins J (1998) Mitochondrial DNA in mammalian reproduction. *Rev Reprod* 3:172-82.
- 1629 Dai Q, Shah AA, Garde RV, Yonish BA, Zhang L, Medvitz NA, Miller SE, Hansen EL, Dunn CN, Price TM  
 1630 (2013) A truncated progesterone receptor (PR-M) localizes to the mitochondrion and controls cellular  
 1631 respiration. *Mol Endocrinol* 27:741-53.
- 1632 Daum B, Walter A, Horst A, Osiewacz HD, Kühlbrandt W (2013) Age-dependent dissociation of ATP synthase  
 1633 dimers and loss of inner-membrane cristae in mitochondria. *Proc Natl Acad Sci U S A* 110:15301-6.
- 1634 Divakaruni AS, Brand MD (2011) The regulation and physiology of mitochondrial proton leak. *Physiology*  
 1635 (Bethesda) 26:192-205.
- 1636 Doerrier C, Garcia-Souza LF, Krumschnabel G, Wohlfarter Y, Mészáros AT, Gnaiger E (2018) High-Resolution  
 1637 Fluorescence Respirometry and OXPHOS protocols for human cells, permeabilized fibres from small biopsies of  
 1638 muscle, and isolated mitochondria. *Methods Mol Biol* 1782 (Palmeira CM, Moreno AJ, eds): Mitochondrial  
 1639 Bioenergetics, 978-1-4939-7830-4.
- 1640 Doskey CM, van 't Erve TJ, Wagner BA, Buettner GR (2015) Moles of a substance per cell is a highly informative  
 1641 dosing metric in cell culture. *PLoS One* 10:e0132572.
- 1642 Drahota Z, Milerová M, Stieglerová A, Houstek J, Ostádal B (2004) Developmental changes of cytochrome *c*  
 1643 oxidase and citrate synthase in rat heart homogenate. *Physiol Res* 53:119-22.
- 1644 Duarte FV, Palmeira CM, Rolo AP (2014) The role of microRNAs in mitochondria: small players acting wide.  
 1645 *Genes (Basel)* 5:865-86.
- 1646 Ehinger JK, Morota S, Hansson MJ, Paul G, Elmér E (2015) Mitochondrial dysfunction in blood cells from  
 1647 amyotrophic lateral sclerosis patients. *J Neurol* 262:1493-503.
- 1648 Ernster L, Schatz G (1981) Mitochondria: a historical review. *J Cell Biol* 91:227s-55s.

- 1649 Estabrook RW (1967) Mitochondrial respiratory control and the polarographic measurement of ADP:O ratios.  
1650 Methods Enzymol 10:41-7.
- 1651 Faber C, Zhu ZJ, Castellino S, Wagner DS, Brown RH, Peterson RA, Gates L, Barton J, Bickett M, Hagerty L,  
1652 Kimbrough C, Sola M, Bailey D, Jordan H, Elangbam CS (2014) Cardiolipin profiles as a potential biomarker  
1653 of mitochondrial health in diet-induced obese mice subjected to exercise, diet-restriction and ephedrine  
1654 treatment. J Appl Toxicol 34:1122-9.
- 1655 Feagin JE, Harrell MI, Lee JC, Coe KJ, Sands BH, Cannone JJ, Tami G, Schnare MN, Gutell RR (2012) The  
1656 fragmented mitochondrial ribosomal RNAs of *Plasmodium falciparum*. PLoS One 7:e38320.
- 1657 Fell D (1997) Understanding the control of metabolism. Portland Press.
- 1658 Forstner H, Gnaiger E (1983) Calculation of equilibrium oxygen concentration. In: Polarographic Oxygen Sensors.  
1659 Aquatic and Physiological Applications. Gnaiger E, Forstner H (eds), Springer, Berlin, Heidelberg, New  
1660 York:321-33.
- 1661 Garlid KD, Beavis AD, Ratkje SK (1989) On the nature of ion leaks in energy-transducing membranes. Biochim  
1662 Biophys Acta 976:109-20.
- 1663 Garlid KD, Semrad C, Zinchenko V. Does redox slip contribute significantly to mitochondrial respiration? In:  
1664 Schuster S, Rigoulet M, Ouhabi R, Mazat J-P, eds (1993) Modern trends in biothermokinetics. Plenum Press,  
1665 New York, London:287-93.
- 1666 Gerö D, Szabo C (2016) Glucocorticoids suppress mitochondrial oxidant production via upregulation of  
1667 uncoupling protein 2 in hyperglycemic endothelial cells. PLoS One 11:e0154813.
- 1668 Gnaiger E. Efficiency and power strategies under hypoxia. Is low efficiency at high glycolytic ATP production a  
1669 paradox? In: Surviving Hypoxia: Mechanisms of Control and Adaptation. Hochachka PW, Lutz PL, Sick T,  
1670 Rosenthal M, Van den Thillart G, eds (1993a) CRC Press, Boca Raton, Ann Arbor, London, Tokyo:77-109.
- 1671 Gnaiger E (1993b) Nonequilibrium thermodynamics of energy transformations. Pure Appl Chem 65:1983-2002.
- 1672 Gnaiger E (2001) Bioenergetics at low oxygen: dependence of respiration and phosphorylation on oxygen and  
1673 adenosine diphosphate supply. Respir Physiol 128:277-97.
- 1674 Gnaiger E (2009) Capacity of oxidative phosphorylation in human skeletal muscle. New perspectives of  
1675 mitochondrial physiology. Int J Biochem Cell Biol 41:1837-45.
- 1676 Gnaiger E (2014) Mitochondrial pathways and respiratory control. An introduction to OXPHOS analysis. 4th ed.  
1677 Mitochondr Physiol Network 19.12. Oroboros MiPNet Publications, Innsbruck:80 pp.
- 1678 Gnaiger E, Méndez G, Hand SC (2000) High phosphorylation efficiency and depression of uncoupled respiration  
1679 in mitochondria under hypoxia. Proc Natl Acad Sci USA 97:11080-5.
- 1680 Greggio C, Jha P, Kulkarni SS, Lagarrigue S, Broskey NT, Boutant M, Wang X, Conde Alonso S, Ofori E, Auwerx  
1681 J, Cantó C, Amati F (2017) Enhanced respiratory chain supercomplex formation in response to exercise in  
1682 human skeletal muscle. Cell Metab 25:301-11.
- 1683 Hinkle PC (2005) P/O ratios of mitochondrial oxidative phosphorylation. Biochim Biophys Acta 1706:1-11.
- 1684 Hofstadter DR (1979) Gödel, Escher, Bach: An eternal golden braid. A metaphorical fugue on minds and machines  
1685 in the spirit of Lewis Carroll. Harvester Press:499 pp.
- 1686 Illaste A, Laasmaa M, Peterson P, Vendelin M (2012) Analysis of molecular movement reveals latticelike  
1687 obstructions to diffusion in heart muscle cells. Biophys J 102:739-48.
- 1688 Jasienski M, Bazzaz FA (1999) The fallacy of ratios and the testability of models in biology. Oikos 84:321-26.
- 1689 Jepihhina N, Beraud N, Sepp M, Birkedal R, Vendelin M (2011) Permeabilized rat cardiomyocyte response  
1690 demonstrates intracellular origin of diffusion obstacles. Biophys J 101:2112-21.
- 1691 Karnkowska A, Vacek V, Zubáčová Z, Treitli SC, Petrželková R, Eme L, Novák L, Žárský V, Barlow LD, Herman  
1692 EK, Soukal P, Hroudová M, Doležal P, Stairs CW, Roger AJ, Eliáš M, Dacks JB, Vlček Č, Hampl V (2016) A  
1693 eukaryote without a mitochondrial organelle. Curr Biol 26:1274-84.
- 1694 Kenwood BM, Weaver JL, Bajwa A, Poon IK, Byrne FL, Murrow BA, Calderone JA, Huang L, Divakaruni AS,  
1695 Tomsig JL, Okabe K, Lo RH, Cameron Coleman G, Columbus L, Yan Z, Saucerman JJ, Smith JS, Holmes  
1696 JW, Lynch KR, Ravichandran KS, Uchiyama S, Santos WL, Rogers GW, Okusa MD, Bayliss DA, Hoehn KL  
1697 (2013) Identification of a novel mitochondrial uncoupler that does not depolarize the plasma membrane. Mol  
1698 Metab 3:114-23.
- 1699 Klepinin A, Ounpuu L, Guzun R, Chekulayev V, Timohhina N, Tepp K, Shevchuk I, Schlattner U, Kaambre T  
1700 (2016) Simple oxygraphic analysis for the presence of adenylate kinase 1 and 2 in normal and tumor cells. J  
1701 Bioenerg Biomembr 48:531-48.
- 1702 Klingenberg M (2017) UCP1 - A sophisticated energy valve. Biochimie 134:19-27.
- 1703 Koit A, Shevchuk I, Ounpuu L, Klepinin A, Chekulayev V, Timohhina N, Tepp K, Puurand M, Truu L, Heck K,  
1704 Valvere V, Guzun R, Kaambre T (2017) Mitochondrial respiration in human colorectal and breast cancer  
1705 clinical material is regulated differently. Oxid Med Cell Longev 1372640.
- 1706 Komlódi T, Tretter L (2017) Methylene blue stimulates substrate-level phosphorylation catalysed by succinyl-  
1707 CoA ligase in the citric acid cycle. Neuropharmacology 123:287-98.
- 1708 Korn E (1969) Cell membranes: structure and synthesis. Annu Rev Biochem 38:263-88.

- 1709 Lai N, M Kummitha C, Rosca MG, Fujioka H, Tandler B, Hoppel CL (2018) Isolation of mitochondrial  
1710 subpopulations from skeletal muscle: optimizing recovery and preserving integrity. *Acta Physiol*  
1711 (Oxf):e13182. doi: 10.1111/apha.13182.
- 1712 Lane N (2005) *Power, sex, suicide: mitochondria and the meaning of life*. Oxford University Press:354 pp.
- 1713 Larsen S, Nielsen J, Neigaard Nielsen C, Nielsen LB, Wibrand F, Stride N, Schroder HD, Boushel RC, Helge JW,  
1714 Dela F, Hey-Mogensen M (2012) Biomarkers of mitochondrial content in skeletal muscle of healthy young  
1715 human subjects. *J Physiol* 590:3349-60.
- 1716 Lee C, Zeng J, Drew BG, Sallam T, Martin-Montalvo A, Wan J, Kim SJ, Mehta H, Hevener AL, de Cabo R,  
1717 Cohen P (2015) The mitochondrial-derived peptide MOTS-c promotes metabolic homeostasis and reduces  
1718 obesity and insulin resistance. *Cell Metab* 21:443-54.
- 1719 Lee SR, Kim HK, Song IS, Youm J, Dizon LA, Jeong SH, Ko TH, Heo HJ, Ko KS, Rhee BD, Kim N, Han J  
1720 (2013) Glucocorticoids and their receptors: insights into specific roles in mitochondria. *Prog Biophys Mol Biol*  
1721 112:44-54.
- 1722 Leek BT, Mudaliar SR, Henry R, Mathieu-Costello O, Richardson RS (2001) Effect of acute exercise on citrate  
1723 synthase activity in untrained and trained human skeletal muscle. *Am J Physiol Regul Integr Comp Physiol*  
1724 280:R441-7.
- 1725 Lemasters JJ, Nieminen AL, Qian T, Trost LC, Elmore SP, Nishimura Y, Crowe RA, Cascio WE, Bradham CA,  
1726 Brenner DA, Herman B (1998) The mitochondrial permeability transition in cell death: a common mechanism  
1727 in necrosis, apoptosis and autophagy. *Biochim Biophys Acta* 1366:177-96.
- 1728 Lemieux H, Blier PU, Gnaiger E (2017) Remodeling pathway control of mitochondrial respiratory capacity by  
1729 temperature in mouse heart: electron flow through the Q-junction in permeabilized fibers. *Sci Rep* 7:2840.
- 1730 Lenaz G, Tioli G, Falasca AI, Genova ML (2017) Respiratory supercomplexes in mitochondria. In: *Mechanisms*  
1731 *of primary energy trasduction in biology*. M Wikstrom (ed) Royal Society of Chemistry Publishing, London,  
1732 UK:296-337.
- 1733 Liu S, Roellig DM, Guo Y, Li N, Frace MA, Tang K, Zhang L, Feng Y, Xiao L (2016) Evolution of mitosome  
1734 metabolism and invasion-related proteins in *Cryptosporidium*. *BMC Genomics* 17:1006.
- 1735 Luo S, Valencia CA, Zhang J, Lee NC, Slone J, Gui B, Wang X, Li Z, Dell S, Brown J, Chen SM, Chien YH,  
1736 Hwu WL, Fan PC, Wong LJ, Atwal PS, Huang T (2018) Biparental inheritance of mitochondrial DNA in  
1737 humans. *Proc Natl Acad Sci U S A* doi: 10.1073/pnas.1810946115.
- 1738 Margulis L (1970) *Origin of eukaryotic cells*. New Haven: Yale University Press.
- 1739 McDonald AE, Vanlerberghe GC, Staples JF (2009) Alternative oxidase in animals: unique characteristics and  
1740 taxonomic distribution. *J Exp Biol* 212:2627-34.
- 1741 Meinild Lundby AK, Jacobs RA, Gehrig S, de Leur J, Hauser M, Bonne TC, Flück D, Dandanell S, Kirk N, Kaech  
1742 A, Ziegler U, Larsen S, Lundby C (2018) Exercise training increases skeletal muscle mitochondrial volume  
1743 density by enlargement of existing mitochondria and not de novo biogenesis. *Acta Physiol* 222, e12905.
- 1744 Menshikova EV, Ritov VB, Fairfull L, Ferrell RE, Kelley DE, Goodpaster BH (2006) Effects of exercise on  
1745 mitochondrial content and function in aging human skeletal muscle. *J Gerontol A Biol Sci Med Sci* 61:534-40.
- 1746 Menshikova EV, Ritov VB, Ferrell RE, Azuma K, Goodpaster BH, Kelley DE (2007) Characteristics of skeletal  
1747 muscle mitochondrial biogenesis induced by moderate-intensity exercise and weight loss in obesity. *J Appl*  
1748 *Physiol* (1985) 103:21-7.
- 1749 Menshikova EV, Ritov VB, Toledo FG, Ferrell RE, Goodpaster BH, Kelley DE (2005) Effects of weight loss and  
1750 physical activity on skeletal muscle mitochondrial function in obesity. *Am J Physiol Endocrinol Metab*  
1751 288:E818-25.
- 1752 Miller GA (1991) *The science of words*. Scientific American Library New York:276 pp.
- 1753 Mitchell P (1961) Coupling of phosphorylation to electron and hydrogen transfer by a chemi-osmotic type of  
1754 mechanism. *Nature* 191:144-8.
- 1755 Mitchell P (2011) Chemiosmotic coupling in oxidative and photosynthetic phosphorylation. *Biochim Biophys*  
1756 *Acta Bioenergetics* 1807:1507-38.
- 1757 Mogensen M, Sahlin K, Fernström M, Glintborg D, Vind BF, Beck-Nielsen H, Højlund K (2007) Mitochondrial  
1758 respiration is decreased in skeletal muscle of patients with type 2 diabetes. *Diabetes* 56:1592-9.
- 1759 Mohr PJ, Phillips WD (2015) Dimensionless units in the SI. *Metrologia* 52:40-7.
- 1760 Moreno M, Giacco A, Di Munno C, Goglia F (2017) Direct and rapid effects of 3,5-diiodo-L-thyronine (T2). *Mol*  
1761 *Cell Endocrinol* 7207:30092-8.
- 1762 Morrow RM, Picard M, Derbeneva O, Leipzig J, McManus MJ, Gouspillou G, Barbat-Artigas S, Dos Santos C,  
1763 Hepple RT, Murdock DG, Wallace DC (2017) Mitochondrial energy deficiency leads to hyperproliferation of  
1764 skeletal muscle mitochondria and enhanced insulin sensitivity. *Proc Natl Acad Sci U S A* 114:2705-10.
- 1765 Murley A, Nunnari J (2016) The emerging network of mitochondria-organelle contacts. *Mol Cell* 61:648-53.
- 1766 National Academies of Sciences, Engineering, and Medicine (2018) *International coordination for science data*  
1767 *infrastructure: Proceedings of a workshop—in brief*. Washington, DC: The National Academies Press. doi:  
1768 <https://doi.org/10.17226/25015>.

- 1769 Oemer G, Lackner L, Muigg K, Krumschnabel G, Watschinger K, Sailer S, Lindner H, Gnaiger E, Wortmann SB,  
 1770 Werner ER, Zschocke J, Keller MA (2018) The molecular structural diversity of mitochondrial cardiolipins.  
 1771 Proc Nat Acad Sci U S A 115:4158-63.
- 1772 Palmfeldt J, Bross P (2017) Proteomics of human mitochondria. Mitochondrion 33:2-14.
- 1773 Paradies G, Paradies V, De Benedictis V, Ruggiero FM, Petrosillo G (2014) Functional role of cardiolipin in  
 1774 mitochondrial bioenergetics. Biochim Biophys Acta 1837:408-17.
- 1775 Pesta D, Gnaiger E (2012) High-Resolution Respirometry. OXPHOS protocols for human cells and permeabilized  
 1776 fibres from small biopsies of human muscle. Methods Mol Biol 810:25-58.
- 1777 Pesta D, Hoppel F, Macek C, Messner H, Faulhaber M, Kobel C, Parson W, Burtscher M, Schocke M, Gnaiger E  
 1778 (2011) Similar qualitative and quantitative changes of mitochondrial respiration following strength and  
 1779 endurance training in normoxia and hypoxia in sedentary humans. Am J Physiol Regul Integr Comp Physiol  
 1780 301:R1078–87.
- 1781 Price TM, Dai Q (2015) The role of a mitochondrial progesterone receptor (PR-M) in progesterone action. Semin  
 1782 Reprod Med 33:185-94.
- 1783 Puchowicz MA, Varnes ME, Cohen BH, Friedman NR, Kerr DS, Hoppel CL (2004) Oxidative phosphorylation  
 1784 analysis: assessing the integrated functional activity of human skeletal muscle mitochondria – case studies.  
 1785 Mitochondrion 4:377-85. Puntschart A, Claassen H, Jostarndt K, Hoppeler H, Billeter R (1995) mRNAs of  
 1786 enzymes involved in energy metabolism and mtDNA are increased in endurance-trained athletes. Am J Physiol  
 1787 269:C619-25.
- 1788 Quiros PM, Mottis A, Auwerx J (2016) Mitonuclear communication in homeostasis and stress. Nat Rev Mol Cell  
 1789 Biol 17:213-26.
- 1790 Rackham O, Mercer TR, Filipovska A (2012) The human mitochondrial transcriptome and the RNA-binding  
 1791 proteins that regulate its expression. WIREs RNA 3:675–95.
- 1792 Reichmann H, Hoppeler H, Mathieu-Costello O, von Bergen F, Pette D (1985) Biochemical and ultrastructural  
 1793 changes of skeletal muscle mitochondria after chronic electrical stimulation in rabbits. Pflugers Arch 404:1-9.
- 1794 Renner K, Amberger A, Konwalinka G, Gnaiger E (2003) Changes of mitochondrial respiration, mitochondrial  
 1795 content and cell size after induction of apoptosis in leukemia cells. Biochim Biophys Acta 1642:115-23.
- 1796 Rice DW, Alverson AJ, Richardson AO, Young GJ, Sanchez-Puerta MV, Munzinger J, Barry K, Boore JL, Zhang  
 1797 Y, dePamphilis CW, Knox EB, Palmer JD (2016) Horizontal transfer of entire genomes via mitochondrial  
 1798 fusion in the angiosperm *Amborella*. Science 342:1468-73.
- 1799 Rich P (2003) Chemiosmotic coupling: The cost of living. Nature 421:583.
- 1800 Rich PR (2013) Chemiosmotic theory. Encyclopedia Biol Chem 1:467-72.
- 1801 Roger JA, Munoz-Gomes SA, Kamikawa R (2017) The origin and diversification of mitochondria. Curr Biol  
 1802 27:R1177-92.
- 1803 Rostovtseva TK, Sheldon KL, Hassanzadeh E, Monge C, Saks V, Bezrukov SM, Sackett DL (2008) Tubulin  
 1804 binding blocks mitochondrial voltage-dependent anion channel and regulates respiration. Proc Natl Acad Sci  
 1805 USA 105:18746-51.
- 1806 Rustin P, Parfait B, Chretien D, Bourgeron T, Djouadi F, Bastin J, Rötig A, Munnich A (1996) Fluxes of  
 1807 nicotinamide adenine dinucleotides through mitochondrial membranes in human cultured cells. J Biol Chem  
 1808 271:14785-90.
- 1809 Saks VA, Veksler VI, Kuznetsov AV, Kay L, Sikk P, Tiivel T, Tranqui L, Olivares J, Winkler K, Wiedemann F,  
 1810 Kunz WS (1998) Permeabilised cell and skinned fiber techniques in studies of mitochondrial function in vivo.  
 1811 Mol Cell Biochem 184:81-100.
- 1812 Salabei JK, Gibb AA, Hill BG (2014) Comprehensive measurement of respiratory activity in permeabilized cells  
 1813 using extracellular flux analysis. Nat Protoc 9:421-38.
- 1814 Sazanov LA (2015) A giant molecular proton pump: structure and mechanism of respiratory complex I. Nat Rev  
 1815 Mol Cell Biol 16:375-88.
- 1816 Schneider TD (2006) Claude Shannon: biologist. The founder of information theory used biology to formulate the  
 1817 channel capacity. IEEE Eng Med Biol Mag 25:30-3.
- 1818 Schönfeld P, Dymkowska D, Wojtczak L (2009) Acyl-CoA-induced generation of reactive oxygen species in  
 1819 mitochondrial preparations is due to the presence of peroxisomes. Free Radic Biol Med 47:503-9.
- 1820 Schultz J, Wiesner RJ (2000) Proliferation of mitochondria in chronically stimulated rabbit skeletal muscle--  
 1821 transcription of mitochondrial genes and copy number of mitochondrial DNA. J Bioenerg Biomembr 32:627-  
 1822 34.
- 1823 Speijer D (2016) Being right on Q: shaping eukaryotic evolution. Biochem J 473:4103-27.
- 1824 Sugiura A, Mattie S, Prudent J, McBride HM (2017) Newly born peroxisomes are a hybrid of mitochondrial and  
 1825 ER-derived pre-peroxisomes. Nature 542:251-4.
- 1826 Simson P, Jepihhina N, Laasmaa M, Peterson P, Birkedal R, Vendelin M (2016) Restricted ADP movement in  
 1827 cardiomyocytes: Cytosolic diffusion obstacles are complemented with a small number of open mitochondrial  
 1828 voltage-dependent anion channels. J Mol Cell Cardiol 97:197-203.
- 1829 Singh BK, Sinha RA, Tripathi M, Mendoza A, Ohba K, Sy JAC, Xie SY, Zhou J, Ho JP, Chang CY, Wu Y,  
 1830 Giguère V, Bay BH, Vanacker JM, Ghosh S, Gauthier K, Hollenberg AN, McDonnell DP, Yen PM (2018)

- 1831 Thyroid hormone receptor and ERR $\alpha$  coordinately regulate mitochondrial fission, mitophagy, biogenesis, and  
 1832 function. *Sci Signal* 11(536) DOI: 10.1126/scisignal.aam5855.
- 1833 Stucki JW, Ineichen EA (1974) Energy dissipation by calcium recycling and the efficiency of calcium transport in  
 1834 rat-liver mitochondria. *Eur J Biochem* 48:365-75.
- 1835 Tonkonogi M, Harris B, Sahlin K (1997) Increased activity of citrate synthase in human skeletal muscle after a  
 1836 single bout of prolonged exercise. *Acta Physiol Scand* 161:435-6.
- 1837 Torralba D, Baixauli F, Sánchez-Madrid F (2016) Mitochondria know no boundaries: mechanisms and functions  
 1838 of intercellular mitochondrial transfer. *Front Cell Dev Biol* 4:107. eCollection 2016.
- 1839 Vamecq J, Schepers L, Parmentier G, Mannaerts GP (1987) Inhibition of peroxisomal fatty acyl-CoA oxidase by  
 1840 antimycin A. *Biochem J* 248:603-7.
- 1841 Waczulikova I, Habodaszova D, Cagalinec M, Ferko M, Ulicna O, Mateasik A, Sikurova L, Ziegelhöffer A (2007)  
 1842 Mitochondrial membrane fluidity, potential, and calcium transients in the myocardium from acute diabetic rats.  
 1843 *Can J Physiol Pharmacol* 85:372-81.
- 1844 Wagner BA, Venkataraman S, Buettner GR (2011) The rate of oxygen utilization by cells. *Free Radic Biol Med*  
 1845 51:700-712.
- 1846 Wang H, Hiatt WR, Barstow TJ, Brass EP (1999) Relationships between muscle mitochondrial DNA content,  
 1847 mitochondrial enzyme activity and oxidative capacity in man: alterations with disease. *Eur J Appl Physiol*  
 1848 *Occup Physiol* 80:22-7.
- 1849 Watt IN, Montgomery MG, Runswick MJ, Leslie AG, Walker JE (2010) Bioenergetic cost of making an adenosine  
 1850 triphosphate molecule in animal mitochondria. *Proc Natl Acad Sci U S A* 107:16823-7.
- 1851 Weibel ER, Hoppeler H (2005) Exercise-induced maximal metabolic rate scales with muscle aerobic capacity. *J*  
 1852 *Exp Biol* 208:1635-44.
- 1853 White DJ, Wolff JN, Pierson M, Gemmell NJ (2008) Revealing the hidden complexities of mtDNA inheritance.  
 1854 *Mol Ecol* 17:4925-42.
- 1855 Wikström M, Hummer G (2012) Stoichiometry of proton translocation by respiratory complex I and its  
 1856 mechanistic implications. *Proc Natl Acad Sci U S A* 109:4431-6.
- 1857 Williams EG, Wu Y, Jha P, Dubuis S, Blattmann P, Argmann CA, Houten SM, Amariuta T, Wolski W, Zamboni  
 1858 N, Aebersold R, Auwerx J (2016) Systems proteomics of liver mitochondria function. *Science* 352  
 1859 (6291):aad0189
- 1860 Willis WT, Jackman MR, Messer JI, Kuzmiak-Glancy S, Glancy B (2016) A simple hydraulic analog model of  
 1861 oxidative phosphorylation. *Med Sci Sports Exerc* 48:990-1000.
- 1862 Zíková A, Hampl V, Paris Z, Týč J, Lukeš J (2016) Aerobic mitochondria of parasitic protists: diverse genomes  
 1863 and complex functions. *Mol Biochem Parasitol* 209:46-57.

## 1866 Supplement

### 1868 S1. Manuscript phases and versions - an open-access approach

1870 This manuscript on ‘Mitochondrial respiratory states and rates’ is a position statement in the frame of COST Action  
 1871 CA15203 MitoEAGLE. The global MitoEAGLE network made it possible to collaborate with a large number of  
 1872 coauthors to reach consensus on the present manuscript. Nevertheless, we do not consider scientific progress to be  
 1873 supported by ‘declaration’ statements (other than on ethical or political issues). Our manuscript aims at providing  
 1874 arguments for further debate rather than pushing opinions. We hope to initiate a much broader process of  
 1875 discussion and want to raise the awareness of the importance of a consistent terminology for reporting of scientific  
 1876 data in the field of bioenergetics, mitochondrial physiology and pathology. Quality of research requires quality of  
 1877 communication. Some established researchers in the field may not want to re-consider the use of jargon which has  
 1878 become established despite deficiencies of accuracy and meaning. In the long run, superior standards will become  
 1879 accepted. We hope to contribute to this evolutionary process, with an emphasis on harmonization rather than  
 1880 standardization.

1881 *Phase 1* The protonmotive force and respiratory control

1882 [http://www.mitoeagle.org/index.php/The\\_protonmotive\\_force\\_and\\_respiratory\\_control](http://www.mitoeagle.org/index.php/The_protonmotive_force_and_respiratory_control)

- 1883 • 2017-04-09 to 2017-09-18 (44 versions)
- 1884 • 2017-09-21 to 2018-02-06 (44+21 versions)

1885 [http://www.mitoeagle.org/index.php/MitoEAGLE\\_preprint\\_2017-09-21](http://www.mitoeagle.org/index.php/MitoEAGLE_preprint_2017-09-21)

1886 2017-11-11: Print version (16) for MiP2017/MitoEAGLE conference in Hradec Kralove

1887 *Phase 2* Mitochondrial respiratory states and rates: Building blocks of mitochondrial physiology Part 1

1888 [http://www.mitoeagle.org/index.php/MitoEAGLE\\_preprint\\_2018-02-08](http://www.mitoeagle.org/index.php/MitoEAGLE_preprint_2018-02-08)

- 1889 • 2018-02-08 – 2018-12-12 (44 plus 50 Versions)


1890 *Phase 3* 2018-12-12: Mitochondrial respiratory states and rates. Submission to the preprint server [BioRxiv](https://www.biorxiv.org/)

1891 *Phase 4* Journal submission: CELL METABOLISM, aiming at indexing by *The Web of Science* and *PubMed*.

1892  
1893  
1894  
1895  
1896  
1897

## S2. Joining COST Actions

- CA15203 MitoEAGLE - [http://www.cost.eu/COST\\_Actions/ca/CA15203](http://www.cost.eu/COST_Actions/ca/CA15203)
- CA16225 EU-CARDIOPROTECTION - [http://www.cost.eu/COST\\_Actions/ca/CA16225](http://www.cost.eu/COST_Actions/ca/CA16225)
- CA17129 CardioRNA - [http://www.cost.eu/COST\\_Actions/ca/CA17129](http://www.cost.eu/COST_Actions/ca/CA17129)



# Mitochondrial respiratory states and rates:

## Building blocks of mitochondrial physiology

Part 1 - [www.mitoeagle.org/index.php/MitoEAGLE\\_preprint\\_2018-02-08](http://www.mitoeagle.org/index.php/MitoEAGLE_preprint_2018-02-08)

Gnaiger E<sup>1,2</sup>, corresponding author  
355 co-authors, MitoEAGLE Working Group

<sup>1</sup>Medical University Innsbruck  
<sup>2</sup>Oroboros, Innsbruck, Austria

### Aims

Clarity of concept and consistency of nomenclature facilitate effective transdisciplinary communication, education, and ultimately further discovery.

Adhering to uniform standards and harmonizing the terminology concerning mitochondrial respiratory states and rates will support the development of databases of mitochondrial respiratory function in cells, tissues, and species.

### Summary

Recommendations on coupling control states and rates are focused on studies with mitochondrial preparations.

**Fig. 1:** Respiration is defined by O<sub>2</sub> flux balance.

**Fig. 2:** OXPHOS analysis is based on the study of mt- preparations. Metabolic fluxes measured in defined coupling and pathway control states provide insights into the meaning of cellular respiration.

**Fig. 3:** Interpretation of respiratory rates depends critically on appropriate normalization.

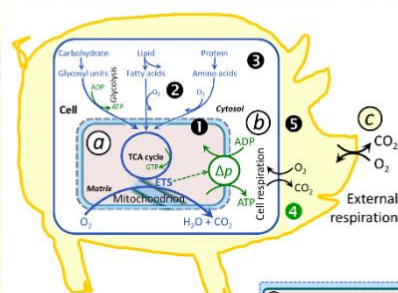


**Figure 1. From mitochondrial to external respiration**

Mitochondrial (mt) respiration is the oxidation of fuel substrates (electron donors) and reduction of O<sub>2</sub> catalysed by the electron transfer system, ETS:

- a** mt-catabolic respiration, excluding
- b** mt-residual oxygen consumption, *Rox*.
- b** Total cellular O<sub>2</sub> consumption, including mt-*Rox*,
- c** non-mt catabolic *Rox*, particularly by peroxisomal oxidases, and
- e** non-mt *Rox* unrelated to catabolism.

**C** External respiration, including aerobic microbial respiration, and extracellular O<sub>2</sub> consumption.

MIPart by Odra Noel

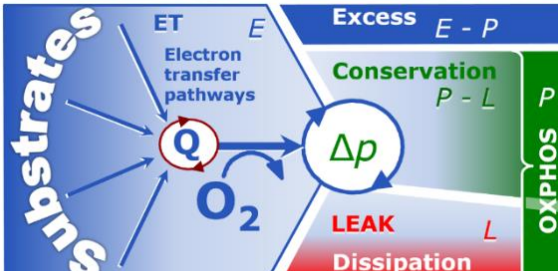


**Figure 2. Respiratory states (ET, OXPHOS, LEAK) and corresponding rates (E, P, L)**



Net OXPHOS-capacity, *P-L*, and excess capacity, *E-P*.

State	<i>J<sub>ko</sub></i>	<i>J<sub>p</sub></i>	$\Delta p$	Inducing factors	Limiting factors
LEAK	<i>L</i> ; low, cation leak-dependent respiration	0	max.	proton leak, slip, and cation cycling	<i>J<sub>p</sub></i> = 0: (1) without ADP, <i>L<sub>S</sub></i> ; (2) max. ATP/ADP ratio, <i>L<sub>T</sub></i> ; or (3) inhibition of the phosphorylation-pathway, <i>L<sub>Only</sub></i>
OXPHOS	<i>P</i> ; high, ADP-stimulated respiration	max.	high	kinetically-saturating [ADP] and [P <sub>i</sub> ]	<i>J<sub>p</sub></i> by phosphorylation-pathway, or <i>J<sub>ko</sub></i> by ET-capacity
ET	<i>E</i> ; max., noncoupled respiration	0	low	optimal external uncoupler concentration for max. <i>J<sub>o, E</sub></i>	<i>J<sub>ko</sub></i> by ET-capacity
ROX	<i>Rox</i> ; min., residual O <sub>2</sub> consumption	0	0	<i>J<sub>o, Rox</sub></i> in non-ET-pathway oxidation reactions	inhibition of all ET-pathways; or absence of fuel substrates

**Figure 3. Normalization of rate**

**A:** Cell respiration is normalized for (1) the experimental **Sample** (flow per object, mass-specific flux, or cell-volume-specific flux); or (2) for methodological reasons for the **Chamber** volume.

**B:** **Flow per cell** [amol O<sub>2</sub> s<sup>-1</sup>·cell<sup>-1</sup>] is flux per chamber volume, *J<sub>v</sub>* [nmol O<sub>2</sub>·s<sup>-1</sup>·L<sup>-1</sup>], divided by cell concentration in the chamber, *N<sub>cell</sub>/V* [cells·L<sup>-1</sup>], which is **Number** analysis. In **Structure** analysis, aerobic cell performance is mt-quality (mt-specific flux, e.g., per citrate synthase, CS) times mt-quantity, or mt-function times mt-structure.

**MitoEAGLE**  
Join  
**COST Action CA15203**

Funded by the Horizon 2020 Framework Programme of the European Union

[www.mitoeagle.org/index.php/MitoEAGLE](http://www.mitoeagle.org/index.php/MitoEAGLE)

1898

**COST Action  
CA15203**

**MitoEAGLE**

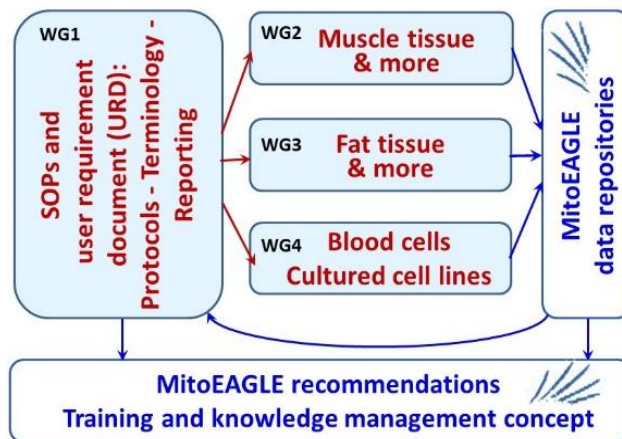
**Evolution Age Gender  
Lifestyle Environment**



**Mission of the global MitoEAGLE network**

in collaboration with the Mitochondrial Physiology Society, MiPs

- Improve our knowledge on mitochondrial function in health and disease with regard to **Evolution, Age, Gender, Lifestyle and Environment**
- Interrelate studies across laboratories with the help of a MitoEAGLE data management system
- Provide standardized measures to link mitochondrial and physiological performance to understand the myriad of factors that play a role in mitochondrial physiology



**Join the COST Action MitoEAGLE - contribute to the quality management network.**



More information:  
[www.mitoeagle.org](http://www.mitoeagle.org)



Funded by the Horizon 2020 Framework Programme of the European Union

